OWTNM 2007

# XVI International Workshop on Optical Waveguide Theory and Numerical Modelling

## Proceedings

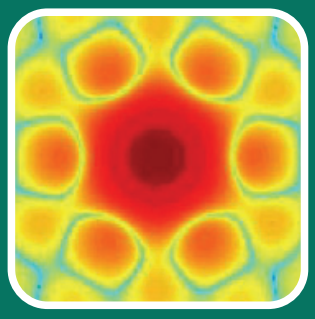

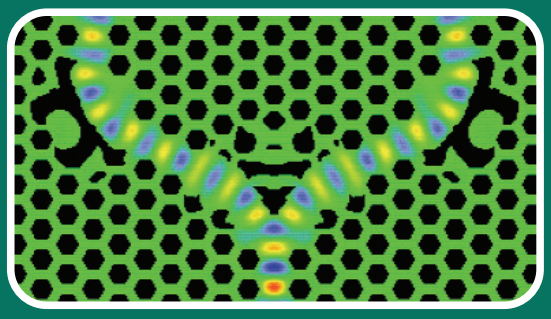

Copenhagen • Denmark • April 27-28 • 2007

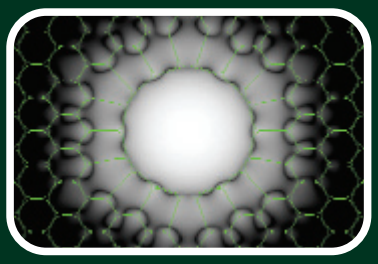

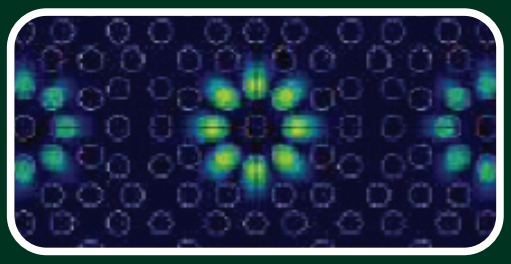

# OWTNM 2007

## XVI International Workshop on Optical Waveguide Theory and Numerical Modelling

27-28 April 2007, Copenhagen, Denmark

## Proceedings

COM•DTU

Department of Communications, Optics & Materials
Technical University of Denmark

**Volume Editors**:
Andrei Lavrinenko
Torben Roland Nielsen
Peter John Roberts

**Contact information:**
Andrei Lavrinenko
COM•DTU
Department of Communications, Optics & Materials
Technical University of Denmark
DTU - Building 345V
DK-2800 Kgs. Lyngby, Denmark
Tel.: +45 4525 6392
Fax.: +45 4593 6581
email: ala@com.dtu.dk

**Web: http://www.com.dtu.dk/**

**2007 Technical University of Denmark**
**Printed in Copenhagen, Denmark**

# Acknowledgements

We would sincerely like to thank, for their interest and financial support:

The Office of Naval Research Global, 223 Old Marylebone Road, London, NW1 5TH, UK[1]

The Danish Technical University, 2800 Kgs. Lyngby, Copenhagen, Denmark

JCMwave, GmbH, Haarer Str. 14a, D-85640 Putzbrunn, Germany

RSoft Design UK Ltd., 11 Swinborne Drive, Springwood Industrial Estate, Braintree, Essex, CM7 2YP, UK

[1] This work relates in part to the Department of Navy Grant N00014-07-1-1060 issued by the Office of Naval Research Global. The United States Government has a royalty-free license throughout the world in all copyrightable material contained herein.
The content of the information does not necessarily reflect the position or the policy of the United States Government.

# Preface

We welcome you all to the 16th International Workshop on Optical Waveguide Theory and Numerical Modelling (OWTNM), which is being held April 27-28 2007 at the Danish Technical University, Copenhagen, Denmark.

The aim of the OWTNM workshop, as in previous years, is to promote interaction between researchers, and to provide a forum for discussion and an exchange of ideas within the field of analytical and numerical waveguide modelling. A key goal of the meeting is to draw attention to encountered difficulties and to highlight currently unsolved problems within the area. Topics of interest include, but are not limited to:

*Theory of passive, active and nonlinear waveguide devices; Simulation and design of photonic integrated systems; Waveguide grating structures; Input/output waveguide coupling aspects; Photonic bandgap structures and photonic crystals; Photonic nanostructures and metamaterials; Plasmonics; Advances in numerical methods; Progress in mode solvers; Mathematical models and numerical methods; Device and system-oriented modeling; Coupling of electronic, photonic, elastic and thermal effects; Solid-state lasers and light-matter coupling in waveguides.*

This year, the OWTNM workshop is collocated with the European Conference on Integrated Optics 2007 (ECIO 2007), which provides an opportunity to connect specialists in numerical methods and modelling with experts on photonic and opto-electronic devices.

The program this year entails 6 invited talks, 26 oral talks and 45 posters arranged in 8 Sessions. We have placed a particular emphasis on the poster session, which is being held mid-morning on the Friday, since this provides a natural forum for a detailed discussion of specific research aspects. We expect that it will boost the working atmosphere and inspire a lot of discussion thereafter.

A collection of papers from the workshop will appear in a special issue of Optical and Quantum Electronics. Details can be found on the workshop website
http://www.dtu.dk/Sites/OWTNM2007/English.aspx

Copenhagen, April 2007

Andrei V. Lavrinenko
Robert John Roberts

# Organizers

## **OWTNM Technical Committee**:

*Trevor Benson, University of Nottingham, UK*
*Peter Bienstman, Ghent University, Belgium*
*Jirí Ctyroký, IREE AS CR, Czech Republic*
*Anand Gopinath, University of Minnesota, USA*
*Hugo J. W. M. Hoekstra, University of Twente, Netherlands*
*Hans-Peter Nolting, HHI Berlin, Germany*
*Olivier Parriaux, University of Saint Etienne, France*
*Reinhold Pregla, FernUniversität Hagen, Germany*
*Christoph Wächter, Fraunhofer IOF, Jena, Germany*
*Andrea Melloni, DEI - Politecnico di Milano, Italy*
*Andrei V. Lavrinenko, COM·DTU, Lyngby Kgs., Denmark*

## **Local Organizing Committee**:

*Andrei V. Lavrinenko (chairman), COM·DTU, Lyngby Kgs., Denmark*
*Ole Bang, COM·DTU, Lyngby Kgs., Denmark*
*Jesper Mørk, COM·DTU, Lyngby Kgs., Denmark*
*Niels Asger Mortensen, MIC, DTU, Lyngby Kgs., Denmark*
*Ejner Nicolaisen, COM·DTU, Lyngby Kgs., Denmark*
*Torben Roland Nielsen, COM·DTU, Lyngby Kgs., Denmark*
*Peter John Roberts, COM·DTU, Lyngby Kgs., Denmark*
*Ole Sigmund, MEK, DTU, Lyngby Kgs., Denmark*

# Programme

# Friday 27.04.2007

8:25 - 8:30 Welcome

8:30 - 10:00 **Session OR-01: Advances in modal methods**

8:30 - 9:00 OR-01.01 *A new look at slanted-wall beam propagation* (Invited)
G. R. Hadley

9:00 - 9:15 OR-01.02 *Helmholtz solver with transparent influx boundary conditions and nonuniform exterior*
R. Stoffer, A. Sopaheluwakan, M. Hammer, E. Van Groesen

9:15 - 9:30 OR-01.03 *Improved 1D mode solver and 2-D bi-directional mode expansion propagation method based on harmonic expansion*
J. Čtyroký

9:30 - 9:45 OR-01.04 *Overcoming the discontinuous fields limitation in Fourier Methods using a novel spectrum splitting strategy*
R. Godoy-Rubio, A. Ortega-Moñux, J. G. Wangüemert-Pérez, I. Molina-Fernández

9:45 - 10:00 OR-01.05 *The perturbation method for photonic crystals using the plane wave expansion*
V. Zabelin, R. Houdré

10:00 - 12:00 **Poster Session PO-01**

PO-01.01 *Pseudo-spectral time-domain simulation of metallic structures*
W. H. P. Pernice, F. P. Payne, D. F. G. Gallagher

PO-01.02 *Simulation of metallic nano-particle composite films using the FDTD method*
W. H. P. Pernice, F. P. Payne, D. F. G. Gallagher

PO-01.03 *New Basis Functions for the Modal Analysis of Integrated Optical Waveguides using the Galerkin Method*
S. Barai, A. Sharma

PO-01.04 *Statistical Analysis of RZ-DPSK Fiber Communication Channels*
T. Broderick, B. Slater, S. Boscolo, S. K. Turitsyn

PO-01.05 *Field representations for optical defect microcavities in 1D grating structures using quasi-normal modes*
M. Maksimovic, M. Hammer, E. van Groesen

PO-01.06 *Optical Analysis of a Microcavity Laser with an Annular Bragg Reflector*
E. I. Smotrova, A. I. Nosich, T. M. Benson, P. Sewell

PO-01.07 *Maximizing the Optical Band Gap in 2D Photonic Crystals*
K. Hougaard, Ole Sigmund

PO-01.08 *Self-consistent FDTD Maxwell-Bloch solver*
T. R. Nielsen, S. Ejsing, A. V. Lavrinenko, J. Mørk

PO-01.09 *Modeling Waveguides with Hole Arrays by Operator Marching and Robin-to-Dirichlet Maps*
L. Yuan, Y. Y. Lu

PO-01.10 *Whispering-Gallery-Mode Resonances in Discrete Luneburg Lenses*
A. I. Nosich, S. Rondineau

PO-01.11 *Dependences of Lasing Thresholds for a Layered Structure on the QW Width*
V. O. Byelobrov, A. I. Nosich

PO-01.12 *Validation of FDTD-2D for high-Q resonances description*
A. V. Boriskin, S. V. Boriskina, A. Rolland, R. Sauleau, A. I. Nosich

PO-01.13 *Benchmark on a slit-groove diffraction problem*
M. Besbes, P. Lalanne

PO-01.14 *Numerical Simulations of New Compact Acousto-Optic Tunable Filters Based on Multi-Reflector Technology*
A. Tsarev, E. Kolosovsky, R. Taziev

PO-01.15 *3D Modelling of Microdisk Resonators Based on Fourier Modal Method*
A. Armaroli, A. Morand, P. Benech, G. Bellanca, S. Trillo

PO-01.16 *Simple approximate method for chromatic dispersion estimation of singlemode optical fiber with an arbitrary coaxial refractive index profile*
V. A. Burdin, A. V. Bourdine

PO-01.17 *Method for high order mode chromatic dispersion estimation*
V. A. Burdin, A. V. Bourdine

PO-01.18 *Optical Fiber Polarization Elements based on Long-Period-Gratings in Photonic Crystal Fibers*
D. C. Zografopoulos, E. E. Kriezis, T. D. Tsiboukis

PO-01.19 *Theoretical Analysis of Square Surface Plasmon Polariton Waveguides*
J. Jung, T. Søndergaard, S. I. Bozhevolnyi

PO-01.20 F*inite-difference time-domain analysis of micro-lens integrated vertical-cavity surface-emitting lasers*
I.-S. Chung, Y. T. Lee

PO-01.21 *Domains tilt effects on the SHG process in PPLN crystals grown by the off-center Czochralski technique*
F.M. Pigozzo, A.-D. Capobianco, N. Argiolas, M. Bazzan, C. Sada

PO-01.22 *Enhancement of the Quality factor of Bloch modes at Gamma-point in a 2D nanopillar Photonic Crystal slab using heterostructures*
L. Ferrier, E. Drouard, X. Letartre, P. Rojo-Romeo, P. Viktorovitch

PO-01.23 *2D modelling of PhC waveguide structures: a comparison of approaches*
I. Richter, J. Čtyroký, M. Šiňor, P. Kwiecien

PO-01.24 *TE and TM mode analysis for a 2D photonic crystal with liquid crystal infiltration*
J. Cos, L. F. Marsal, J. Pallarès, J. Ferré Borrull

PO-01.25 *A methodology for the design of bio-inspired multilayer deflectors*
C. Vandenbem, O. Deparis, M. Rassart, V. L. Welch, V. Lousse, J. P. Vigneron

PO-01.26 *Photonic Crystal Beam Propagation using a Fourth Order Approximation of the Band Diagram*
D. Bernier, E. Cassan, G. Maire, D. Marris-Morini, L. Vivien

PO-01.27 *Fabry-Perot Interferometer with two Waveguide-Grating Mirrors: Influence of Grating Shift*
B. A. Usievich, V. A. Sychugov, J. Kh. Nurligareev

PO-01.28 *Simulation of acousto-optical interaction in a Mach-Zehnder interferometer*
M. B. Dühring, O. Sigmund, J. S. Jensen

PO-01.29 *A 'Couplonic' Approach to Out-Of-Phase Coupled Periodic Waveguides*
Y. G. Boucher, A. V. Lavrinenko, D. N. Chigrin

PO-01.30 *Metamaterials based on Nanocavities*
C. Rockstuhl, T. Zentgraf, T. P. Meyrath, H. Giessen, T. Pertsch, F. Lederer

PO-01.31 *Analysis and Design of MMI-Based Racetrack Resonators*
T. T. Le Laurence, W. Cahill

PO-01.32 *Demultiplexing optical signals using chirped two-dimensional photonic crystals*
D. Biallo, A. D'Orazio, M. De Sario, V. Marrocco, V. Petruzzelli, F. Prudenzano

PO-01.33 *Modeling of Multimodal Effects in Two-port Ring-Resonator Circuits for Sensing Applications*
H. P. Uranus, H. J. W. M. Hoekstra, R. Stoffer

PO-01.34 *BPM Simulation of SNOM Measurements of Waveguide Arrays Induced by Periodically Poled BNN Crystals*
J. Lamela, F. Jaque, E. Cantelar, D. Jaque, A. A. Kaminskii, G. Lifante

PO-01.35 *Rigorous modeling of cladding modes in photonic crystal fibers*
L. Rindorf, O. Bang

PO-01.36 *Donor and acceptor modes in nonlinear microstructured optical fibers*
M. Zacares, G. Renversez, F. Drouart, G. March, A. Nicolet, A. Ferrando

PO-01.37 *Q-Factor Calculations with the Finite-Difference Time-Domain Method*
A. Ivinskaya, A. V. Lavrinenko

PO-01.38 *Wave Chaotic Behaviour Generated by Linear Systems*
V. A. Buts, A. G. Nerukh, N. N. Ruzhytska, D. A. Nerukh

PO-01.39 *A variational formulation of guided wave scattering problems*
M. Hammer

PO-01.40 *Slow-light enhanced optical detection in liquid-infiltrated photonic crystals*
M. E. V. Pedersen, L.S. Rishøj, H. Steffensen, S. Xiao, N.A. Mortensen

PO-01.41 *Breakdown of Wigner-Weisskopf theory for spontaneous emission: A quantitative analysis*
P. Kristensen, B. Tromborg, P. Lodahl, J. Mørk

PO-01.42 *Band Structure Calculation Methods for complex and frequency dependent Photonic Crystals*
M. Bergmair, K. Hingerl

PO-01.43 *Multistable Lasing in Coupled Microcavities and Nanopillar Waveguides: Mode Switching Dynamics*
S. V. Zhukovsky, D. N. Chigrin, A. V. Lavrinenko, J. Kroha

PO-01.44 *Parallelogramic metal gratings as a benchmark for the modal- and diffraction-order-based slicing techniques*
M. Foresti, A. V. Tishchenko

PO-01.45 *Competing quadratic and cubic nonlinear phenomena in metamaterials*
D. de Ceglia, A. D'Orazio, M. De Sario, V. Petruzzelli, F. Prudenzano, M. A. Vincenti, M. G. Cappeddu, M. J. Bloemer, M. Scalora

12:00 - 13:00 **Lunch**

13:00 - 14:15 **Session OR-02: Analysis of fibers**

13:00 - 13:30 OR-02.01 *An adaptive finite element method for the optimization of photonic crystal fibers* (Invited)
S. Burger, J. Pomplun, F. Schmidt

13:30 - 13:45 OR-02.02 *Transformation of Radiating Cylindrical Waves between Skew Axes and Application to an Optical Fiber Helix*
I. D. Chremmos, N. K. Uzunoglu

13:45 - 14:00 OR-02.03 *Air-clad fibers: pump absorption assisted by chaotic wave dynamics*
N. A. Mortensen

14:00 - 14:15 OR-02.04 *Spectral properties of splay-aligned mesogens in liquid crystal photonic bandgap fibres*
G. Tartarini, R. Palermo, F. Cornazzani, T. T. Alkeskjold, A. Bjarklev, P. Bassi

14:15 - 14:30 **Break**

14:30 - 16:30 **Joint Session OR-03/OWTNM & FC/ECIO**
**Modelling of passive and active nanophotonics components**

14:30 - 15:00 OR-03.01 *Modeling photonic crystal and plasmonic devices* (Invited)
S. Fan

15:00 - 15:15 OR-03.02 *On Meta-Meta-Materials – an approach for magnetic resonances in the visible*
C. Rockstuhl, T. Scharf, T. Pertsch, F. Lederer

15:15 - 15:30 OR-03.03 *Tailoring group velocity by topology optimization*
R. Stainko, O. Sigmund

15:30 - 15:45 OR-03.04 *Accurate analysis of modal and leaky characteristics of silicon-on-insulator photonic wires*
H.-C. Chang, S.-M. Hsu, C.-P. Yu

15:45 - 16:00 OR-03.05 *SOI grating structure for perfectly vertical fiber coupling*
G. Roelkens, D. Van Thourhout, R. Baets

16:00 - 16:15 OR-03.06 *Spatial and Spectral Distributed Multi Population Rate Equations Model for Quantum Dot Superluminescent Diodes*
M. Gioannini, I. Montrosset

16:15 - 16:30 OR-03.07 *Full-vectorial time-domain modelling of photonic crystal semiconductor lasers*
W. H. P. Pernice, D. F. G. Gallagher, F. P. Payne

16:30 - 17:00 **Break**

17:00 - 18:00 **Session OR-04 : Light emission and radiation extraction**

17:00 - 17:30 OR-04.01 *Efficient modeling of nonlinear wave propagation and radiation dynamics in nano-photonic systems* (Invited)
K. Busch

17:30 - 17:45 OR-04.02 *Modelling light extraction in 3D organic LEDs containing photonic crystals*
P. Bienstman, P. Vandersteegen, R. Baets

17:45 - 18:00 OR-04.03 *Emission in periodic waveguides: computational concepts and applications*
G. Lecamp, J.-P. Hugonin, P. Lalanne

19:00 - **Workshop Dinner**

## Saturday 28.04.2007

8:30 - 10:00 **Session 5: Modelling of optical waveguides**

8:30 - 9:00 OR-05.01 *Plasmonic waveguides and components* (Invited)
O. J. F. Martin

9:00 - 9:15 OR-05.02 *Numerical modelling on new nano-photonic SOI waveguide structures for multi-reflector filtering devices*
A. V. Tsarev

9:15 - 9:30 OR-05.03 *2D Numerical model of bent waveguide using RCWA and PML developed to simulate a spectrograph in integrated optics*
B. Martin, A. Morand, P. Benech, G. Leblond, S. Blaize, G. Lerondel, P. Royer, E. Lecoarer

9:30 - 9:45 OR-05.04 *Backreflection modelling in rough waveguides*
R. Costa, F. Morichetti, A. Melloni

9:45 - 10:00 OR-05.05 *Inverse method for the reconstruction of refractive index profile and power management in gradient index optical waveguides*
N. E. Nikolaev, V. V. Shevchenko

10:00 - 10:30 **Break**

10:30 - 12:00 **Session OR-06: Numerical methods in photonics**

10:30 - 11:00 OR-06.01 *Recent Advances on Finite Element Algorithms and their Applications to Photonics* (Invited)
H. E. Hernandez Figueroa

11:00 - 11:15 OR-06.02 *A new split step non-paraxial finite difference method for 3-D wave propagatio*n
D. Bhattacharya, A. Sharma

11:15 - 11:30 OR-06.03 *General covariance in computational electrodynamics*
D. M. Shyroki, J. Lægsgaard, O. Bang, A. V. Lavrinenko

11:30 - 11:45 OR-06.04 *Computing photonic crystal point defect modes by Dirichlet-to-Neumann maps*
S. Li, Y. Y. Lu

11:45 - 12:00 OR-06.05 *Finite element time domain modelling of $90^0$ sharp bends*
A. Agrawal, B. M. A. Rahman, K. T. V. Grattan, S. S. A. Obayya

12:00 - 13:00 **Lunch**

13:00 - 15:00 **Session OR-07 Modelling of linear and nonlinear cavities and waveguides**

| | | |
|---|---|---|
| 13:00 - 13:30 | OR-07.01 | *Revisiting the Rayleigh hypothesis: impacts on future electromagnetic theory and numerical modelling* (Invited)<br>A. V. Tischenko |
| 13:30 - 13:45 | OR-07.02 | *Simulation of resonance modes in pillar-type cavities using finite element methods*<br>B. Kettner, F. Schmidt, L. Zschiedrich |
| 13:45 - 14:00 | OR-07.03 | *Influence of geometry on the quality factor of a micro pillar*<br>N. Gregersen, T. R. Nielsen, J. Mørk |
| 14:00 - 14:15 | OR-07.04 | *Control of near-field pattern in 2D circular resonator by adjusting in time of media parameters*<br>N. K. Sakhnenko, A. Nerukh |
| 14:15 - 14:30 | OR-07.05 | *Beam propagation method for simulation of quantum dot flared laser and SLD*<br>P. Bardella, I. Montrosset, J. M. Blanco Triana |
| 14:30 - 14:45 | OR-07.06 | *Models of non-stationary light beam propagation for non-linear waveguide excitation problems*<br>E. A. Romanova, V. Janyani, A. Vukovic, P. Sewell, T. Benson |
| 14:45 - 15:00 | OR-07.07 | *Model of the refractive index change induced by a single femtosecond pulse*<br>J. S. Petrovic, V. Mezentsev, I. Bennion |

15:00 **Closing of the Workshop**

# Abstracts

# A New Look at Slanted-Wall Beam Propagation

G. Ronald Hadley
*Sandia National Laboratories, Albuquerque, New Mexico, USA*
*grhadle@sandia.gov*

Here we present a derivation of finite difference equations for 1D beam propagation through waveguides whose dielectric interfaces are slanted in arbitrary fashion with respect to the propagation direction.

## Summary

It is well known that the use of a rectangular grid for beam propagation of light through structures whose dielectric interfaces slant with respect to the direction of propagation is problematic. Numerical errors resulting from this approach are particularly troublesome for high-contrast waveguides, and include spurious energy loss due to scattering from the "stair-steps" and non-physical mode mixing. Previous attempts to address this issue [1]-[4] have usually employed some form of coordinate transformation. These methods are quite accurate for structures with special geometries, but lack sufficient generality to be useful for structures that meander or change waveguide widths in complicated or unpredictable ways. In particular, the analysis of a new problem requires constructing a new transformation. In contrast to this approach, we address the need for a finite difference equation that allows each grid point to move arbitrarily (constrained only by limits on the maximum angle) between adjacent propagation planes (see Fig. 1), so that both the motion of boundaries and the location of grid points for optimum field resolution may be independently and dynamically adjusted.

Unfortunately, the complete loss of symmetry that results from allowing independent motion of grid points leads to considerable problems with energy conservation. Thus, many finite difference equations are possible that reduce to the correct propagation equation in the limit of zero grid size, but most of these do not conserve energy, and in fact in some cases this non-conservation can extend over many orders of magnitude. To address this issue, we derive general conditions on the 1D finite difference equations that must be satisfied in order to guarantee the existence of a conserved quadratic form. With these conditions as a guide, we have successfully derived wide-angle finite difference equations for 1D propagation that conserve energy for realistic problems to better than 1%, while reproducing accurate propagation constants for the simple case of a slanted waveguide of constant cross section.

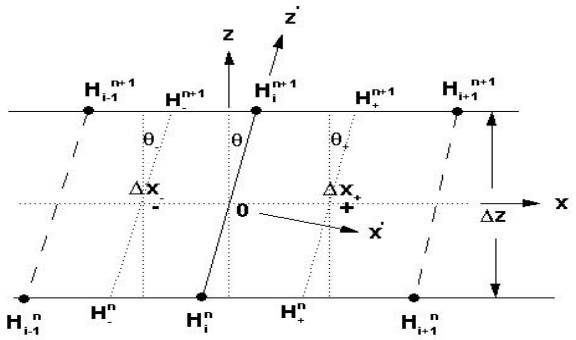


Fig. 1 Schematic of region surrounding grid point *i* at propagation planes *n*, *n+1* including notation. Although not subscripted in the figure to simplify notation, the angles $\theta, \theta_{\pm}$ all will in general be different at each grid point

## References

[1] P. Sewell, T. M. Benson, P. C. Kendall and T. Anada, "Tapered beam propagation", Electron. Lett. Vol. 32, pp.1025-1026(1996).
[2] J. Yamauchi, J. Shibayama and H. Nakano, "Finite-difference beam propagation method using the oblique coordinate system", Electron. And Communications in Japan, Part 2, Vol. 78, pp.20-27(1995).
[3] Y.-P. Chiou and H.-C. Chang, "Beam propagation method for analysis of z-dependent structures that uses a local oblique coordinate system", Opt. Lett. Vol. 23, pp.998-1000(1998).
[4] D. Z. Djurdjevic, T. M. Benson, P. Sewell, and A. Vukovic, IEEE J. Lightwave Tech. Vol. 22, pp.2333-2340(1999).

.

# Helmholtz solver with transparent influx boundary conditions and nonuniform exterior

R. Stoffer, A. Sopaheluwakan, M. Hammer and E. van Groesen
*MESA+ Institute for Nanotechnology, AAMP group, University of Twente,*
*P.O. Box 217, 7500 AE Enschede, The Netherlands*
*r.stoffer@math.utwente.nl*

Boundary conditions for a 2D finite element Helmholtz solver are derived, which allow scattered light to leave the calculation domain in the presence of outgoing waveguides. Influx of light, through a waveguide or otherwise, can be prescribed at any boundary.

In the simulation of integrated optical structures, the boundaries of the calculation window are an important issue. They should act as if they were not there; in principle the boundary conditions should incorporate the solution of the equations in the exterior. Thus, scattered light from structures in the interior should leave the domain unobstructed, and it must be possible to prescribe the influx of light from the exterior to the interior. Such Transparent Influx boundary conditions (TIBC's) can be described in terms of a so-called Dirichlet-to-Neumann (DtN) operator, which relates the field on the boundary to its normal derivative, such that the solution represents only outfluxing fields. Similarly, influxed fields may be prescribed. In [1], approximations of the DtN operator are applied on a computational domain with a smooth boundary; these operators are local. Contrarily, [2] describes operators for the boundaries of a rectangular domain; the respective TIBC's are nonlocal, expressing the field in the exterior as a series of Fourier modes. The method in [2] is limited to problems with a uniform exterior. This paper extends this method to structures in which half infinte straight waveguides extend from the boundary. The fields on the boundary are projected onto a modal basis associated with the waveguides, instead of on a Fourier basis. The example in Figure 1 clearly shows proper influx through a waveguide and outflux through all waveguides and into free space.

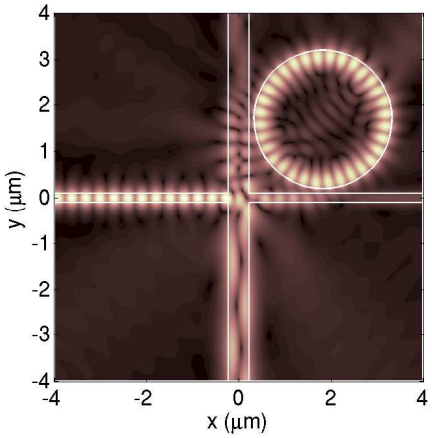


Figure 1: Finite element simulation (TE polarization, absolute value) of a waveguide crossing with a small disk. Parameters: Background refractive index 1.45, waveguide and disk refractive index 3.4, waveguide widths 0.2 $\mu$m (horizontal), 0.45 $\mu$m (vertical), disk radius 1.5 $\mu$m, gap between disk and waveguides 0.1 $\mu$m. At the boundaries fields are projected onto modes that are calculated using a window that is three times as wide as the shown finite element window. The field expansion consists of 147 terms on the western and eastern boundary and 149 on the north and south boundary.

*This research was supported by NanoNed, a national nanotechnology program coordinated by the Dutch Ministry of Economic Affairs.*

## References

[1] F. Schmidt, *Computation of discrete transparent boundary conditions for the 2D Helmholtz equation*, Optical and Quantum Electronics, **30**, 427–441 (1998).

[2] J. B. Nicolau and E. van Groesen, *Hybrid analytic-numerical method for light through a bounded planar dielectric structure*, Journal of Nonlinear Physics and Materials, **14**, 161 (2005).

# Improved 1D mode solver and 2-D bi-directional mode expansion propagation method based on harmonic expansion

Jiří Čtyroký
*Institute of Photonics and Electronics ASCR, v.v.i., Chaberská 57, 18251 Praha 8, Czech Republic* [1]
ctyroky@ufe.cz

A simple but efficient 1-D mode solver based on harmonic expansion was extended to more general boundary conditions, and its convergence for TM modes was improved. It was implemented into a 2-D bi-directional mode expansion propagation algorithm.

## Summary

At OWTNM 2005 we reported on a simple but efficient 1-D mode solver based on harmonic expansion. Its application in a 2-D bi-directional mode expansion propagation algorithm was described in [1]. Proper truncation (Fourier factorization) rules [2, 3] are fully implemented in the method. It can be easily applied to lossy media and allows for a very simple implementation of perfectly matched layers in terms of complex co-ordinate stretching [4] without the need of complex root searching. The bi-directional mode expansion propagation method based on this algorithm results in a very simple and strictly reciprocal algorithm.

The algorithm described in [1] was limited to fields with dominant components satisfying Dirichlet conditions at the boundaries of a computational window, *i.e.*, to TE fields between electrically conducting walls or TM fields between magnetically conducting walls. In the present contribution, the algorithm is generalized to any combination of electric and/or magnetic walls (with or without PMLs). It allows not only to fully utilize a pertinent symmetry of the problem to reduce the computational effort but also to better mimic the plane-wave excitation of the structure. Moreover, for TM modes between electric walls, a modified algorithm with significantly improved convergence was found and will be reported.

The similarities and differences of the method compared to the Fourier modal method will be briefly discussed, and some aplications of the method will be presented, too.

## References

[1] J. Čtyroký, *Opt. Quantum Electron.*, **38**, 45-62 (2006).
[2] C. Sauvan, P. Lalanne, and J.-P. Hugonin, *Opt. Quantum Electron.*, **36**, 271-284, (2004).
[3] J. P. Hugonin, P. Lalanne, I. d. Villar, *et al.*, *Opt. Quantum Electron.*, **37**, 107-119 (2005).
[4] W. C. Chew, J. M. Jin, and E. Michielsen, *Microwave and Opt. Technol. Lett.*, **15**, 383-369 (1997).

# Overcoming the discontinuous fields limitation in Fourier Methods using a novel spectrum splitting strategy

R. Godoy-Rubio, A. Ortega-Moñux, J. G. Wangüemert-Pérez, I. Molina-Fernández
*Dpto. Ingeniería de Comunicaciones, Universidad de Málaga, Campus Teatinos s/n,, 29071, Málaga, Spain*
*faligr@ic.uma.es, aom@ic.uma.es,gonzalo@ic.uma.es, imf@ic.uma.es*

In this work we present a novel strategy to dramatically improve the convergence rates of FFT-based Mode Solvers. The new formulation satisfies the electromagnetic boundary conditions at material interfaces.

## Summary

It is well known that the problem of slow convergence rates of the first implementations of Fourier Decomposition Methods (FDM) were solved, almost simultaneously, in [1][2][3], wherein the authors proposed a new Fourier factorization rule (known as Inverse Rule), instead of Laurent's rule, to correctly perform the product of discontinuous functions. Unfortunately, this technique cannot be directly applied to FFT-based electromagnetic solvers, like the recently proposed FFT-based Mode Solver (FFT-MS) [4], because the product terms in the wave equation are solved in the space domain. In this work we present a novel strategy to dramatically improve the convergence rates of FFT-based methods. Making use of simple signal filtering concepts and fundamental properties of Fourier series, it is possible to accurately obtain the discontinuous field profiles and their propagation constants with low number of harmonics, even in strongly guiding conditions. This technique has been exhaustively assessed in 1D situations. Fig. 1 shows the relative error of the normalized propagation constant for the fundamental TM mode of a high index contrast ($n_1$=1, $n_2$=3.5) slab waveguide. As illustrated in this figure, the obtained results show a similar accuracy as the one obtained with Inverse rule based methods and almost three orders of magnitude improvement with respect to the previous FFT-MS [4] and Laurent's rule based methods. Preliminary results have also been obtained for 2D situations with excellent performance. Fig. 2 shows the x-component of the electric field profile of the SOI photonic wire proposed in the European COST P11 action. Note in this figure the abrupt discontinuity of the field in the dielectric interfaces at $x$= ±0.25μm. The calculated effective index $N_{eff}$= 2.41234 is in good agreement to previously published results.

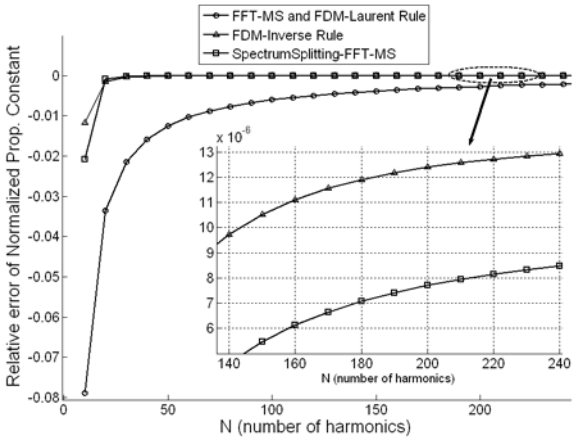


Figure 1: High index contrast slab waveguide.

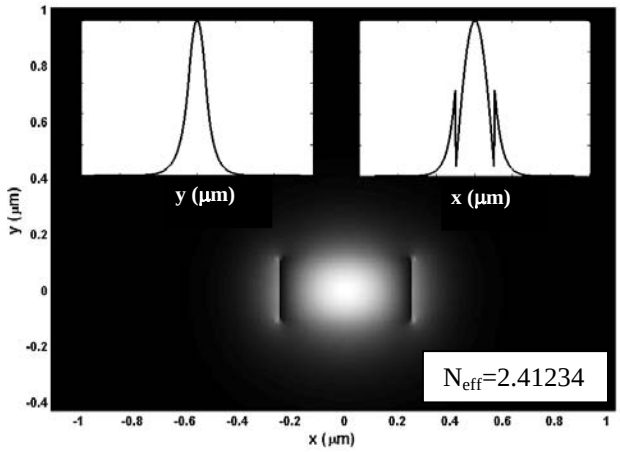


Figure 2: SOI Photonic wire results.

### References

[1] G. Granet and B. Guizal, J. Opt. Soc. Am. A. **13**, 1019-1023 (1996).
[2] P. Lalanne and G. M. Morris, J. Opt. Soc. Am. A. **13**, 779-784 (1996).
[3] L. Li, J. Opt. Soc. Am. A. **13**, 870-1876 (1996).
[4] A. Ortega-Moñux, J.G. Wangüemert-Pérez, I. Molina-Fernández, E. Silvestre and P. Andrés, IEEE Photonics Tech. Lett. **18**, 1128-1130 (2006).

# The perturbation method for photonic crystals using the plane wave expansion

Vasily Zabelin* and Romuald Houdré
*Institut de Photonique et d'Electronique Quantique, Ecole Polytechnique Fédérale, Lausanne, Switzerland*
**vasily.zabelin@epfl.ch*

A novel method for calculation of photonic crystal properties using the perturbation theory is presented. The method is based on the plane wave expansion scheme and can handle the variation of the permittivity and photonic crystal geometry.

## Summary

Photonic crystals (PhC) are one of the key elements of the modern integrated optics. Utilization of PhC-based structures allows us to tailor light propagation properties and create such devices as waveguides, microcavities, optical filters etc. The design of these devices requires an extensive numerical modelling to determine, for example, the dispersion relation for the propagating modes, frequency, field distribution, and the quality factor for the localized states. The computation speed becomes one of the critical parameters, because a large series of the calculation is usually required to find an optimal design.

The formalism of the perturbation theory, widely used in quantum mechanics, is very promising for the calculation of the response of the device properties to small variation of different parameters of the PhC structure. Unfortunately, the standard perturbation theory approach is hardly applicable for most of photonic crystals because of the high index contrast [1]. In this work we present another approach, based on the plane wave expansion method [2], which has been proved to be a powerful and efficient tool for determining the light propagation properties for any 2D periodic structure. The representation of the permittivity and the electromagnetic field distributions as a set of plane waves allows us to introduce the continuous variation of PhC structure parameters and overcome the problem of the permittivity discontinuity [1]. The developed method calculates the change of the state frequency and the field distribution as a result of the PhC parameters perturbation.

This method can handle variations of a PhC element (hole or pillar) permittivity, atom size, and atom position. Such perturbed elements can be arbitrarily distributed in the PhC computational super-cell, which allows one to simulate the effects like PhC infiltration, variation of a cavity geometry etc. The computation procedure requires only one calculation of the frequency and the field distribution of the Bloch modes for the given Bloch vector and then determines the corrections as functions of the introduced perturbation parameter. It is much faster than the usual device design approach, which uses a series of the calculations, because the longest step (determination of the eigenvalues and the eigenvectors of a large matrix) is performed only once. This becomes especially important for designing high-Q cavities, because it requires a big super-cell, greatly decreased computation speed. The variation of the localized state field distribution, obtained by the presented method, also allows one to estimate the change of the quality factor [3], which is very helpful to design the better cavity.

Another possible application of the method, such as modelling of PhC optical tuning using liquid crystal infiltration, are also discussed.

## References

[1] M. Skorobogatiy, S. G. Johnson, S. A. Jacobs, and Y. Fink, Phys. Rev. E, **67**, 046613 (2003)
[2] M. Plihal and A.A. Maradudin, Phys. Rev. B, **44** (16), 8565-8571, (1991)
[3] D. Englund, I. Fushman, and J. Vuckovic, Optics Express, **13** (16), 5961-5975 (2005)

# Pseudo-spectral time-domain simulation of metallic structures

Wolfram H. P. Pernice[1], Frank P. Payne[1] and Dominic F. G. Gallagher[2]
[1] *University of Oxford, Department of Engineering Science, Oxford, OX1 3PJ, UK*
wolfram.pernice@eng.ox.ac.uk

[2] *Photon Design, 34 Leopold Street, Oxford, OX4 1TW, UK*

We present a pseudo-spectral approach for simulating the optical properties of metallic structures. Dispersion is introduced through auxiliary differential equations for Drude-Lorentz material models. A novel averaging approach is applied to avoid errors from material discontinuities present in spectral elements.

## Summary

The pseudo-spectral time-domain (PSTD) method has attracted increasing interest for the time domain simulation of electromagnetic problems [1]. Due to its exponential convergence, spatial resolution can be limited to as few as two points per wavelength. This feature results in both savings of computational memory and time, making it possible to investigate more complex problems. With increasing interest in plasmonic devices and metal nano-particle structures, it is important to be able to simulate dispersive materials. In this article we introduce the PSTD method extended with auxiliary differential equations for the numerical investigation of metals. Our formulation only requires additional storage for polarization fields, thus making it memory efficient. The PSTD method is usually expressed in curvilinear coordinates in order to be able to efficiently approximate irregular material boundaries. However, this increases the computational load significantly, as 18 derivatives have to be calculated for each time-step. In addition, the curvilinear approach results in a small time-step when small geometrical features are described by a single spectral element. We have therefore used rectilinear coordinates, which reduces the number of derivatives needed to 6. For curved surfaces an averaging approach is required to describe the resulting dielectric function at each grid point. As shown for the FDTD method, using an effective permeability yields poor results. We therefore average the electric flux density at grid points that lie on material interfaces. This approach results in new updating equations for the electric fields while leaving the updating equations for the metallic polarization fields unchanged. We present results demonstrating, that even dispersive elements smaller than the grid spacing can be modeled accurately.

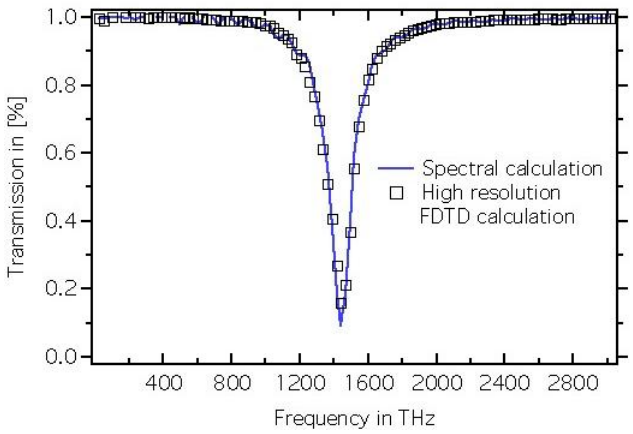


*Fig. 1. Transmission spectrum obtained for a 20 nm thick gold disk.*

We evaluated our algorithm by simulating transmission through thin layers of metals. Furthermore, in order to evaluate the averaging approach, we calculated the transmission spectrum for a gold nano-particle. Comparison with the FDTD method demonstrates the validity of the algorithm as depicted in figure 1.

## References

1. G.X. Fan, Q.H. Liu and J.S. Hesthaven, IEEE Trans. Geos. Rem. Sens., **40**, 1366–1373, (2002).

# Simulation of metallic nano-particle composite films using the FDTD method

Wolfram H. P. Pernice[1], Frank P. Payne[1] and Dominic F. G. Gallagher[2]
[1] *University of Oxford, Department of Engineering Science, Oxford, OX1 3PJ, UK*
wolfram.pernice@eng.ox.ac.uk

[2] *Photon Design, 34 Leopold Street, Oxford, OX4 1TW, UK*

We present an efficient formulation for the FDTD simulation of granular films. Composite materials consisting of a dielectric matrix with inclusions of metallic nano-particles are investigated and show close agreement with theoretical results.

## Summary

Research on metal nano-particle composite films has been of particular interest due to the possibility to tune the optical properties of the film by varying solely the volume percentage of nano-particles [1]. The numerical investigation of structures composed of such materials remains a challenging problem, because of the small feature size of the particles compared to the optical wavelength. In this article we propose an efficient approach to model the optical properties of granular nano-particle films. As suggested by [2] the dielectric constant of composite materials with a filling fraction (1-*x*) of metal can be described by an extended version of the Maxwell-Garnett theory for a mixture of a metal and a dielectric with permittivity functions $\varepsilon_m$ and $\varepsilon_d$, respectively

$$\varepsilon(\omega) = \varepsilon_d \frac{(1-x+xL_m)\varepsilon_m(\omega)+(1-L_m)x\varepsilon_d}{L_m x\varepsilon_m(\omega)+(1-L_m x)\varepsilon_d} \qquad (1)$$

The particle shape is included through the depolarizability parameter $L_m$. We approximate the dielectric function of the metal with a Drude-Lorentzian model with N poles, which describes the material behavior in the optical range very accurately. The resulting dielectric function for the granular material cannot be used in the FDTD directly, therefore we transform it into a sum of alternative Lorentzians. Equation (1) is first expressed in pole-residue form. Subsequently, we group terms with complex conjugate poles to construct a new Lorentzian. The final approximation to the composite dielectric function uses the same number of poles as the function used to describe the metal. We include the Lorentzian model in the FDTD method through auxilliary differential equations. The applicability of our approach is demonstrated by simulating reflectance spectra of composite layers. As shown in figure 1, the results agree very well with analytical calculations. In particular the predicted red-shift in resonance frequency [2] is also observed.

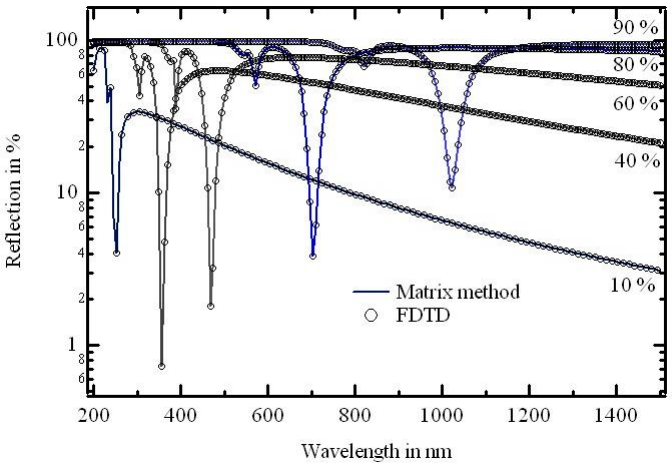


*Fig. 1. Reflection spectra calculated for varying silver content in a 50 nm thick quartz film.*

## References

[1] L. M. Liz-Marzan, Langmuir, **22**, 32-41 (2006).
[2] R. W. Cohen, G. D. Cody, M. D. Coutts and B. Abeles, Phys. Rev. E, **8**, 3689-3703 (1973).

# New Basis Functions for the Modal Analysis of Integrated Optical Waveguides using the Galerkin Method

Samit Barai and Anurag Sharma
*Physics Department, Indian Institute of Technology Delhi, New Delhi – 110016, India*
*asharma@physics.iitd.ac.in*

A new set of basis functions based on truncated Gaussian wavelets produces a sparse eigenvalue equation when the wave equation is solved by the Galerkin method. The results for diffused planar waveguides show a significant reduction in computation time and improvement in accuracy.

## Summary

The efficiency of optical waveguide analysis by the Raleigh-Ritz method and the Galerkin method depends critically on the choice of basis functions. The Hermite-Gauss (HG) functions have often been used. Recently, a new scheme has been devised to generate a set of basis functions by systematically deriving a sequence of functions from a single predefined function [1,2]. The method has the advantage of dealing with a single optimization parameter. In all these methods, the resulting matrix is generally dense and the evaluation of matrix elements also requires numerical integration on infinite or large range. We present here a new set of basis functions, which leads to a sparse matrix and the effort on the numerical integrations involved is also greatly economized.

We define a train of truncated Gaussian wavelets as

$$\varphi_i(x) = e^{-(x-i\Delta x)^2/[c(m\Delta x)^2]} - e^{-1/c} \quad \text{for} \quad (i-m)\Delta x < x < (i+m)\Delta x$$
$$= 0 \quad \text{elsewhere;} \qquad \text{with} \quad i = 0,\pm1,\pm2,...$$

where $\Delta x$ is the distance between consecutive wavelets $c$ is a constant and $m$ decides the number of defined points in the wavelet and hence the bandwidth ($4m$-1) of the final sparse matrix of the eigenvalue equation. A typical wavelet is shown in Fig. 1 for $m = 2$.

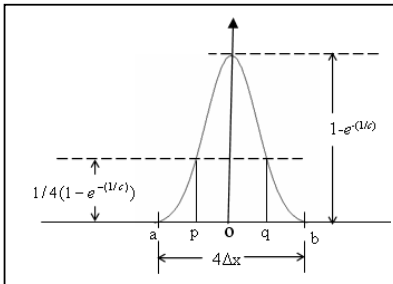

Fig. 1 Truncated Gaussian Wavelet ($m$=2).

As an example, we consider a diffused planar waveguide with a Gaussian profile: $n^2(x) = n_c^2$ for $x < 0$ and $n^2(x) = n_s^2 + 2n_s\Delta n \exp(-x^2/w^2)$ for $x > 0$, where, $n_s$ is the substrate index, $n_c$ is the cover index, $\Delta n$ is the peak index change and $w$ is the effective width. Table I shows a comparison of normalized propagation constant $b = [(\beta/k_0)^2 - n_s^2]/(2n_s\Delta n)$ as a function of normalized frequency $V = k_0 w\sqrt{(2n_s\Delta n)}$, for $TE_0$ mode calculated using 35 HG and TGW ($m$=3) functions. Figure 2 shows the comparison of computation time. These results show amply the advantage of considerably reduced computation effort that we obtain with our method. The work for rectangular waveguides is in progress and will be reported at the Workshop.

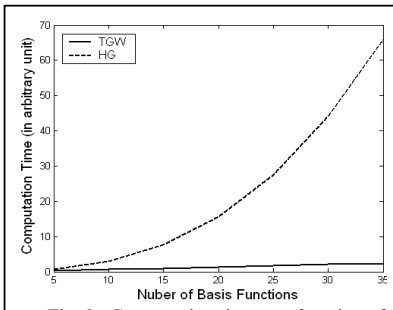

Fig. 2 Computation time as a function of number of functions for the $TE_0$ mode.

**Table I**: $b$ vs $V$ for the $TE_0$ mode

| $V$ | HG | TGW ($m$ = 2) | TGW ($m$ = 3) | TGW ($m$=4) | Exact |
|---|---|---|---|---|---|
| 2.0 | 0.076 | 0.079 | 0.082 | 0.082 | 0.082 |
| 3.0 | 0.269 | 0.273 | 0.274 | 0.274 | 0.275 |
| 4.0 | 0.409 | 0.412 | 0.412 | 0.412 | 0.413 |

$n_c = 1.0$, $n_s = 2.177$, $\Delta n = 0.043$, $\lambda = 1.3$ μm.

## References

[1] J.D. Manacini, V. Fesssatidis, Q. Haider, S.P. Brown, Physics Letters A **274**, 170-173 (2000).
[2] C. Stubbins and K.Das, Phys. Rev. A **47**, 4506-4509 (1993).

# Statistical Analysis of RZ-DPSK Fiber Communication Channels

Terence Broderick, Brendan Slater, Sonia Boscolo, and Sergei K. Turitsyn
*Photonics Research Group, School of Engineering and Applied Science, Aston University, Birmingham B4 7ET, UK.* broderit@aston.ac.uk

We present an analysis of the received signal probability density functions in a practical fiber-optic communication channel utilizing the return-to-zero differential phase-shift keying modulation format.

## Summary

An important and yet unsolved problem in fiber-optic communication channels using the differential phase-shift keying (DPSK) signal modulation format is a reliable and simple estimation of the bit-error rate (BER). An accurate evaluation of the BER is a critically important issue in the design of fiber-optic systems. Since direct measurements of very low BERs can be difficult, indirect statistical and numerical methods for system performance evaluation are imperative. Various $Q$-factor methods are available for the BER estimation in DPSK systems [1], which are based on a Gaussian or modified Gaussian approximation for the signal statistics. However, the accuracy of such methods is strongly dependent on the particular scenario analyzed. To understand if any reliable generic rules can be found at all for DPSK systems, an exact knowledge of the behaviour of the probability density functions (PDFs) for the relevant quantities of the received signal is highly desirable. In this paper, we analyze the PDFs of the received current and differential phase in return-to-zero (RZ) DPSK transmission systems. As an example, we consider a typical non-slope matched submarine link at 20 Gb/s channel rate. Details of the numerical modelling will be given in the workshop. Figure 1 shows an example of PDFs for 33% and 20% duty cycle pulses obtained at similar values of BER (approximately $10^{-3}$). It can be seen that the actual distributions deviate from the Gaussian or modified Gaussian approximations. In particular, the kurtosis of the actual PDFs indicates that such distributions are in general of leptokurtic type with a more acute "peak" and "fat tails" than the corresponding normal distributions. The latter suggests that more of the variance is due to rare extreme deviations. We observe that in the considered parameter range, this "non-gaussianicity" of the PDFs increses with decreasing pulse width. To assess the type of the observed distributions, we use a tail-fitting approach based on the extreme value theory [2]. In the long-tailed (high kurtosis) case the distribution tails decay similar to the tails of the Pareto distribution, which behaves like a polynomial and, thus, is a simple fitting tool for our model. Full results of this study will be presented in the workshop, with a focus on the dependence of the PDFs' behaviour on the pulse duty cycle and the transmission distance.

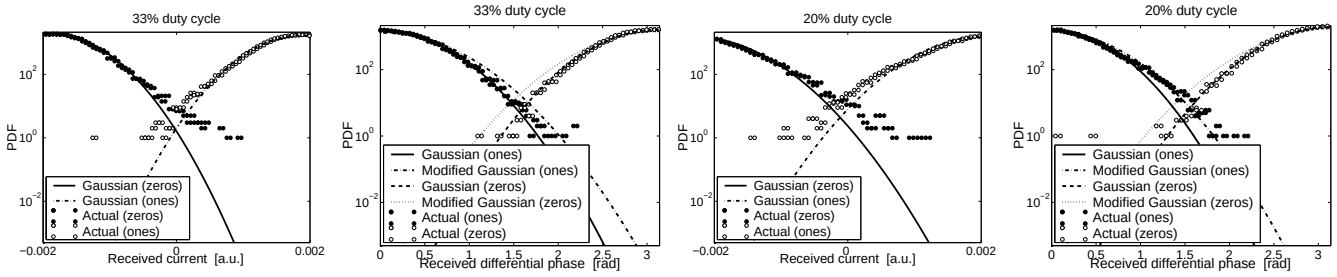


**Fig. 1** Distributions of received current and differential phase for the "ones" and the "zeros": actual distributions and approximations.

## References

[1] N. S. Bergano et al., IEEE Photon. Technol. Lett. **5**, 304–306 (1993); C. C. Hiew et al., IEEE Photon. Technol. Lett. **16**, 2619–2621 (2004).

[2] B. Finkenstädt and H. Rootzén, *Extreme Values in Finance, Telecommunications and the Environment*, Monographs on Statistics and Applied Probability (Chapman & Hall/CRC, New York, 2003).

# Field representations for optical defect microcavities in 1D grating structures using quasi-normal modes

M. Maksimovic, M. Hammer, E. van Groesen
*MESA$^+$ Institute for Nanotechnology, University of Twente, Enschede, The Netherlands*
*m.maksimovic@math.utwente.nl*

Quasi-Normal Modes are used to characterize transmission resonances in 1D optical defect cavities and the related field approximations. Using a mirror field and the relevant QNM, a variational principle permits to represent the field and the spectral transmission close to resonances.

## Summary

When subjected to external excitation, dielectric optical gratings show a resonant response in the time or frequency domain, which can be tailored by inclusion of defects. One can view the structures as open systems which permit the leakage of energy to the exterior, described by the Helmholtz equation with outgoing wave boundary conditions. This constitutes an eigenvalue problem for complex frequencies and the associated field profiles, or quasi-normal modes (QNMs). A theoretical framework for an overall description of optical 1D systems via QNMS is given in [1] and for periodic structures in [2]. We consider single and multiple defect cavities in finite gratings; the theory of [1, 2] has been adapted and implemented in terms of a standard Transfer-Matrix Method . A time-independent perturbation theory for QNM eigenfrequencies is given.

The complex eigenvalues appear to correspond to the position and quality of resonances in the spectral transmission [3]. Splitting the total field of the transmission problem into incoming and scattered parts, as an alternative to [1, 2] we investigated a QNM expansion of only the scattered field, and the related expressions for the transmission and compared to the exact TMM reference. Adequate approximations require summation over many basis modes, even in a spectral region of isolated defect resonances in the band-gap. It turns out that the variational form of the transmission problem [3, 4] offers a resourceful alternative. Using a combination of the mirror field of the structure (without defect) and only one/few relevant QNM(s) as a template, the restriction of the functional of [3, 4] yields an excellent field representation, together with a reasonable approximation of the spectral transmission.

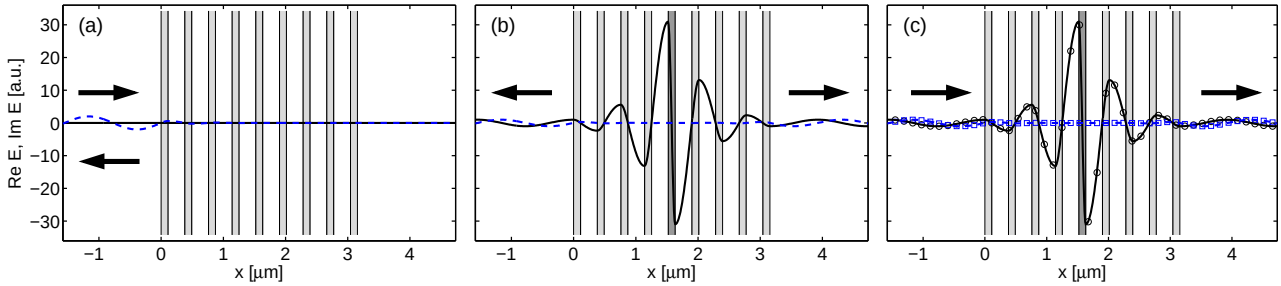


*Figure 1: 1D (defect) grating, field patterns for a (defect) frequency at the center of the bandgap, real (continuous) and imaginary parts (dashed); (a) full reflection for the grating without defect, (b) QNM associated with the defect structure, higher refractive index in the central layer, (c) field associated with the full transmission through the defect grating, variational approximation based on (a, b) (lines) and TMM reference (markers).*

**References**

[1] E.S.C. Ching, et al. Reviews of Modern Physics, Vol. 70, No. 4, pp.1545-1554, 1998.
[2] A. Settimi, et. al., Physical Review E,68: 026614111 , 2003.
[3] A. Sopaheluwakan. *Characterization and Simulation of Localized States in Optical Structures.* University of Twente, Enschede, The Netherlands, 2006. Ph.D. Thesis.
[4] E. van Groesen, J. Molenaar. *Continuum Modeling in the Physical Sciences,* SIAM publishers, March 2007.

# Optical Analysis of a Microcavity Laser with an Annular Bragg Reflector

Elena I. Smotrova[1], Alexander I. Nosich[1], Trevor M. Benson[2] and Phillip Sewell[2]
[1] *Institute of Radio-Physics and Electronics NASU, Kharkov 61085, Ukrain*e
*elena_smotrova@yahoo.com*

[2] *George Green Institute for Electromagnetics Research, University of Nottingham, NG7 2RD, UK*

Lasing spectra and thresholds of an annular Bragg reflector equipped with an active region are studied.

## Summary

Key elements of compact integrated circuits are microcavity lasers due to their small size and very low threshold operation. Ring and disk lasers utilize whispering-gallery (WG) modes that experience almost total internal reflection at the cavity rim. These modes operate under extremely low threshold pumping energy. Further reduction of microcavity size leads to the increasing of mode threshold as far as low-order lasing modes are non-WG modes. There are several ways to improve this situation. The first one is to collect small microdisks in a cyclic photonic molecule [1]. Due to the optical field interference we can achieve the thresholds lower than in a single cavity. However, this requires accurate tuning of the distance between the adjacent disks (for WG modes) or brining them together (for non-WG modes) [1, 2]. The second way is to imbed the microdisk into the annular Bragg reflector (ABR). ABRs have the advantage of in-plane radial optical confinement [3]. Here we present the 2D optical analysis of microdisk surrounded with ABR (Fig. 1). In this paper we will focus on the $H_z$ polarized modes. Our study is based on the Lasing eigenvalue problem (LEP) [4], which enables one to find not only the lasing frequencies but the thresholds as well. LEP statement implies that the field function satisfies Helmholtz equation with a complex–valued parameter $\nu^2 : \nu = \alpha_{eff} - i\gamma, \quad \gamma > 0$ inside the cavity or $\nu = 1$ otherwise, transparent boundary conditions and Sommerfeld radiation condition. Here, $\gamma$ is a threshold value of material gain needed to force the mode lasing. Hence, our eigenparameters are pairs of real values: lasing wavelengths $\lambda_n$ and thresholds $\gamma_n$. For the circular cavities, one can use the separation of variables to convert the boundary-value problem to matrix equations. Corresponding determinantal equations are solved numerically to quantify eigenfrequencies and thresholds.

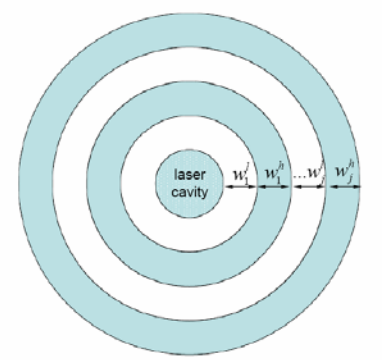

Fig. 1. Microdisk inside ABR in 2D

Numerical analysis shows that the lowest-mode thresholds are affected by two factors. The first is the distance from the cavity with an active region to the ABR and the second is the number of pairs of layers of lower and higher refractive indices in the ABR. We discuss how it is possible to optimize the configuration of the studied microlaser to achieve the lowering of the thresholds.

## References

[1] E.I. Smotrova et al, IEEE Photonics Technology Lett., **18**, 1993-1995, (2006).
[2] E.I. Smotrova et al, Optics Lett., **31**, 921-923, (2006).
[3] A. Jebali et al., J. Appl. Phys., **96**, 3043-3049 (2004).
[4] E.I. Smotrova et al, IEEE J. Selected Topics in Quantum Electronics, **11**, 1135-1142, (2005).

# Maximizing the Optical Band Gap in 2D Photonic Crystals

Kristian Hougaard and Ole Sigmund
*MEK•DTU, Department of Mechanical Engineering, NanoDTU, Technical University of Denmark, DK-2800 Kgs Lyngby, Denmark*
kh@mek.dtu.dk

Topology optimization is used to find the 2D photonic crystal designs with the largest relative photonic band gaps. Starting points for the topology optimization are found with an exhaustive binary search on a low resolution grid.

## Summary

We find the 2D photonic crystal designs showing the largest photonic band gaps obtainable. TM, TE and complete band gaps are investigated, and two kind of structures are considered: Structures in a square lattice, with 45 degrees symmetry and structures in a triangular lattice with 30 degrees symmetry.

We use a topology optimization code, implemented in Comsol Multiphysics, to find the optimal structures, and this method is described in detail. The optimization algorithm uses repeated finite element analysis of the eigenvalue problem on a domain with Bloch periodic boundary conditions combined with a sensitivity analysis of the solutions. The starting point for the topology optimization needs to be chosen carefully, because of the existence of many local minima. The initial structures are found using an exhaustive search on a low resolution grid where all pixels in the design space can be either material (silica) or air.

After the exhaustive search, the structures resulting in the largest band gaps are used as starting points for the topology optimization code. An example of an optimized structure found with our topology optimization code is shown in Fig. 2. The final structure is the structure with the largest band gap between the $5^{th}$ and $6^{th}$ band, and is an example of a structure which could not have been designed without an optimization tool. Based on our findings we formulate a general theory for the geometries of optimal band gap structures.

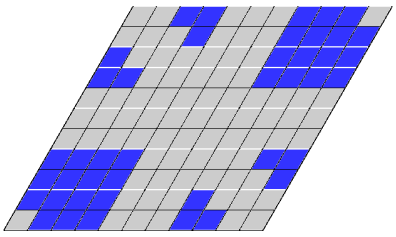

*Figure 1: Cell structure, found in the initial search, which have a TE band gap between the $5^{th}$ and the $6^{th}$ band.*

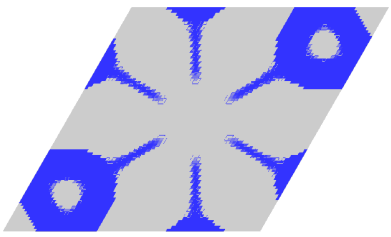

*Figure 2: Optimized cell structure found with the topology optimization code, where the structure in Figure 1 was used as starting point.*

## References

[1] J.D. Joannopoulos, *Photonic Crystals – Molding the flow of light,* University Press, (1995).
[2] M. P. Bensøe and O. Sigmund, *Topology Optimization, Thery, Methods and Applications*, Springer Verlag (2002).

# Self-consistent FDTD Maxwell-Bloch solver

Torben R. Nielsen, Simon Ejsing, Andrei V. Lavrinenko and Jesper Mørk
*COM•DTU, Department of Communications, Optics and Materials, Technical University of Denmark,*
*DK-2800 Kgs Lyngby, Denmark*
trn@com.dtu.dk

We report on the development of a general semi-classical description of the light-matter interaction by combining the finite-difference-time-domain (FDTD) and the density matrix methods. Pulse propagation in a quantum dot (QD) semiconductor waveguide is numerically investigated.

## Summary

In waveguide geometries the group velocity of an optical signal is modified by waveguide and material dispersion. Quantum dots (QDs) embedded in a photonic crystals (PC) membrane waveguide is one possible candidate for achieving such dispersion engineering. Optical buffering by slow light (SL) based solely on material dispersion such as electromagnetically induced transparency has attracted much attention lately [1]. We present here a one-dimensional fully self-consistent finite-difference-time-domain (FDTD) model for pulse propagation in a SL QD medium, treating the electromagnetic fields and the microscopic polarization on an equal footing.

We consider a one-dimensional QD waveguide geometry where the electrical field is propagated along the waveguide ($z$) axis according to

$$\frac{\partial}{\partial t}E_x = -\frac{1}{\varepsilon_b}\frac{\partial}{\partial z}H_y - \frac{1}{\varepsilon_b}\frac{\partial}{\partial t}P_x\{E_x\} \cdot \qquad (1)$$

The macroscopic polarization is given by $\boldsymbol{P} = \Sigma\, \boldsymbol{\mu}_{ij}\, \rho_{ij}$ where $\boldsymbol{\mu}_{ij}$ are the microscopic dipole moments and $\rho_{ij}$ are the elements of the density matrix which are propagated in time accordingly to the Liouville equation. The light-matter interaction is treated within the dipole approximation. When implemented on a FDTD grid the Liouville equation is solved at every grid point. Together with Amperes law for propagating the magnetic field strength, we solve numerically the set of equations without any further approximations. The numerical method is similar to that of Ref. [2].

In this paper, we examine a slow light configuration which is excited in the cascade arrangement [1], i.e. the probe beam is resonant with the QD electron-hole ground state transition, while a strong (control) beam is applied between the QD electron ground state and a third excited electron state. We study the influence of probe-pulse width and dephasing using realistic parameters for semiconductor structures. Slow-down is observed for picosecond pulses with a group velocity corresponding to the analytic results of Ref. [1]. Shorter pulses are strongly distorted and depending on parameters one may observe broadening or break-up of the pulse (see Fig. 1).

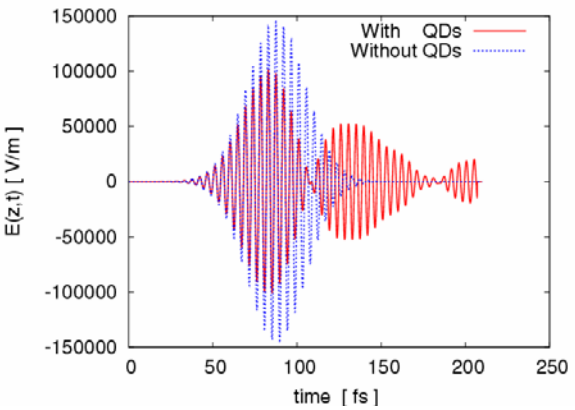


**Figure 1:** Probe field monitored at exit of waveguide (short pulses). Without (blue) and with embedded QDs (red) in the waveguide.

## References

[1] C. J. Chang-Hasnain et al., ”Variable Optical Buffers Using Slow Light in Semiconductor Nanostructures”, Proc. IEEE, **9**, 1884 (2003)

[2] R. W. Ziolkowski et al., “Ultrafast pulse interaction with two-level atoms”, Phys. Rev. A, **53**, 3082 (1995)

# Modeling Waveguides with Hole Arrays by Operator Marching and Robin-to-Dirichlet Maps

Lijun Yuan and Ya Yan Lu

*Department of Mathematics, City University of Hong Kong*
*Kowloon, Hong Kong*

A numerical method is developed for 2D slab waveguide structures with hole arrays in the core. The method relies on marching a pair of operators using Robin-to-Dirichlet maps of the segments containing holes.

**Summary**

Waveguide structures with large longitudinal variations are important in many applications [1]. Numerical methods are needed to analyze and design these structures. Many of these structures contain segments that are invariant in the longitudinal direction. For such a piecewise uniform structure, a number of efficient numerical methods have been developed. The most widely used methods rely on separation of variables and eigenfunction expansions in each uniform segment. The bidirectional beam propagation methods apply operator rational approximation techniques for fast marching of the forward and backward wave field components in each uniform segment. The recently developed Dirichlet-to-Neumann (DtN) map method [2] uses a highly accurate Chebyshev collocation scheme to discretize the longitudinal variable $z$ in the computation of the DtN map of a uniform segment. These methods take advantage of the special geometric feature of the structure and they are more efficient than general purpose methods such as the finite-difference time-domain method.

If the structure is not piecewise uniform in the longitudinal direction, such as the slab with holes studied in [1], we typically approximate it numerically by a structure with many small uniform segments. Clearly, this is not an efficient process, since the crude "staircase" approximation to curved dielectric interfaces gives rise to large errors unless the length of the segments (in the $z$ direction) is sufficiently small. In this paper, we develop a numerical method for two-dimensional slab waveguide structures with hole arrays. More specifically, starting from a straight slab waveguide, we create a $z$-varying waveguide structure by inserting a finite array of holes in the waveguide core. The structure can be divided into a finite number of non-uniform segments each containing exactly one hole in the core. Let the segments be separated by $z_0$, $z_1$, ..., $z_m$. The problem is to find the transmitted and reflected fields for an incident field given in $z < z_0$. As in [2] and [3], the problem can be solved if we are able to calculate two operators $Q_0$ and $Y_0$ satisfying $Q_0\, u(\cdot, z_0) = \partial_z u(\cdot, z_0)$ and $Y_0\, u(\cdot, z_0) = u(\cdot, z_m)$, where $u$ is the $y$-component of the electric or magnetic fields depending on the polarization. Similarly, we can define operators $Q_j$ and $Y_j$ at $z_j$. In turns out that $Q_m$ is known from the radiation condition for $z \geq z_m$ and $Y_m$ is the identity operator. In [2], we have used the DtN map $M$ of the segment $(z_{j-1}, z_j)$ to find the operators $Q_{j-1}$ and $Y_{j-1}$ assuming that $Q_j$ and $Y_j$ are given. The operator $M$ for a uniform segment is obtained by a Chebyshev collocation scheme for discretizing $z$. In this paper, we first develop marching formulas for $Q_{j-1}$ and $Y_{j-1}$ using the Robin-to-Dirichlet (RtD) map which seems to be more robust than the DtN map. Next, we develop an efficient method for computing the RtD map for non-uniform segments containing holes in the waveguide core. Numerical examples are used to illustrate the efficiency and accuracy of the new method.

## References

[1] J. S. Foresi, P. R. Villeneuve, et al., Nature, **390**, 143-145 (1997).
[2] L. Yuan and Y. Y. Lu, IEEE Photonic Technology Letters, **18**, 1967-1969 (2006).
[3] Y. Huang and Y. Y. Lu, Journal of Lightwave Technology, **24**, 3448-3453 (2006).

# Whispering-Gallery-Mode Resonances in Discrete Luneburg Lenses

Alexander I. Nosich [1] and Sebastien Rondineau [2]
[1] *IRE NASU, Kharkiv 61085, Ukraine,* [2] *University of Colorado, Boulder, CO 80309, USA*

*anosich@yahoo.com*

An accurate mathematical and numerical analysis of a discrete spherical Luneburg lens fed by elementary dipoles is fully presented.

## Summary

Luneburg introduced the lens named after him as a dielectric sphere with a varying refractive index $n=[2-(r/r_{\max})^2]^{1/2}$. More practical are discrete lenses (DLLs) first introduced into microwave antenna technology in the late 1950's. The spherical symmetry of the lens offers a rare opportunity to solve analytically the wave scattering problems by reducing them to the Mie series – see, e.g., [1] for a DLL fed by a Huygens source and [2] for numerical optimization study.

No surprise that today dielectric lenses are the key components of all infrared and terahertz systems and normally are integrated with tiny printed feeds. However accurate modeling of such combined structures is a challenging task. GO/PO approaches fail to reproduce the field features associated with wavelength-size printed elements. Conventional MoM codes can hit "numerical wall" if applied to a 20-λ DLL with a printed feed. Such a structure should display a complicated interplay of both ray-like *and* mode-resonance phenomena.

We have developed a powerful full-wave tool for a DLL integrated with a conformal printed feed. We demonstrate that this is possible provided that one uses the concept of analytical regularization, or analytical preconditioning, and reduces the scattering problem to a Fredholm second kind matrix equation [3]. Numerical solution of 20-λ and greater integrated DLL takes seconds of a desktop computer time, and accuracy is well-controlled and can be refined.

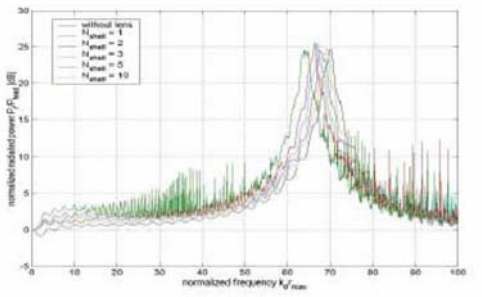


*Fig. 1. Normalized radiated power for DLLs with N shells fed by a printed feed excited by a slot as a function of normalized frequency, $k_0 r_{\max}$.*

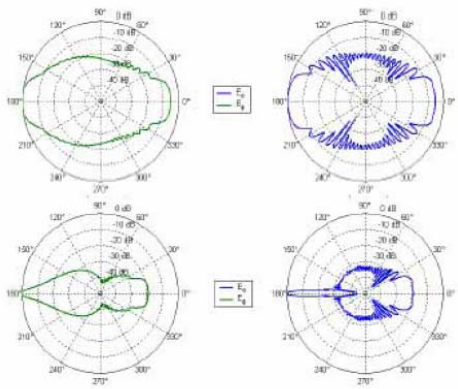

*Fig.2. Far field patterns for DLL in broad resonances in Fig.1. $N=0$ (no lens), $k_0 r_{ext}=70.15$ for the top row, $N=10, k_0 r_{ext}=69.43$ for the bottom one. The E(H)-plane is on the left (right) side.*

An accurate mathematical and numerical analysis of both dipole-fed and disk-fed DLL is presented. The problem is cast into a coupled set of dual-series equations for the field expansion coefficients, and then to an infinite-matrix equation having favorable features. Analytical regularization is based here on the explicit inversion of the static part of the full-wave equations. Such a procedure leads to the guaranteed convergence and controlled accuracy of computations. Because of its semi-analytical nature, the implemented algorithm is accurate and very economic in both CPU time and memory requirements.

We demonstrate that the smaller the number of layers in DLL, the greater the effect of the whispering-gallery mode resonances (Fig. 1). These resonances spoil the lens-caused collimating of the dipole or printed-feed radiation because their far fields display many sidelobes of equal intensity (Fig. 2). Therefore double-shell spherical lenses may display a degraded performance at certain wavelengths.

## References

[1] H. Mieras, IEEE Trans. Antennas Propagat. **30**, 1221-1224 (1982).
[2] H. Mosallaei, Y. Rahmat-Samii, IEEE Trans. Antennas Propagat. **49**, 60-69 (2001).
[3] A.I. Nosich, IEEE Antennas Propagat. Magazine. **42**, 34-49 (1999).

# Dependences of Lasing Thresholds for a Layered Structure on the QW Width

Volodymyr O. Byelobrov, Alexander I. Nosich

volodia.byelobrov@gmail.com
*Institute of Radiophysics and Electronics NASU, ul. Proskury 12, Kharkiv 61085, Ukraine*

Optical modes and linear thresholds of lasing for a quantum well (QW) sandwiched between two distributed Bragg reflectors (DBRs) are investigated as a specific eigenvalue problem with "active" imaginary part of the QW refractive index.

## Summary

QWs embedded in epitaxially grown semiconductor microcavities are widely used in photonics [1,2]. We consider a layered structure consisting of the cavity whose width is $w_c$, sandwiched between two DBRs. Inside the cavity, shifted by the distance $b$ from its middle line, sits a QW (or active layer) of the width $w_a$ (Fig. 1). Therefore we model the active layer by a refractive index with a complex value, $\nu = \alpha_c - i\gamma$, while adjacent layers have the same real values of this index, $\alpha_c$. For this structure we introduce a lasing eigenvalue problem (LEP) [3,4] and reduce it to the following equation

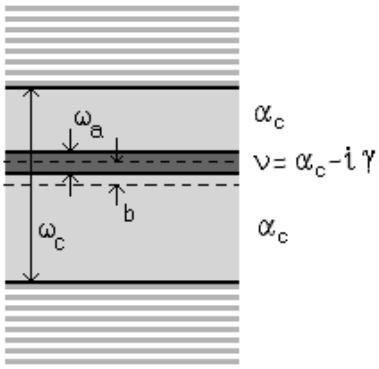


Figure 1. Sketch of layered structure

$$e^{-i2\kappa(\alpha_c - i\gamma)(w_a/w_c)} = R_1 R_2, \qquad R_{1,2} = \frac{R_{B,T} e^{i\kappa\alpha_c[1\pm(2b\mp w_a)/w_c]} + R_a}{1 + e^{i\kappa\alpha_c[1\pm(2b\mp w_a)/w_c]} R_{B,T} R_a}, \quad R_a = \frac{i\gamma}{2\alpha - i\gamma},$$

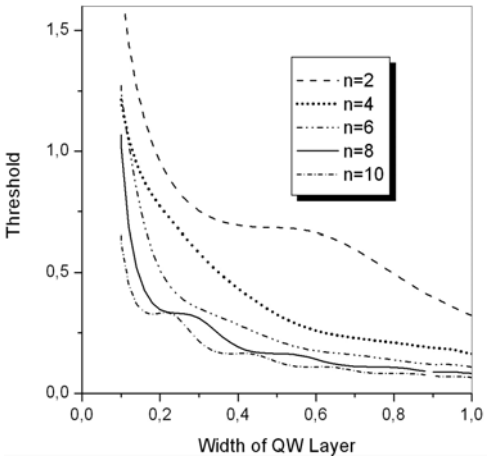


Figure 2. Dependences of thresholds on the relative width of QW in a GaAs cavity suspended in air. $b$=0, $n$ is modal index.

where $R_{B,T}$ are reflectivities of the bottom and top DBRs, respectively. We computed the thresholds by iterations, starting from this value for the QW occupying entire cavity and using a two-parameter Newton method. The results given in Fig. 2 show that the thresholds grow up if the relative width of active layer shrinks. We present here only thresholds for the even modes of the GaAs cavity with a QW in the middle however the behavior of the odd modes is the generally similar. Unlike thresholds, the lasing wavelengths are very stable with respect to the QW width. This is because they are determined mainly by the width of the cavity.

We discuss how placing the cavity equipped with QW between two DBRs effects the lasing wavelengths and thresholds. We also estimate the fractions of modal power leaking into the top and bottom media through the DBRs as a function of the layer pairs in reflectors.

## References

[1] G. M. Yang, et al., J. Appl. Phys., **78,** 3605-3609 (1995).
[2] X. H. Zhang, et al., Appl. Phys. Lett., **88,** 191111 (2006)
[3] E.I. Smotrova, A.I. Nosich, Optics and Quantum Electronics, **36**, 213-221 (2004).
[4] E. I. Smotrova , et al., IEEE J Selected Topics in Quantum Electronics, **11,** 1135-1142 (2005)

# Validation of FDTD-2D for high-*Q* resonances description

Artem V. Boriskin, Svetlana V. Boriskina, Anthony Rolland, Ronan Sauleau, Alexander I. Nosich

[1] *Institute of Radiophysics and Electronics NASU, ul. Proskury 12, Kharkiv 61085, Ukraine.*
*a_boriskin@yahoo.com*

[2] *IETR, University of Rennes 1, Campus de Beaulieu, bat 11D, 35042 Rennes Cedex, France*

[3] *Kharkiv National University, Svobody Sqr. 4, Kharkiv 61077, Ukraine.*

The validation of the FDTD-2D algorithm accuracy for the description of the WGM resonances in circular dielectric resonators is considered. The Mie-type series solution is used as a reference. A loss of accuracy near to high-*Q* resonances is demonstrated for the near- and far-field characteristics.

## Summary

FDTD is a powerful method widely applied for the analysis of a wide range of electromagnetic problems [1]. It has gained popularity thanks to simplicity of implementation of numerical algorithms, which are flexible to scatterer geometries and capable of providing informative and reasonably accurate results. The main well-known drawback of the FDTD-3D versions is extremely heavy requirements to computer resources especially in the open-domain and resonance problems. Another drawback, which can easily spoil the analysis of fine resonance effects, is a loss of accuracy near to natural frequencies of studied objects [2]. This drawback often escapes attention although it is intrinsic for any 2-D and 3-D version of FDTD and can become a bottleneck in the analysis of small-size dielectric lenses or resonators. This is because in the electromagnetic and optical behavior of such scatterers internal resonances play dominant role - see, e.g.,[3-4]

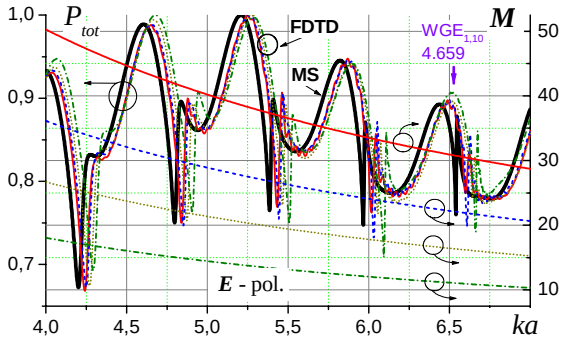


Fig. 1. Normalized far-field characteristics of the line current source illuminating a quartz ($\varepsilon = 4.0$) circular cylinder computed by FDTD and MS, respectively. A family of four curves for FDTD is for different mesh sizes. Mesh size parameter values for each curve are represented by lines of corresponding types associated with the right axis. The mesh size at any frequency point can be estimated as $\lambda_0/M$.

Unfortunately, there are very few papers focused on the validation of the FDTD codes as to reliable characterization of resonance phenomena in dielectric scatterers. As FDTD does not have any in-built criterion of accuracy, it can only be estimated via comparison with more advanced methods providing controllable precision, e.g. Mie-type (MS) series for the circular cylindrical resonator.

The aim of the paper is to assess the accuracy of a standard FDTD-based numerical algorithm in the analysis of the near and far fields of dielectric cylinders. To achieve the goal, we consider circular dielectric resonators excited by the line current sources and demonstrate the failure of FDTD algorithm to characterize high-*Q* whispering-gallery-mode (WGM) resonances. We do this by comparison with the exact Mie-series solutions. The near-field and far-field characteristics are studied for resonators of various sizes, made of quartz and silicon. Both the *E*- and the *H*-polarizations are considered. The computational error, i.e. a resonance frequency shift observed for the FDTD solution, is analyzed and compared for several WGMs having different *Q*-factors.

## References

[1] K.L. Shlager, J.B. Schneider, *IEEE Antennas Propagation Magazine*, **37**(4), 39-57 (1995).
[2] G.L. Hower, R.G. Olsen, *et al.*, *IEEE Trans. Antennas Propag.*, **41**(7), 982-986 (1993).
[3] S.V. Boriskina, T.M. Benson, *et al.*, *J. Optical Soc. America A*, **21**(3), 393-402 (2004).
[4] A.V. Boriskin, S.V. Boriskina, *et al.*, *Microwave Optical Techn. Letters*, **43**(6), 515-158 (2004).

# Benchmark on a slit-groove diffraction problem

M. Besbes and P. Lalanne
*Laboratoire Charles Fabry de l'Institut d'Optique, CNRS, Univ Paris-Sud, Campus Polytechnique, RD 128, 91127 Palaiseau, France.*

Because Maxwell's equations for linear materials are exact, computation plays a crucial role in the analysis of light scattering by subwavelength structures in metallo-dielectric structures. In this work, we benchmark several fully-vectorial methods on a basic scattering problem governing the physics of the electromagnetic interaction between subwavelength apertures on a metal film. The two-dimensional geometry under study is depicted in Fig. 1. It is composed of a groove and of a slit etched both into a silver film on a glass substrate. The center-to-center distance between the slit and the groove is denoted by *d* in the following. The other parameters like the silver dielectric constant, the metallic film thickness are given in the caption. Several reasons have motivated the choice of the specific geometry depicted in Fig. 1, like for instance the availability of experimental data [Gay et al., Nature Phys. **2**, 262 (2006)], the related embodiment of a variety of physical leading to an oscillatory behaviour of the transmitted power as a function of *d*, the existence of a discrepancy between numerical predictions and experimental data [Lalanne & Hugonin, Nature Phys. **2**, 551 (2006)] providing different interpretations for the mechanisms responsible for the interaction at the metallo-dielectric interface, and another discrepancy between purely numerical data obtained with Finite-Difference Time Domain (FDTD) and modal methods. Our objective is thus to lift off these discrepancies and to provide an overview of the present state-of-art in the field of computational plasmonics.

Several groups in European countries and in the United States have been contacted to participate to the benchmark. Most of them have positively responded and have been able to provide numerical data in a short 45-day lap of time. The results provided as a poster at the conference will show computational results obtained with 11 numerical methods, belonging to four very different categories : Finite Element Methods (Besbes et al., Pereira et al.), FDTD (Kozacki, Baida et al., Sukharev et al.), modal methods including a-FMM (Hugonin et al., Granet et al., Pereira et al., CAMFR (Bienstman) , MOL (Helfert), and Volume Integral Methods (Pereira et al.).

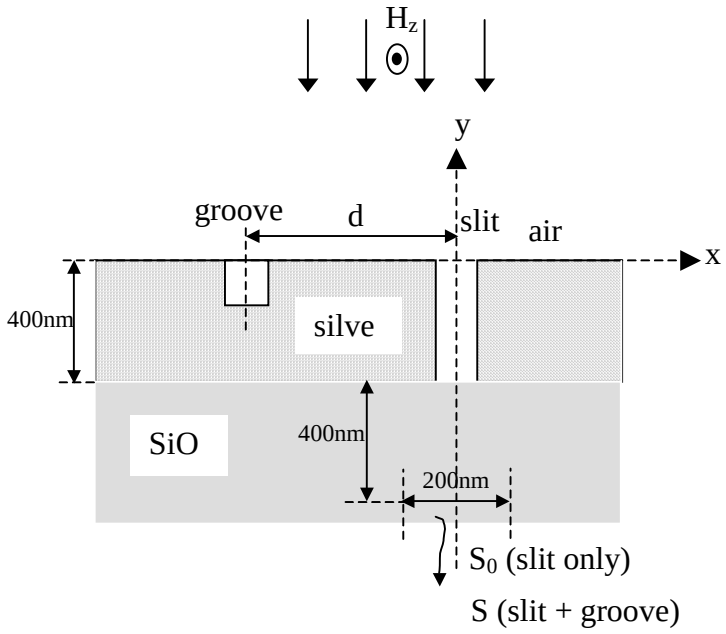


Figure 1. Slit-groove doublet considered in this work. The center-to-center slit-groove separation distance is denoted by *d*. All computations have been performed for $\varepsilon_{Ag}$ = -33.22+1.1700i, a value as close as possible of the silver permittivity used in the experiment, for an illumination with a plane wave normally incident from air (n = 1) at $\lambda$ = 852 nm, for groove and slit widths of 100 nm and for a groove depth of 100 nm. The metallic film deposited onto a semi-infinite glass (n = 1.48) substrate in (a) is 400-nm thick.

# Numerical Simulations of New Compact Acousto-Optic Tunable Filters Based on Multi-Reflector Technology

Andrei Tsarev, Eugeny Kolosovsky and Rinat Taziev

*Laboratory of Optical Materials and Structures*
*Institute of Semiconductor Physics, Siberian Branch of Russian Academy of Science*
*Prospect Lavrenteva, 13, Novosibirsk, 630090, Russia*
*tsarev@isp.nsc.ru*

*The new compact noncollinear acousto-optic tunable filter based on multi-reflector beam expanders has been studied by FDTD method and under spectral approximation for the case of chalcogenide $As_2S_3$ glass waveguide on $LiNbO_3$ substrate. Multiple computer experiments demonstrate the device proof-of-concept.*

## Summary

This paper present result of numerical simulations of noncollinear acousto-optic tunable filters (AOTF) based on multi-reflector (MR) beam expanders [1]. Studding of compact MR-AOTF is performed by finite difference time domain (FDTD) method that demonstrates the device proof-of-concept. Large devices with practically need parameters utilizing the high dense ITU grid (25 GHz and smaller) are examined under spectral approximation. To fasten simulations 3D structure has been replaced by 2D analogy using the effective index method (EIM) that decomposes 3D strip waveguide into two 2D slab waveguides.

By this approach, we examine MR-AOTF by means of 2D FDTD method by software tool FullWAVE from RSoft Design Group, Inc. [2]. Typical results of simulation of the device that contains two beam expanders with 32 partial reflectors and AO grating are presented in Fig.1. Effect of phase grating induced by SAW is examined by static grating of refractive index with period around $L$ = 1.2 μm, and aperture $L$ = 50 μm. Parameters of waveguide structure basically correspond to the case of chalcogenide $As_2S_3$ glass on $LiNbO_3$ substrate.

**Acknowledgments.** We would like to thank Company RSoft Design Group, Inc. that provides the FDTD software [2]. This work has been supported by Grant No 05-02-08118-ofi-a from Russian Foundation for Basic Research.

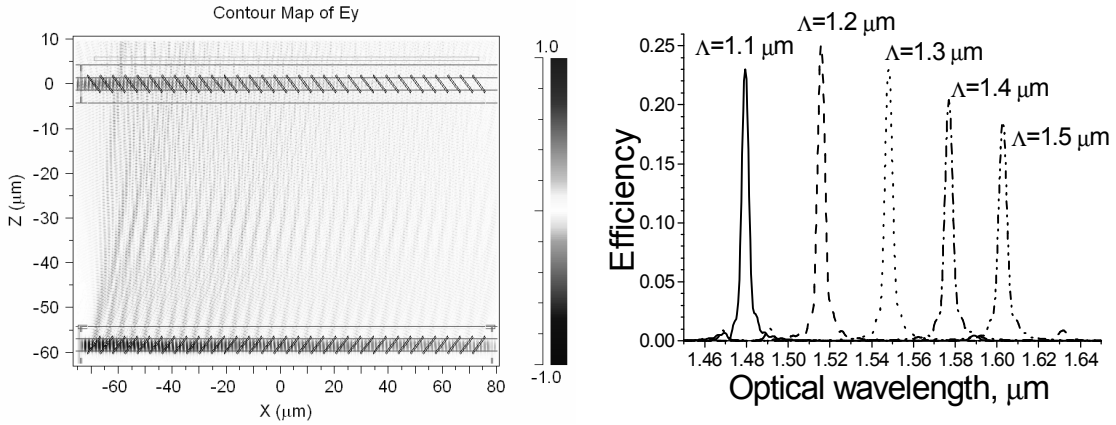


Fig. 1. Optical field propagation (a) and frequency response (b) of AO tunable filter formed by two multi-reflector beam expanders with 32 partial reflectors. FDTD simulation.

## References

[1] A.V. Tsarev, Beam-expanding device, USA Patent No. 6,836,601, Dec. 28, 2004.
[2] www.rsoftdesign.com.

# 3D Modelling of Microdisk Resonators Based on Fourier Modal Method

Andrea Armaroli,[1,2] Alain Morand,[1] Pierre Benech,[1] Gaetano Bellanca,[2] and Stefano Trillo[2]

[1] *IMEP, Institut de Microélectronique, Electromagnétisme et Photonique, UMR 5130, INPG-UJF-CNRS, 3, parvis Louis Neel, BP 257, 38016, Grenoble Cedex 1, France*

[2] *ENDIF, Engineering Department, University of Ferrara, via Saragat 1, blocco A, 44100, Ferrara, Italy*

andrea.armaroli@unife.it

We implemented a numerical tool for the 3D modelling of dielectric microdisk cavities. Based on the Fourier expansion of dielectric permittivity and fields along the axial direction, it allows to compute resonant wavelengths, quality factors, and field distributions.

## Summary

Microresonators are among the most interesting devices for next-generation photonic circuits and their modelling is a crucial and challenging task. Finite Difference Time Domain (FDTD) is computationally demanding, while approximated but somehow coarse approaches are also available (e.g. based on Effective Index or Film Mode Matching) [1].

An accurate and fast analysis of resonant modes of cylindrical microcavities can be faced by decomposing the structure in homogeneous layers along the radial direction and describing the field in each of them by means of a modal expansion. We find that a proper description of radiation and evanescent part of the spectrum is crucial in order to estimate properly the quality factor of high performance microresonators.

Rigorous Coupled Wave Analysis (RCWA), also known as Fourier Modal Method, computes the modes of the real structure as Bloch modes of a periodic one. This approximation can be improved by implementing suitable boundary conditions [2].

The resulting approach is quite straightforward: we use a common harmonic basis instead of physical modes and matrix multiplications instead of overlap integrals, otherwise needed.

We developed interface conditions, considering the different coordinate system and propagation basis (expressed by Bessel-Hankel functions), and, in free oscillation regime, obtained a homogeneous problem with complex solutions giving access to the resonant wavelengths of the structure.

We show an example of resonant mode computed by means of our algorithm in figure 1.

Our method is quite promising and, to the best of our knowledge, constitutes a novel approach to the description of such cutting-edge devices. We believe that the performances of the method can be further improved by overcoming the present limitations on the convergence.

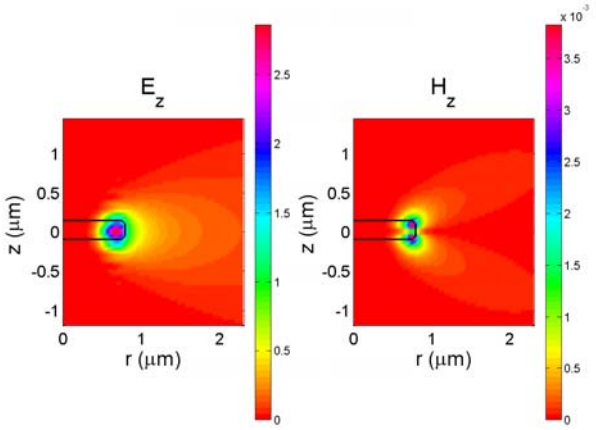


Figure 1: Cross section view of a TM resonant mode of a 1.54μm diameter disk in SOI technology.

This work was partially supported by the Marie Curie Early Stage Research Training Project 504195 EDITH.

## References

[1] T. M. Benson et al., in *Frontiers in Planar Lightwave Circuit Technology: Design, Simulation and Fabrication*, (S. Janz, J. Čtyroký, and S. Tanez eds.), Springer 2006.

[2] J.P. Hugonin and P.Lalanne, JOSA A 22 (9), 1844-1849 (2005).

# Simple Approximate Method for Chromatic Dispersion Estimation of Singlemode Optical Fiber with an Arbitrary Coaxial Refractive Index Profile

Vladimir A. Burdin[1,2] and Anton V. Bourdine[1,2]
[1]*Department of Communication Lines, Povolzhskaya State Academy of Telecommunications and Informatics (PSATI), 67, Moscow Av., Samara, Russia;*
burdin@psati.ru

[2]*Research & Development Co. "CommunicationAutomationMounting" Ltd. (R&D Co."CAM" Ltd.), 76, Mitchurin Str, 443110, Samara, Russia*
bourdine@samara.ru

Simple method for estimation of chromatic dispersion slope for weakly guiding singlemode optical fiber with an arbitrary coaxial refraction index profile is described.

## Summary

We propose an approximate method for the chromatic dispersion calculation of the weakly guiding singlemode optical fibers with an arbitrary coaxial refraction index profile. Chromatic dispersion parameter D is determined by the second derivation of propagation constant β [1,2], which can be evaluated by the waveguide parameter U [1,2]. Core refraction index and it's derivation are estimated from Sellmeier equation [2]. It is proposed to determine parameter U as a results of method of small normalized frequency approach and modified Gaussian approximation [3,4]. To estimate an accuracy of proposed method, two samples of $GeO_2$ doped fibers [5] were considered. Comparison results of calculation and measured dispersion slopes, mentioned in sample specifications [5], are shown on Fig. 1. The difference between theoretical and measured results is about 1…6 ps/(nm·km). Accuracy is not so good, however it is acceptable for coarse estimation.

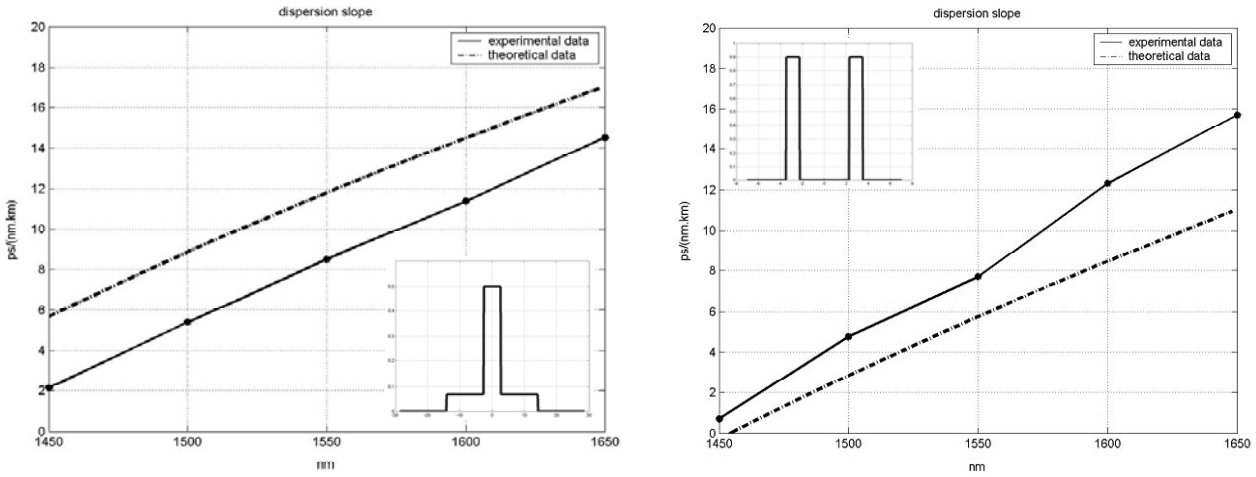


**Figure 1.** Dispersion slopes of fiber samples.

## References

[1] A. Snyder, J. Love. *Optical Waveguide Theory* (Moscow, Radio i Svyaz, 1987).
[2] K. Okamoto. *Fundamentals of Optical Waveguides* (Academic Press, San Diego, 2000).
[3] V. Burdin. *Fundamentals of Piecewise Regular Fiber Optic Transmission Lines Modeling* (Radio i Svyaz, Moscow, 2002).
[4] V. Burdin, R. Andreev, D. Praporshchikov, Proc. SPIE, **5485** (2005).
[5] S. Matsuo and S. Tanigava, Patent RU 2 216 029 (2003).

# Method for High Order Mode Chromatic Dispersion Estimation

Vladimir A. Burdin[1,2] and Anton V. Bourdine[1,2]
[1]*Department of Communication Lines, Povolzhskaya State Academy of Telecommunications and Informatics (PSATI), 67, Moscow Av., Samara, Russia;*
burdin@psati.ru

[2]*Research & Development Co. "CommunicationAutomationMounting" Ltd. (R&D Co."CAM" Ltd.), 76, Mitchurin Str, 443110, Samara, Russia*
bourdine@samara.ru

Approximate method for high order guided mode chromatic dispersion estimation in weakly guiding single-cladding optical fibers with an arbitrary graded refractive index profile is represented.

## Summary

We present an approximate method for chromatic dispersion estimation of arbitrary order guided modes, propagating along the core of the weakly guiding single-cladding optical fiber with an arbitrary refractive index profile. It is offered to evaluate chromatic dispersion parameter D, ps/(nm·km), by the well-known formula of first and second derivatives of the propagation constant β [1], which is expressed by core mode parameter U [2]. Proposed method is based on extension of modified Gaussian approximation [3]. Here core region refractive index is represented as the set of N claddings in which the refractive index can be taken as a constant. This representation allows to write variational expression for the core mode parameter U, characteristic equation of the equivalent normalized mode field radius $R_0$ , and their derivatives in the form of finite nested sums. Some results of dispersion curve calculation, been obtained for optical fiber with ideal profiles by proposed method and exact solution, are shown on Fig. 1. In all cases, a good accuracy is noticed.

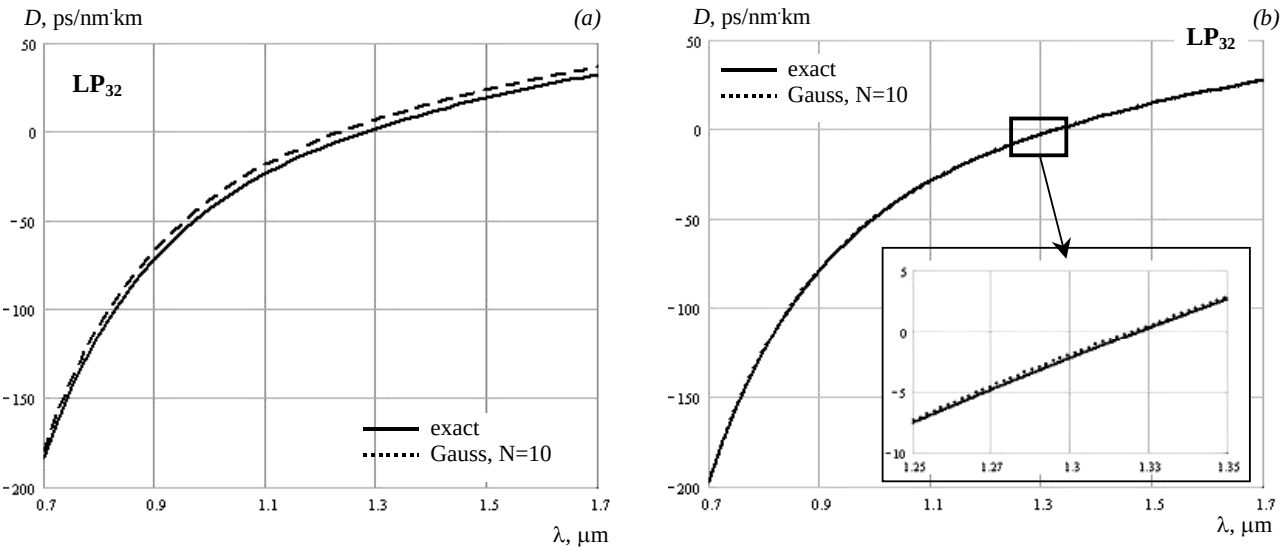


**Figure 1.** Chromatic dispersion curves of guided mode $LP_{32}$: (a) step index fiber 50/125; (b) graded fiber 50/125 with ideal non-limited parabolic index profile

## References

[1] K. Okamoto, *Fundamentals of Optical Waveguides* (Academic Press, San Diego, 2000).
[2] A. Snyder and J. Love, *Optical Waveguide Theory* (Moscow, Radio i Svyaz, 1987).
[3] A.V. Bourdine, Computer Optics, **26**, 7-15 (2004).

# Optical Fiber Polarization Elements based on Long-Period-Gratings in Photonic Crystal Fibers

Dimitrios C. Zografopoulos, Emmanouil E. Kriezis, and Theodoros D. Tsiboukis
*Department of Electrical and Computer Engineering, Aristotle University of Thessaloniki, Thessaloniki GR-54124, Greece*
dzogra@auth.gr, mkriezis@auth.gr, tsibukis@auth.gr

The polarization properties of long-period-gratings written in birefringent photonic crystal fibers are theoretically investigated. Thermal tuning is assessed and preliminary results suggest ample tuning of the resonant wavelengths.

## Summary

Long-period-gratings (LPGs) inscribed in conventional optical fibers have found many interesting applications, such as in optical filtering, gain flattening, and sensing devices, or as fiber polarizing elements [1,2]. Photonic crystal fibers (PCFs) constitute a special class of optical fibers which has been under intense study in the last years, since their microstructure allows for the sophisticated tailoring of their properties. Moreover, tunable properties may also be achieved by infiltrating the cladding holes of a PCF with a material whose properties may be externally controlled. The properties of LPG-PCFs have been the subject of significant research as well, since the demonstration of the first gratings inscribed in PCFs [3].

In the present we analyze the polarization properties of LPG birefringent PCFs [4] by means of a multipole method [5]. Numerical studies show that the coupling between the fundamental birefringent guided mode (Fig. 1(a)) and the cladding modes, which is induced by the LPG, is highly polarization dependent. This leads to ample separation of the grating's Bragg resonances corresponding to the two polarization states. We further show that extensive thermal tuning of these resonances is possible by infiltrating the cladding holes with an isotropic fluid (Fig. 1(b)). Thus, such PCFs may find interesting applications as tunable wavelength selective polarization elements.

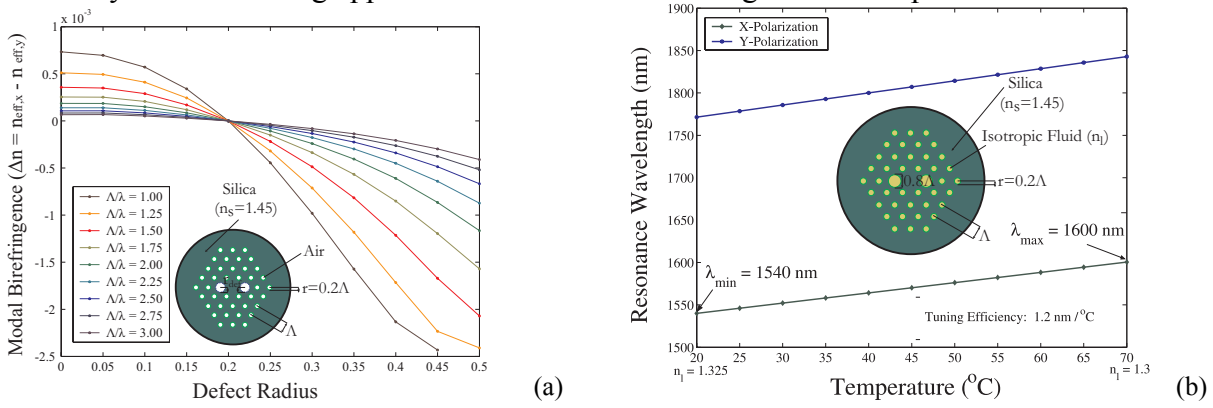


*Figure 1*: (a) Modal birefringence values for the fundamental guided mode of a PCF with an asymmetrical core, and (b) thermal tuning of the polarization-dependent resonance wavelengths of a LPG highly-birefringent PCF infiltrated with an isotropic fluid.

## References

[1] A.S. Kurkov, M. Douay, O. Duhem *et al.*, Elect. Lett. **33**, 616-617, 1997.
[2] B. Ortega, L. Dong, W.F. Liu *et al.*, IEEE Phot. Tech. Lett. **9**, 1370-1372, 1997.
[3] B.J. Eggleton, P.S. Westbrook, R.S. Windeler *et al.*, Opt. Lett. **24**, 1460-1462, 1999.
[4] M. Szpulak, J. Olszewski, T. Martynkien *et al.*, Opt. Commun. **239**, 91-97, 2004.
[5] T.P. White, B.T. Kuhlmey, R.C. McPhedran *et al.*, J. Opt. Soc. Am. B **19**, 2322-2330, 2002.

*This work was supported by the Greek General Secretariat of Research & Technology (PENED03/Grant: 03ED936).*

# Theoretical Analysis of Square Surface Plasmon Polariton Waveguides

Jesper Jung, Thomas Søndergaard, and Sergey I. Bozhevolnyi
*Department of Physics and Nanotechnology, Aalborg University, Skjernvej 4A, DK-9220 Aalborg Øst, Denmark*

jung@physics.aau.dk

Utilizing the finite element method (FEM) the electromagnetic modes of square cross section metal waveguides are calculated at telecom wavelengths (~1550 nm). Unlike thin metal strip waveguides the square waveguide supports long-range surface plasmon polariton waves for both polarizations.

## Summary

A recently studied component with integrated optics in mind is the thin metal strip waveguide (t<<w - inset Fig. 1). This component offers waveguiding with strongly confined mode fields and propagation lengths in the millimeter range. A major drawback though is that long-range propagation is only supported for one orientation of the electric field. In this work we utilize the FEM for studying a square (t=w) surface plasmon polariton waveguide (SSPPW) with a gold core surrounded by a lossless dielectric polymer of benzocyclobutene (BCB). We will show that this waveguide is not polarization sensitive, and that long-range guiding is still possible. Long-range guiding was recently observed experimentally for both polarizations [1]. SSPPWs have also been studied theoretically to some extent utilizing the method of lines [2]. A presentation will be given of mode dispersion, propagation lengths, and field distributions including mode size for sub and supra wavelength SSPPWs. An example of the mode index vs core size is given in Fig. 1. For t=w=200nm the two degenerate modes $ss^0_{bx}$ and $ss^0_{by}$ have a propagation length of app. 2mm. The $ss^0_{bx}$ ($ss^0_{by}$) mode is polarized mainly along the *x*-axis (*y*-axis) (Fig. 2). These two SPP modes make long-range polarization-independent plasmonic signal transmission possible.

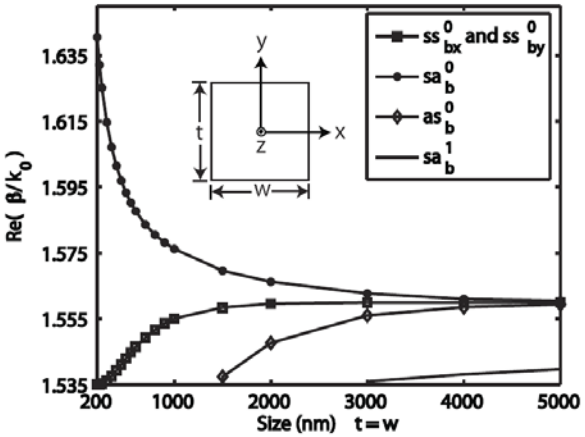


**Fig. 1:** Real part of mode index versus the size of the square gold core (λ=1550nm).

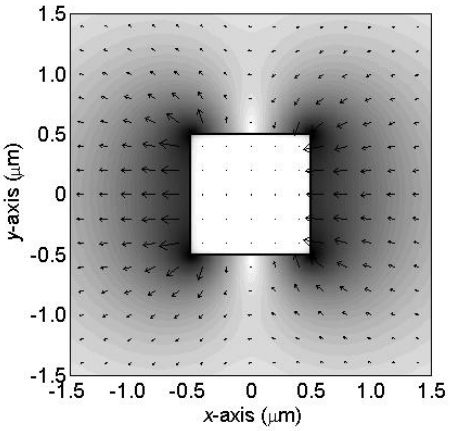


**Fig. 2:** Magnitude and orientation of electric field in the *xy*-plane ($ss^0_{bx}$).

## References

[1] K. Leosson et. al., Opt. Express **14**, 314-319 (2006).

[2] P. S. J. Berini, "Optical Waveguide Structures", US patent number 6,741,782, http://www.uspto.gov/, (2003).

# Finite-difference time-domain analysis of micro-lens integrated vertical-cavity surface-emitting lasers

Il-Sug Chung[1] and Yong Tak Lee[2]

[1] *COM•DTU, Department of Communications, Optics and Materials, Technical University of Denmark, DK-2800 Kgs Lyngby, Denmark*

isc@com.dtu.dk

[2] *Department of Information and Communications, Gwangju Institute of Science and Technology, Gwangju, 500-712, Republic of Korea*

Optical modes of vertical-cavity surface-emtting lasers with micro-lens monolithically integrated onto the top distributed Bragg reflector are analyzed by using finite-difference time-domain method.

## Summary

Micro-lens monolithically integrated with vertical-cavity surface-emitting lasers (VCSELs) reduces the beam divergence of output, leading to better coupling efficiency with optical fibers for regular optical fiber communications and providing collimated beams for free space optical interconnects. Recently-reported micro-lens integration technique has a few advantages over the conventional method [1]. In this method, a self-aligned micro-lens is formed onto the top distributed Bragg reflector (DBR) by using wet oxidation, as schematically shown in Figure 1.

In this report, we analyze the optical modes of VCSELs with micro-lens integrated onto the top DBR by using finite-difference time-domain (FDTD) method. Far-field pattern (Figure 2), the quality factor, and the threshold gain of the fundamental mode are investigated as a function of the radius of curvature of micro-lens. In addition, optimized thickness of the micro-lens layer is discussed considering the constructive interference condition at the outermost layer [2]. This outermost layer effect is often utilized for surface-relieved VCSELs to control the size of optical modes [3].

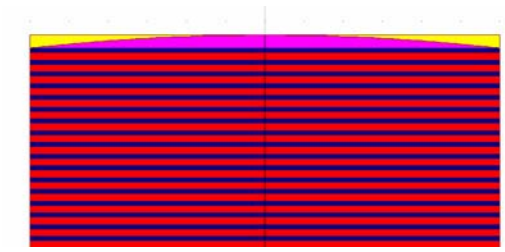

Figure 1: A micro-lens is formed onto the top DBR of a top-emission VCSEL.

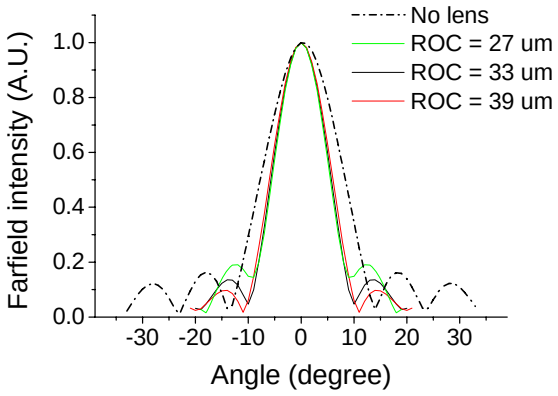


Figure 2: Far-field patterns of VCSELs with micro-lens of different radius of curvatures (ROCs).

## References

[1] K. S. Chang, *et al*., IEEE Photon. Tech. Lett., **18**, 2203-2205 (2006).
[2] I.-S. Chung, *et al*., J. Appl. Phys., **96**, 2423-2427 (2004).
[3] Å. Haglund, *et al*., IEEE Photon. Tech. Lett., **16**, 368-370 (2004).

# Domains tilt effects on the SHG process in PPLN crystals grown by the off-center Czochralski technique

F.M. Pigozzo[1], A.-D. Capobianco[1], N. Argiolas[2], M. Bazzan[2], C. Sada[2]
[1]*DEI Department, University of Padova, Via Gradenigo 6/b, 35131 Padova, Italy*
superg@ray.dei.unipd.it

[2]*Physics Department, University of Padova, Via Marzolo 8, 35131 Padova, Italy*

## Summary

Lithium niobate is a well-known ferroelectric material widely exploited in the field of nonlinear optics. The realization of engineered domain structures in a single crystal, in fact, has opened the way to many applications of scientific and technological interest such as second harmonic based laser sources. In particular the periodic modulation of the non linear optical coefficients, achieved in Periodically Poled Lithium Niobate (PPLN) crystals, was exploited to obtain high second harmonic generation via the Quasi-Phase Matching technique. From a structural point of view, the inversion of the spontaneous polarization should not affect at all the refractive index of uniaxial ferroelectric crystals. However, it was reported [1] that PPLN crystals prepared by the electric field poling technique illuminated by a laser beam give rise to a diffraction pattern. This fact indicates that the poling process induces a modification of the linear optical properties of the crystal. As a consequence a periodic modulation of the refractive index linked to the domain structure appears. Experimental data indicates that the refractive index modulation have essentially a sinusoidal profile with a period equal to that of the domain structure. This is in contrast to the picture commonly reported in literature [2] that refractive index modifications appear only at the domain walls due to the associated strain [3]. The same phenomenon occurs also in PPLN prepared by the Czochralski off-center technique where the domain structure extends throughout the whole crystal volume. Although these crystals are expected to have ferroelectric domain boundaries parallel to the direction of the spontaneous polarization, in this work we show that a domain wall tilting is present. By exploiting the High Resolution X-Ray Diffraction technique [4] in reciprocal space mapping mode, in fact, we report that the angle between the domain border and the spontaneous polarization directions is different from zero, reaching a value as high as 5 degrees. Moreover the ferroelectric domains present a bent shape that resembles the growth interface. It is worth mentioning that the presence of a modulation in the linear refractive index and the presence of domain wall tilting can affect the second harmonic generation (SHG) efficiency. A systematic analysis to simulate this effect by numerical integration of governing equations is therefore mandatory [5]. To this goal, by means of a wide angle non linear BPM we have simulated field propagation in presence of tilted domains at various angles; although at the output the SH wave remains almost collinear with FF wave, an appreciable reduction of the conversion efficiency (up to 20%) was predicted. Preliminary measurements of SHG performed on real samples affected by tilted domains confirm this trend.

## References

[1] M. Müller, E. Soergel, K. Buse, C. Langrock , MM. Fejer, J.App.Phys. **97**, 044102-1-044102-4 (2005).
[2] S. Kim , V. Gopalan, Mat.Sci.Eng. B. **120,** 91-94 (2005).
[3] T. Jach, S. Kim, V. Gopalan, S. Durbin, D. Bright, Phys. Rev.B **69,** 064113-064122 (2004).
[4] M. Bazzan, N. Argiolas, C. Sada, E. Cattaruzza, Applied Physics Letters **89**, 062901-3 (2006).
[5] E. Autizi, A.D. Capobianco, FM. Pigozzo, N. Argiolas, M. Bazzan, E. Cattaruzza, P. Mazzoldi, C. Sada, Opt.Quant.Elec. **38,** 177-185 (2006).

# Enhancement of the Quality factor of Bloch modes at Γ-point in a 2D nanopillar Photonic Crystal slab using heterostructures

L. Ferrier, E. Drouard, X. Letartre, P. Rojo-Romeo and P. Viktorovitch
*Institut des Nanotechnologies de Lyon (INL, UMR CNRS 5270), Ecole Centrale de Lyon*
*36 avenue Guy de Collongue, 69134 Ecully Cedex, France*
Lydie.Ferrier@ec-lyon.fr

Photonic heterostructures [1] are used to increase the quality factor of slow Bloch modes located around the Γ-point in 2D nanopillar Photonic Crystal (PC) slabs. 3D calculations show an enhancement of at least 5.

## Summary

2D nanopillar PC structures formed in high index contrast silicon on insulator slabs are investigated. The principal motivation of this work lies in that nanopillar arrays should be easily combined with refractive structures (e. g. micro-wire waveguides), unlike 2DPC consisting in hole lattices. Such an association is expected to lead to both new functionalities and higher integration. In addition, waveguided Bloch modes in 2DPC slabs can be coupled in a controlled way to the radiated modes. For example, it is well known that non-degenerate Bloch modes with $k_{//}=0$ (i.e. at the Γ-point) can not couple to a vertical plane wave for symmetry reasons [2]. Thus, in compact structures operating at the Γ-point, the photon lifetime is mainly controlled by in plane losses occurring at the lateral edges of the PC [3]. Such losses may be kept low owing to the low group velocity of the mode located at a high symmetry point.
In order to increase the Q-factor without increasing the mode volume, we use a heterostructure (fig. 1), where the pillars of the surrounding rows have a different radius to inhibit the lateral leakages, leading to an improved lateral confinement of the photons inside the structure. Figure 2 shows the computed Q-factor (using 3D FDTD) of the first Γ-point mode of the inner structure consisting of an 11*11 nanopillar square lattice, as a function of the filling factor (ff) of the surrounding structure and for different numbers of confining rows. A Q factor of 3750 can thus be achieved, instead of 650 without any surroundings rows.
A phenomenological model will be used to explain the numerical results.

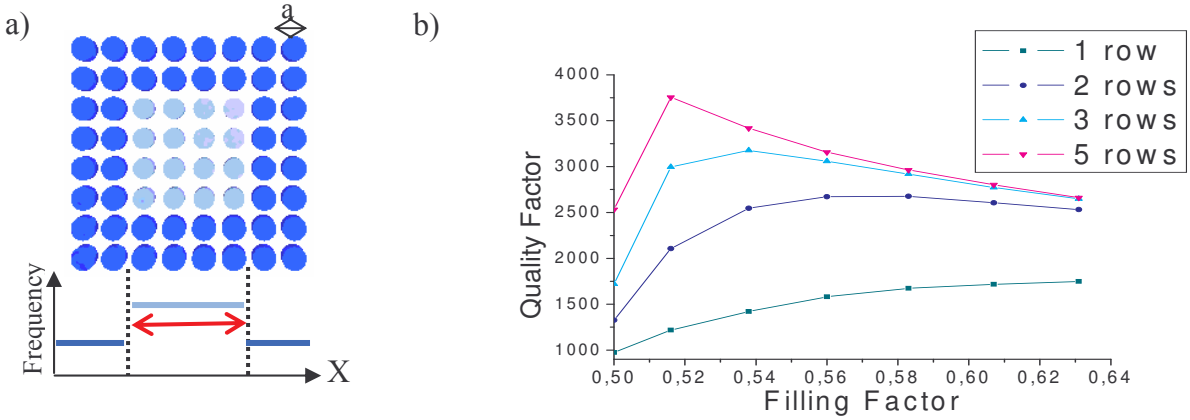


**Fig1**: a) Schematic view of the heterostructure and the corresponding band diagram showing the mode confinement. b) Quality factors of an 11*11 pillar array (silicon in silica, ff = 50% and a = 0.58 µm, height 0.3 µm), as a function of the surrounding filling factor, and for different number of rows.

## References

[1] B.S. Song *et al.*, Nature materials **4,** 207 (2005)
[2] T. Ochiai and K. Sakoda, Physical Review B **63**, 125107 (2001)
[3] X. Letartre *et al.*, IEEE Journal of Lightwave Technology **21**, 1691 (2003)

# 2D Modelling of PhC Waveguide Structures: a Comparison of Approaches

Ivan Richter[1], Jiří Čtyroký[2], Milan Šiňor,[1] and Pavel Kwiecien[1]
[1] *Czech Technical University in Prague, Faculty of Nuclear Sciences and Physical Engineering, Department of Physical Electronics, Břehová 7, 11519 Prague 1, Czech Republic*
richter@troja.fjfi.cvut.cz

[2] *Institute of Photonics and Electronics, Academy of Sciences of the Czech Republic, Chaberská 57, 18251 Prague 8, Czech Republic*

2D structures of PhC waveguides are modelled in various configurations, including rectangular, chessboard and circular building blocks of rectangular and triangular grid, both of direct and inverse type. Mode matching and FDTD techniques, namely CAMFR, BEX tool, and F2P tools are compared.

## Summary

Today, photonic crystals (PhC) or photonic band gap (PBG) structures, and more generally photonic structures based on PhC, still represent very promising structures of artificial origin. Since such structures exhibit very specific properties and characteristics that can be very difficult (or even impossible) to realise by other means, they represent a significant part of new artificially made metamaterials. In order to fully explore the advantages of such structures, before the actual design and fabrication part of the process, the modelling and optimization part is preceding, clearly with many benefits of such an approach. Obviously, development and testing of numerical modelling tools on one side, and analysis and design of novel perspective PhC-based structures on the other side, are strongly interconnected. In this contribution, we have selected one special modelling problem, namely a two – dimensional PhC waveguide structure, mainly to compare and discuss various numerical approaches and tools. Although such a problem has already been extensively studied, there is still a lot space left, especially in terms of a particular comparison of numerics such as those presented here. For the purpose of our study, we have applied several numerical tools, primarily (1) both the standard (CAMFR software package) and modified two-dimensional bidirectional expansion and propagation method (BEX tool [1,2]), and (2) the 2D finite-difference time-domain (FDTD) method with perfectly matched layers (F2P package [3]). Also, the plane wave expansion (PWE) method (MIT MPB software package) has been used.

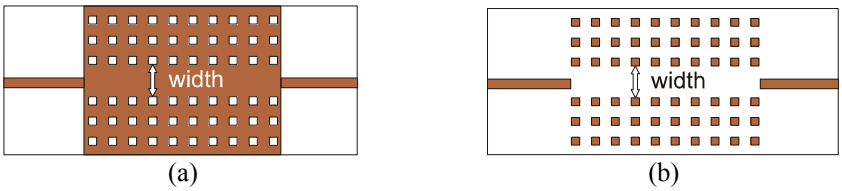


**Fig. 1.** Two types of rectangular PhC waveguide structures studied, with (a) air holes and dielectric guide, and (b) with dielectric rods and air guide.

Namely, we have concentrated on several examples of structures, comparing two types of guides, dielectric-rode type and air-hole type, with several geometries, especially rectangular lattice with either rectangular or chessboard inclusions (see Fig. 1). The modelling results are compared and discussed.

## References

[1] J. Čtyroký, Opt. and Quantum Electron. **38**, 45-62, (2006).
[2] J. Čtyroký, I. Richter, M. Šiňor, Opt. and Quantum Electron. **38**, *in print*, (2007).
[3] I. Richter, M. Šiňor, A. Haiduk, poster (Frontiers in Optics – OSA Annual Meeting, Laser Science XXII, October 2006, Rochester, USA).

# TE and TM mode analysis for a 2D photonic crystal with liquid crystal infiltration

Joaquín Cos, Lluís F. Marsal, Josep Pallarès and Josep Ferré Borrull
Nanoelectronic and Photonic Systems
*D.E.E.E.A., Universitat Rovira i Virgili, Avda. Països Catalans 26, 43007 Tarragona, Spain*
lluis.marsal@urv.net

A theoretical study of 2D photonics crystals made of anisotropic materials is presented. We analyzed the TE and TM modes for a 2D silicon photonic crystal with liquid crystal scatters in the XY plane and a 2D liquid crystal photonic crystal with silicon scatters in the XY plane. First we studied different design parameters, as geometries, radius, etc, in order to perform a suitable band gap. Next, changes of the photonics band structures by rotating directors of liquid crystals in the YZ plane are discussed. These structures can be employed in all-optical devices.

## Summary

Photonic crystals (PhC) offer many important possibilities to control light propagation. Nowadays there is a big interest in the fabrication of PhC based devices with tunable optical properties controlled by the operating conditions or an external field. Two of the most promising ways to achieve such functionality is by filling the holes of 2D silicon PhC with liquid crystals (LC) [1] or by surrounding the silicon pillars of 2D PhC with LC [2].

In the present contribution we studied band structure of 2D PCs made of anisotropic material (E7 liquid crystal) by the plane-wave method (PWM) method [3]. Changes of the photonics band structures by rotating directors of LC are analyzed.

We perform the analysis for two structures:

1. Silicon ($n=3.478$) PhC with a triangular lattice (lattice constant $a$) of circular LC ($n_o=1.522$ $n_e=1.706$) with radius $R=0.423a$. In this structure, as we can see in Fig.1, varying the directors angle we can observe a band gap shift.
2. LC ($n_o=1.522$ $n_e=1.706$) PhC with a triangular lattice (lattice constant $a$) of circular Silicon ($n=3.478$) with radius $R=0.224a$. As we can see in Fig. 2 this structure can be used as switch.

## References

[1] H. Takeda and K. Yoshino, Phys. Rev. E **70**, 026601 (2004).
[2] Y. Y. Wang and L. W. Chen, Opt. Express 14 **22**, 10580-10587 (2006).
[3] K. Busch and S. John, Phys. Rev. E **58**, 3896 (1998).

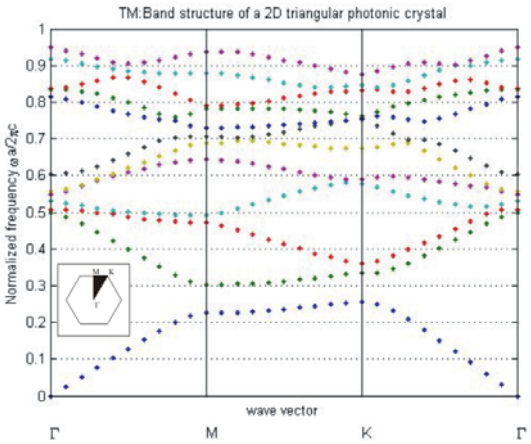


Fig. 1. TM band structure of a 2D triangular silicon photonic crystal with liquid crystal scatters ($\theta=5\pi/12$).

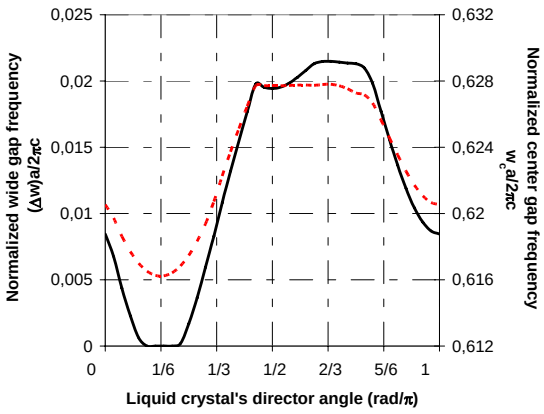


Fig. 2. LC's director angle dependences of wide gap (solid line) and center gap (dashed line) in the TM modes of a 2D LC photonic crystal with silicon scatters.

# A methodology for the design of bio-inspired multilayer deflectors

C. Vandenbem, O. Deparis, M. Rassart, V. L. Welch, V. Lousse, J. P. Vigneron
*Laboratoire de Physique du Solide, University of Namur, 61 rue de Bruxelles, 5000 Namur, Belgium*
cedric.vandenbem@fundp.ac.be

Photonic-crystal theory applied to multilayer stacks gives the relevant quantities useful for the design of light deflecting devices. We propose a methodology which highlights the influence of each parameter and enables prediction of the visual effects, reducing therefore needs of extensive calculations from Maxwell equations.

## Summary

In the living world, a careful study of some Coleoptera specimens shows us that multilayer stacks in the animal's exocuticle can lead to versatile visual effects. Periodic stacks give rise to specular reflection with changing coloration. The ventral part of *Chrysochroa vittata* appears red under normal incidence and reveals a bluish green under grazing angles [1]. In the case of *Hoplia coerulea*, the reflection peak lies in the blue and moves slightly as the angle of incidence increases [2]. Besides, chirped stacks lead to stable metallic coloring (*Chrysina resplendens*). Extraordinarily, a simple combination of air and biological material similar to cellulose is used to produce all these lamellar structures.

Our major aim is to elucidate the change of the reflection peak as a function of the incidence angle. The model is based on a semi-infinite 1D photonic crystal, in which the unit cell is approximated by averaging refractive index in long wavelength regime. The dominant reflected wavelength and the width of the photonic bandgap can be predicted [1, 3]. Different designs can be compared on the basis of the spectral richness [3], which gives the range of wavelengths that is spanned by the dominant reflected wavelength as the angle is changed. A first application of the spectral richness concept is to reproduce multilayer reflectors with a different combination of materials but having the same visual aspect as the biological template [1]. Another application is to design mirrors with completely different visual aspects, using the same combination of materials but adjusting the thickness ratio of the two materials. By this way, we can create multilayer stacks reflecting light like *Hoplia coerulea* or like *Chrysochroa vittata*.

The concept of dominant reflected wavelength is also useful to design narrowband filters. Chirped multilayer films exhibit high reflectivity within a broad range of the electromagnetic spectrum. This broadband reflectance is formed by the additions of several reflection peaks. If the different peaks could shift by the same amount as the angle of incidence is changed, then the reflectance spectrum as a whole would be preserved. The later design is even more attractive with a transmission window for which the quality factor is maintained when the angle of incidence is varied [4]. Adding a defect, which here takes the form of a local alteration of the thicknesses of two layers, creates the filter window. The methodology described here allows us to exploit valuable design ideas from various biological lamellar structures in order to realize versatile mirrors and filters.

## References

[1] J. P. Vigneron, M. Rassart, C. Vandenbem, V. Lousse, O. Deparis, L. P. Biró, D. Dedouaire, A. Cornet and P. Defrance, Phys. Rev. E **73**, 041905 (2006).
[2] J. P.Vigneron, J.-F. Colomer, N. Vigneron and V. Lousse, Phys. Rev. E **72**, 061904 (2005).
[3] O. Deparis, C. Vandenbem, M. Rassart, V. L. Welch and J. P. Vigneron, Opt. Express **14**, 3547-3555 (2006).
[4] O. Deparis, C. Vandenbem and J. P. Vigneron, Opt. Lett. **32**, to be published (2007).

# Photonic Crystal Beam Propagation using a Fourth Order Approximation of the Band Diagram

Damien Bernier, Eric Cassan, Guillaume Maire, Delphine Marris-Morini, Laurent Vivien
*Institut d'électronique Fondamentale, Université Paris Sud CNRS UMR 862, Bat. 220, 91405 Orsay,France*
*damien.bernier@ief.u-psud.fr*

This paper deals with the propagation of optical beams in photonic crystals (PC) using a fourth order approximation of the PC band structure. The effect of fourth order on beam shape is shown and compared with FDTD simulations in a "superlens" photonic crystal configuration.

## Summary

Photonic crystals (PC) have attracted a growing interest for several years due to their unique ability to tailor light properties. Among mechanisms that rely on propagation of light, attention has been specially paid to superprism, superlens, and self-collimating structures [1]. The popular Finite Difference Time Domain (FDTD) is a robust and straightforward method available for the study of these effects but suffers from several drawbacks as: i) light propagation typically occurs within some tens of μms in semiconductor planar devices leading to heavy and memory-consuming simulations, ii) no clear understanding of refraction properties is possible with direct temporal computations. Alternatively, a reliable effective index method has been proposed by Momeni and co-workers that allows the description of light propagation in PC areas [2]. This method is based on the estimation of a propagation operator that is obtained using successive derivatives of PC bandstructure in each localized region under interest in k-space. This operator is then used for the propagation of a set of plane waves, enabling calculations of arbitrary shaped optical pulses both in 2D-PC or 3D geometries (2D planar PCs). We have implemented this method using PC bandstructures calculated in a previous step using the MIT Photonic-bands software [3]. Several 2D-planar strong index contrast PC configurations have been studied. Figure 1 shows a 2D-FDTD field map obtained with a superlens configuration using a 45°-rotated square silicon on insulator (SOI) slab PC. Field profiles have been estimated with second, third, and fourth-order approximations of PC bandstructure and compared with FDTD-calculated field maps.

It has been found that the four-order approximation of PC bandstructure is necessary for the accurate description of the light intensity shape in PC areas, especially when Gaussian pulses suffer from strong spatial distortion, as shown in figure 2. Possible approximations of the propagation operator will be discussed in the final communication; several examples will be presented and accuracy of numerical estimations of the successive bandstructure derivatives will be discussed.

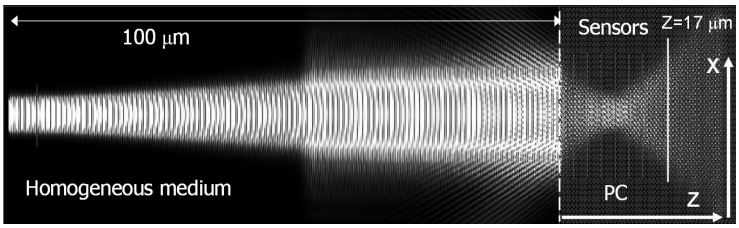


Figure 1: Focalization in PC superlens: FDTD-calculated beam intensity of a 4 μm wide incident Gaussian beam.

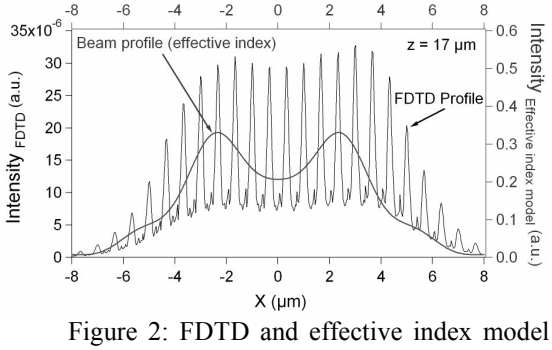


Figure 2: FDTD and effective index model beam profiles at z=17μm within PC.

## References

[1] T. F. Krauss, Phys. Stat. Sol. (A) **197**, 688-702 (2003).
[2] B. Momeni et al, J. Lightwave Technol. **23**, 1522-1532 (2005).
[3] S. G. Johnson et al, Optics Express **8**, no. 3, 173-190 (2001).

# Fabry-Perot Interferometer with two Waveguide-Grating Mirrors: Influence of Grating Shift

Boris A. Usievich, Vladimir A. Sychugov and Jamil Kh. Nurligareev
*Laser Materials and Technology Research Center, General Physics Institute, Russian Academy of Sciences, 119991, Vavilov Street 38, Moscow, Russia*
borisu@kapella.gpi.ru

Fabry-Perot interferometer with two identical waveguide gratings mirrors is studied. It is found that breaking the symmetry by shifting gratings or by slanting the incident beam give rise to additional resonances.

## Summary

Pass band filters are the important elements in spectroscopy, spectrum analysis and WDM communications. Narrow-band optical filters remain subjects of intense research and development [1, 2]. In its simplest form a pass band filter is a Fabry-Perot with two multilayer mirrors. We reported recently [3] as one solution for narrowing the transmission peak without unreasonably increasing the number of layers is to replace one multilayer mirror by the waveguide grating mirror (WGM) which, as is known from [4], can exhibit a sharp and close to 100% abnormal reflection in narrow spectral and angular ranges. Searching for new areas for application of WGMs, we studied a structure of the Fabry-Perot interferometer with two WGMs with the identical characteristic parameters. We found earlier [5,6] that in-phase and anti-phase structures give rise to different resonance positions in the case of small distance between the mirrors due to coupling between the waveguides. In this paper we study the effect of grating's phase shifting in more details for the normal incidence of light on the filter (Fig. 1). It is found that the symmetry play the crucial role in this situation. If the phase shift between two gratings $\Delta\varphi$ is not equal to zero (in-phase) or $\pi$ (anti-phase) then in addition to the shifting of the resonance found in earlier works there are additional resonances nearby whose positions, widths and amplitudes depend on $\Delta\varphi$. It is also found that these additional resonances also appear when the incidence is not strictly normal (Fig. 2).

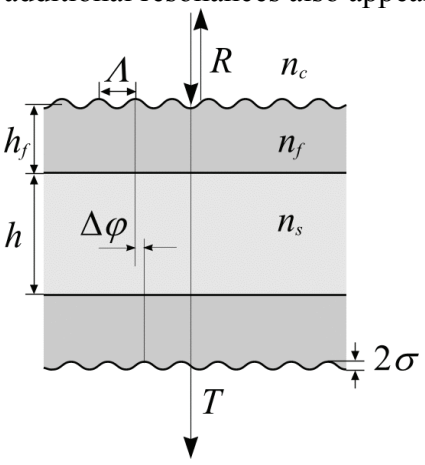


Fig. 1: Scheme of the filter

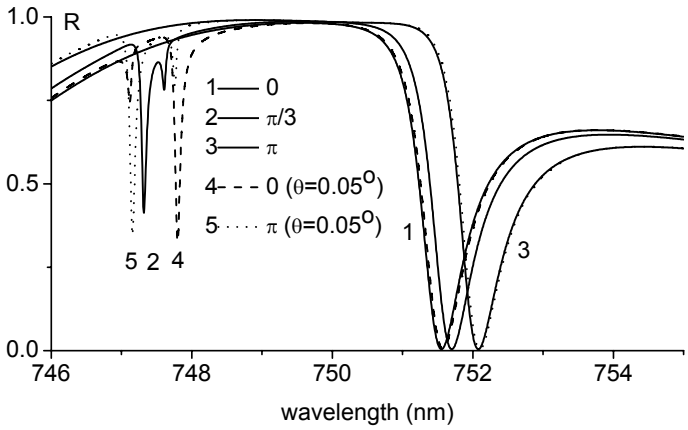


Fig. 2: Reflection of the filter

## References

[1] I.F. Kanaev, V.K. Malinovskii, N.V. Surovtsev, Phys. Solid State **42**, 2142 (2000).
[2] N. Destouches, J.-C. Pommier, O. Parriaux at all., Opt. Express 14(26), 12613-12622 (2006).
[3] B.A. Usievich et al, Opt. Quant. Elect. **36** (1-3), 109-117 (2004).
[4] G.A. Golubenko et al, Kvant. Elektron. (Moskow) **12**, 1334 (1985).
[5] B.A.Usievich, V.A.Sychugov, Laser Physics, **14**, 1110-1114 (2004).
[6] B.A.Usievich, V.A.Sychugov, Proc. OWNTM 2006, 44 (2006).

# Simulation of acousto-optical interaction in a Mach-Zehnder interferometer

Maria B. Dühring, Ole Sigmund and Jakob S. Jensen
*Department of Mechanical Engineering, MEK, NanoDTU, Technical University of Denmark, DK-2800 Kgs. Lyngby, Denmark*
mbd@mek.dtu.dk

The acousto-optical modulation of light in a Mach-Zehnder interferometer affected by a surface acoustic wave, is simulated by the finite element method. It is discussed how the modulation can be improved based on a parameter study of the geometry.

## Summary

A new way to control and modulate light in waveguide structures is to let the light interact with surface acoustic waves (SAW) [1]. SAWs are elastic waves that propagate along a material surface, they consist of a longitudinal and a shear component and they have most of their energy density concentrated within one wavelength of the surface [2]. In [3] it is explained how a SAW can be employed to modulate the output light of a GaAs Mach-Zehnder interferometer (MZI) and experimental results with a relative modulation depth of 40 % are presented. To modulate the light using a MZI a SAW is transmitted perpendicularly to the two waveguide arms and the elastic stress field from the SAW results in a periodic change of the refractive index and therefore a periodical phase change in the waveguide arms. At a wave crest the refractive index will increase and at a trough it will decrease. Thus, if the distance between the arms is chosen as an unequal multiple of half the SAW wavelength the light at the output waveguide will interfere constructively and destructively in a periodic way and the MZI can hence be used as an optical switch. To understand and improve the interaction of the elastic field from the SAW with the optical field in the waveguides a numerical model of the MZI is constructed. The generation of the SAW by interdigital transducers is studied using a 2D finite element model of a piezoelectric, anisotropic material implemented in the high-level programming language Comsol Multiphysics. By calculating the stresses in the waveguide arms introduced by the SAW the changes in refractive indices are obtained from Pockels constants. This model is then coupled to an optical model where the time independent wave equation is solved as an eigenvalue problem giving the effective refractive index of the lowest modes in the waveguide arms. Numerical results of the modulation for MZIs of both GaAs and Si are presented. Based on results from a parameter study of the geometry it is discussed how the acousto-optical modulation can be improved.

## References

[1] M. M. de Lima Jr. and P. V. Santos, (2005), “Modulation of photonic structures by surface acoustic waves”, *Rep. Prog. Phys.*, 68 1639-1701.
[2] K.-Y. Hashimoto, “Surface acoustic wave devices in telecommunications modeling and simulation”, Springer, Berlin, 2000, ISBN 3-540-67232-X.
[3] M. M. de Lima Jr., M. Beck, R. Hey and P. V. Santos, “Compact Mach-Zehnder acousto-optic modulator”, *Applied Physics Letters*, 89, 121104 (2006).

# A "Couplonic" Approach to Out-Of-Phase Coupled Periodic Waveguides

Yann G. Boucher[1], Andrei V. Lavrinenko[2] and Dmitry N. Chigrin
[1] *ENIB/RESO Lab, CS 73862, F-29238 Brest cedex 3, France*
boucher@enib.fr
[2] *COM•DTU, Technical University of Denmark, DK-2800 Kgs Lyngby, Denmark*
[3] *Physikalisches Institut, Universität Bonn, Nussallee 12, D-53115 Bonn, Germany*

We investigate the peculiar properties of out-of-phase coupled periodic waveguides in the frame of a systematic coupled-mode analysis, with special emphasis on internal symmetries at the scale of a unit cell.

## Summary

In spite of its intrinsic limitations, the scalar Coupled Mode Theory (CMT) applied to coupled periodic waveguides (CPW) appears especially appealing, with simple and accurate all-analytical results that remain essential for good physical insight. In the special case of mutually shifted CPW, though, discrepancy is sometimes observed between CMT predictions and full-wave analysis [1]. The aim of this work is to help clarifying the problem by using a formal approach based essentially on symmetry arguments (such as space reversal). For the sake of clarity, we assume that the unit cell of each waveguide is lossless and symmetric.

In terms of CMT, the system is described by a (4x4) linear evolution operator. In the in-phase case, the problem is best expressed in the even/odd eigenmode basis, since even and odd supermodes appear totally decoupled, with a lift of degeneracy affecting their propagation constant, thus the position of their Bragg resonance. In the half-period shift case (phase opposition), a decoupling occurs, since the co-propagating even mode couples back into the contra-propagating odd mode and *vice versa*. In the general case, the even/odd decomposition remains of course totally valid as a linear basis, but even and odd modes are no longer decoupled.

On the other hand, for in-phase configuration at least, the continuous CPW is formally similar to a discrete system made of multi-port networks interconnected by segments of transmission lines [2]. It is therefore tempting to extend that analogy. Possible configurations are depicted in Fig. 1, where the unit cell is made of identical three-port networks (this means implicitly that the co-directional coupling and the contra-directional cross-coupling share the same strength). With a judicious translation of the reference planes along the axis of the lower waveguide, the scattering parameters of the unit cell in the shifted configuration (c) exhibit exactly the same form as in the configuration (a). This suggests that decomposition in terms of parity could become relevant again, provided we generalise the notion of "even" and "odd" supermodes by taking the shift into account properly.

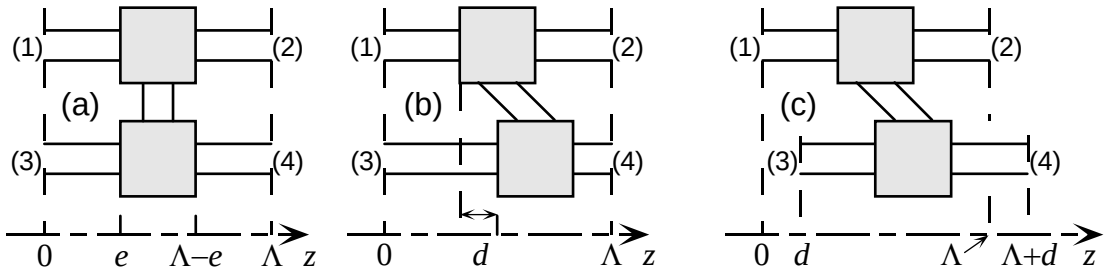


*Figure 1: Discrete unit cell made of two identical three-port networks interconnected by segments of transmission lines. (a) symmetrical configuration; (b) shifted configuration; (c) shifted configuration with a d-translation of the lower reference planes.*

## References

[1] A.V. Lavrinenko, D.N. Chigrin, OWTNM 2005, Grenoble, April 2005.
[2] Y.G. Boucher, *Fundamental of Couplonics*, Proc. SPIE Vol. 6182, 61821E, 2006.

# Metamaterials based on Nanocavities

C. Rockstuhl[1], T. Zentgraf[2,3], T. P. Meyrath[2,3], H. Giessen[2,3], T. Pertsch[1], and F. Lederer[1]

[1] *Friedrich-Schiller-Universität Jena, Max-Wien-Platz 1, 07743 Jena, Germany*
carsten.rockstuhl@uni-jena.de

[2] *Max Planck Institute for Solid State Research, Heisenbergstr. 1, 70569 Stuttgart, Germany*

[3] *University of Stuttgart, Pfaffenwaldring 57, 70550 Stuttgart, Germany*

We theoretically and experimentally investigate metamaterials consisting of holes in thin metallic sheets that resemble nanocavities or nanoapertures. Resonances of these structures relate to guided modes localized inside the nanocavities. Their impact on effective material parameters is discussed.

## Summary

Metamaterials (MM) are artificial media consisting of (usually) periodically arranged unit cells. Light propagation in such media is governed by the dispersion relation of Bloch-periodic eigenmodes. If one aims to allocate effective material parameters, light propagation has to be dominated by the fundamental eigenmode. Resonances are usually employed to obtain strongly dispersive effective material parameters. Presently, two resonance mechanisms are predominantly used. The first is based on Mie-resonances in high permittivity spheres [1]. The second is based on plasmon resonances excited in appropriately shaped single or coupled metallic elements [2].

Here we outline a third resonance mechanism that can be used in the design of MMs. It consists of nanoapertures in thin metallic sheets. These structures show resonances in the excitation of localized fields that relate to guided modes in an infinitely extended metallic waveguide. We outline our design approach by analyzing complementary split-ring-resonators and complementary nanowires. These geometries are schematically shown in Fig. 1.

In this contribution, we will introduce the idea of employment of resonances in nanocavities in the design of MMs and show experimental and theoretical results. The fundamental mechanisms are outlined, practical implementations are presented, and their disadvantages as well as their advantages in comparison to other approaches in the design of MMs will be discussed.

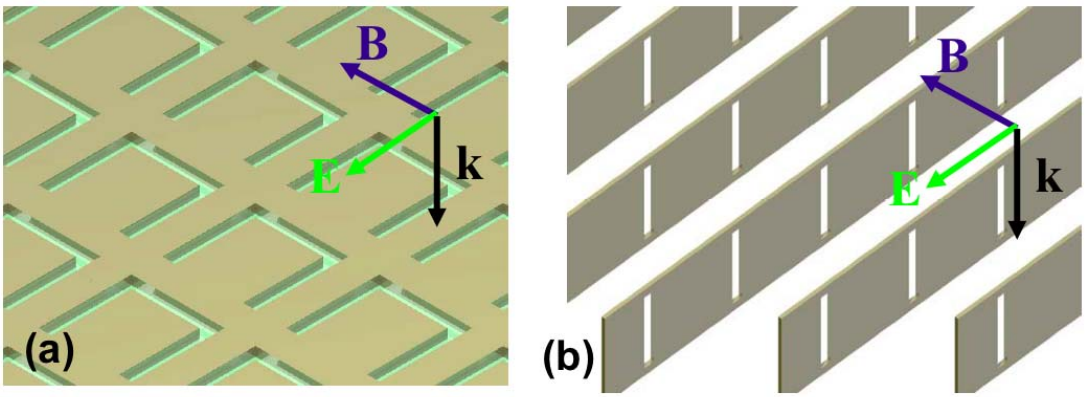


Fig. 1: Geometry for a complementary split-ring-resonators and a complementary wire in thin metallic sheets.

## References

[1] V. Yannopapas and A. Moroz, J. Phys.: Condes. Matter **17**, 3717-3734 (2005).
[2] J. P. Pendry et al. IEEE Trans. Microwave Theory Tech. **47**, 2075-2084 (1999).

# Analysis and Design of MMI-Based Racetrack Resonators

Thanh Trung Le and Laurence W. Cahill
*Department of Electronic Engineering La Trobe University, Melbourne, Victoria 3086, Australia*
tt18le@students.latrobe.edu.au , l.cahill@latrobe.edu.au

The analysis and design of an optical ring or racetrack resonator based on a multimode interference (MMI) coupler with variable coupling is presented in this paper. We consider the conditions on the MMI coupler for optimum performance of the device, taking into account both bending loss and the effect of the higher order modes in the ring.

## Summary

The MMI-based racetrack resonator comprises a tunable 2x2 MMI coupler and a racetrack, as shown in figure 1. A similar structure has been analysed previously [1]. However, the splitting ratio of the MMI coupler is limited if conventional MMIs are used. It is possible to implement tunable power splitting couplers by using angled MMI couplers, butterfly MMI couplers or region index modulation couplers. In this paper, we investigate these options. We take into account the losses from the MMI coupler as well as the ring resonator bending loss and propagation loss. In addition, the effect of higher order modes in the ring waveguide on the performance of the device is included.

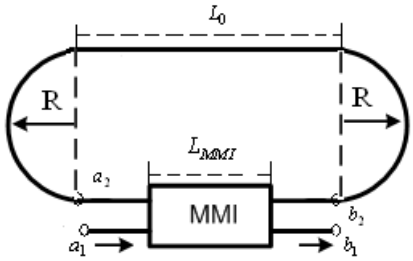


Fig. 1 Configuration of a racetrack resonator based on a variable MMI coupler.

By using the transfer matrix method, the normalized power at the coupler output can be found from

$$\left|b_1/a_1\right|^2 = \left|(t_{11} + k_{12}\alpha_1 x_1 \exp(j\phi_1)) + \alpha_2 \exp(j\phi_2)(k_{13} + k_{12}\alpha_1 x_2 \exp(j\phi_1))(y_1 + y_2 x_1)/(1 - x_2 y_2 \alpha_1 \exp(j\phi_2))\right|^2 \quad (1)$$

where $t_{ij}$ and $k_{ij}$ (i,j=1,2,3) are the transmission and coupling coefficients of the fundamental mode and the first order mode between straight waveguides and the racetrack resonator, $x_1 = k_{21}/(1 - t_{22}\alpha_1 \exp(j\phi_1))$, $x_2 = k_{23}/(1 - t_{22}\alpha_1 \exp(j\phi_1))$

$y_1 = (k_{31} + \alpha_2 k_{32} k_{21} \exp(j\phi_1))/(1 - t_{32}t_{23}\alpha_1\alpha_2 \exp j(\phi_1 + \phi_2) - t_{33}\alpha_2 \exp(j\phi_2))$, $\phi_i = 2\pi n_{effi}(L_0 + 2\pi R)/\lambda$

$y_2 = (\alpha_2 k_{32} t_{22} \exp(j\phi_1))/(1 - t_{32}t_{23}\alpha_1\alpha_2 \exp j(\phi_1 + \phi_2) - t_{33}\alpha_2 \exp(j\phi_2))$, $\lambda$ is the optical wavelength, $n_{effi}$ (i=1,2) are the effective refractive indices and $\alpha_i$ (i=1,2) are the propagation losses of the modes respectively. Polarisation effects may be included and the approach can be extended also to multiple rings.

Numerical simulations demonstrate the characteristics of the device and enable the parameters of the MMI coupler to be chosen in order to achieve the desired performance.

## References

[1] Driessen, A. et al., *Proc. SPIE,* **5956**, pp. 59560 Q-1 – 59560Q-14, 2005.
[2] Caruso, L.; Montrosset, I., *IEEE J. Light. Technol.*, **21**, no.1,pp. 206- 210, Jan 2003.
[3] Melloni, A., *Opt. lett.*, **28**, no17, pp. 1567-1569, 2003.

# Demultiplexing optical signals using chirped two-dimensional photonic crystals

D.Biallo[1] , A. D'Orazio[1] , M. De Sario[1], V. Marrocco[1], V. Petruzzelli[1] and F. Prudenzano[2]
[1] *Dipartimento di Elettrotecnica ed Elettronica, Politecnico di Bari, Via Re David 200, 70125, Bari Italy*

dorazio@poliba.it

[2] *Dipartimento di Ingegneria dell'Ambiente e per lo Sviluppo Sostenibile-Seconda Facoltà di Ingegneria, Taranto, Via del Turismo 8, 74100, Taranto,Italy.*

## Summary

Recently some innovative works concerning new demultiplexing configurations in 2D-PC have been reported in literature. A multi-wavelength drop operation in [1] is obtained by connecting different PC regions characterized by different lattice constant, namely the in-plane hetero-photonic crystal (IP-HPC). The heterostructure interfaces between adjacent photonic crystal regions can act as wavelength selective mirrors: in this way the signal is reflected back by each interface, coupled to high-Q microcavities and dropped to output PC waveguides. The demultiplexing functionality can be accomplished considering the variation of the air-hole radii of the PC waveguide along the propagation direction of the PBG waveguide as the incident light signal propagates trough an input waveguide [2,3]. The device is based on the concept that varying the air-hole radii along the sides of the PBG input waveguide the transmission bands of the waveguide modes shift. In this paper a design of a novel demultiplexing system in 2D-PC technology is proposed. The design exploits the cascade of different PCs, characterized by the variation of the period along the ΓK direction only (differently from the heterostructure) and it is able to isolate the optical signals using PC waveguides only. A W1 waveguide, acting as input waveguide, crosses the entire structure and side W1 waveguides, placed in each PC section, are able to collect the output signals. The value of the lattice constant in the ΓK direction is progressively decreased using a constant step (5 nm or 10 nm smaller with respect to the value of the lattice constant considered in the previous section), thus provoking the blue-shift of the cutoff wavelengths of the propagating modes. As the input signal propagates, some wavelengths are filtered by the following sections, as the lattice constant decreases, so the part of the signal which is not supported by the rest of the input waveguide is reflected back. Side output channels are opportunely placed in order to let the forward and backward signals interfere in a constructive way, thus allowing the collection of each dropped signal at the output.

## References

[1] H. Takano, Bong-Shik Song, T. Asano and S. Noda, "Highly efficient multi-channel drop filter in a two-dimensional hetero photonic crystal", Optics Express vol. 14, N. 8, pp. 3491-3496, 17 April 2006.

[2] A. Shinya,S. Mitsugi, E. Kuramochi and M. Notomi, "Ultrasmall multi-channel resonant-tunnelling filter using mode gap of width-tuned photonic-crystal waveguide", Optics Express, Vol. 13, N. 11, pp. 4202-4209, 30 May 2005.

[3] T. Niemi, L.H. Fradsen, K. K. Hede, P. I. Borel and M. Kristensen, "Wavelength-division demultiplexing using photonic crystal waveguides", IEEE Photonics Technology Letters, Vol. 18, N. 1, January 2006.

# Modeling of Multimodal Effects in Two-port Ring-Resonator Circuits for Sensing Applications

H.P. Uranus[1], H.J.W.M. Hoekstra[1], and R. Stoffer[2]
[1]*IOMS Group and* [2]*AAMP Group, MESA+ Institute for Nanotechnology, University of Twente, PO Box 217, 7500 AE, Enschede, The Netherlands*
*e-mail: h.p.uranus@ewi.utwente.nl, h.j.w.m.hoekstra@ewi.utwente.nl, r.stoffer@ewi.utwente.nl*

Multimodal effects in two-port ring-resonator circuits for sensing applications were modeled using a transfer matrix method and previously published rigorous 3-D modeling tools. Device parameters which are relevant for evaluating sensing performance are numerically deduced from the model. Some examples will be given.

## Summary

A two-port ring resonator (TPRR) circuit is an interesting integrated optical structure for sensing applications. One of the widely used criteria for designing such a structure is its monomodality, which leads to a simple and well-understood model. However, achieving such a monomodal condition is not always trivial and may conflict with other design criteria and fabrication technology limitations. For structures based on high-contrast materials, especially in the short wavelength regime (e.g. in the visible wavelengths where absorption of watery solution is low), such a monomodal condition generally requires small waveguide dimensions which might be beyond the capability of the available fabrication technology. In some circumstances, the application of the monomodality requires sacrificing the optimal value of other device parameters. A monomodal waveguide normally has a relatively weakly confined modal profile. Consequently, for such a situation, scattering loss, substrate leakage loss, and bend loss, are generally higher than for a well confined mode. Since modal loss plays an important role as a limiting factor for the resolution of ring resonator sensing platform, enforcing monomodality might end-up with a low resolution.

Considering the implications discussed in the previous paragraph, in some circumstances, relaxing the monomodality design criteria might be an alternative choice. In such design, multimodal effects take place as intermodal coupling is unavoidable, e.g. in the coupler region. We should note that different modes have different values for the modal loss (which implies different values for the required coupling constant to interrogate the sensing analyte effectively) due to different modal field confinement, in addition to different modal effective indices (which implies different values of resonant wavelength). Such differences help to separate the contribution of each individual mode to the response curve of the device. Hence, a multimodal TPRR, if carefully designed, could still work as a good sensing platform. For designing such a multimodal TPRR, a corresponding model is important. In this work, we present a model for evaluating the multimodal effects in the TPRR, using a transfer matrix method and previously published 3-D rigorous vectorial modeling tools (i.e. coupled mode theory [1] and mode solvers [2], [3]), taking also the effect of substrate leakage loss, scattering loss, and bend loss of each individual mode as well as waveguide dispersion and coupling between such modes into account. Using the model, we numerically deduce device parameters which are relevant for evaluating sensing performance, i.e. power transmittance, amplitude transmission coefficients, Q-factor, group index, and sensitivity of transmittance and phase shift to an infinitesimal change in the measurand refractive index. Some examples will be given.

## References

[1]. R. Stoffer, K.R. Hiremath, M. Hammer, L. Prkna, and J. Čtyroký, Opt. Commun., **256**, 46-67 (2005).
[2]. L. Prkna, M. Hubálek, and J. Čtyroký, J. Selected Topics in Quantum Elect., **11**, 217-223 (2005).
[3]. H.P. Uranus and H.J.W.M. Hoekstra, Opt. Express, **12**, 2795-2809 (2004).

# BPM Simulation of SNOM Measurements of Waveguide Arrays Induced by Periodically Poled BNN Crystals

Jorge Lamela[1], Francisco Jaque[1], Eugenio Cantelar[1], Daniel Jaque[1], Alexander A. Kaminskii[2] and Ginés Lifante[1]

[1] *Departamento de Física de Materiales, C-IV. Universidad Autónoma de Madrid. 28049-Madrid, Spain.*
gines.lifante@uam.es

[2] *Russian Academy of Science, Inst Crystallog., Moscow 119333, Russia*

The simulation of light propagation, using standard BPM, in one-dimensional waveguide arrays in BNN crystals is presented. The waveguide arrays were produced by domain inversion induced during the crystal growth. SNOM measurements, using collection mode, are compared with the BPM simulations.

## Summary

Waveguide arrays can be fabricated in $Ba_2NaNb_5O_{15}$ crystals as consequence of periodically inverted domain structures [1]. The one-dimensional domains may act as planar waveguides due to a local increase of the refractive index. This structure can be studied by Scanning Near Field Optical Microscopy (SNOM) working in collection mode. In this configuration, light is collected at the end of the crystal when the sample is illuminated from the other end, allowing sub-wavelength spatial resolution. Figure (bottom) shows the BPM simulation of the waveguide array using 633 nm light. It can be observed that light is mostly confined into the high index regions, giving rise to a high contrast pattern (upper part of the figure, selected from the central part of the BPM simulation). Right side of the figure shows a SNOM image of the collected light at the polished end-face of the BNN crystal, using a 200 nm diameter fibre tip. Both period and contrast are in agreement with the simulation results, indicating that BPM is an adequate tool for analysing SNOM images under sub-wavelength resolution.

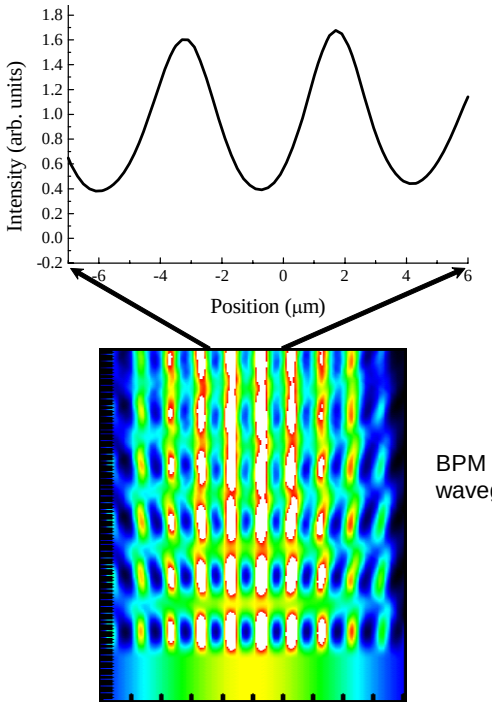


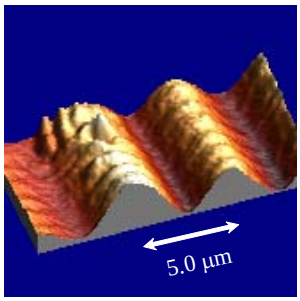


SNOM using collection mode



BPM simulation of the waveguide array

## References

[1] S. Kin and V. Gopalan, Materials Science and Engineering B 120, 91-94 (2005).

# Rigorous modeling of cladding modes in photonic crystal fibers

Lars Rindorf and Ole Bang
*COM•DTU, Department of Communications, Optics and Materials,*
*Technical University of Denmark, DK-2800 Kgs. Lyngby, Denmark*

We study the cladding modes of a photonic crystal fiber (PCF) with a finite size cladding using a finite element method. The cladding consists of seven rings of air holes with bulk silica outside.

In an optical fiber for optical communication the information is carried in the so-called core mode which has extremely low losses. The fiber also supports a number of higher order modes which typically attenuate over a couple of centimeters. A long period grating uses a resonant coupling between the core mode and a cladding mode modes. The coupling is dependent on the effective indices and the symmetry of the modes. The resonance condition is $\lambda = \left(n_{eff,co}(\lambda) - n^{(i)}_{eff,cl}(\lambda)\right)\Lambda_G$. For a step index fiber solutions may be found analytically, however, for a PCF powerful numerical methods must be employed. The true dielectric structure of a PCF is difficult to model due to the bulk silica beyond the air holes and the air around silica rod. A mode solver thus has to deal with a high number of bulk modes and can experience problems with both accuracy and convergence in some methods, such as the planewave method. When solving for the core mode the bulk and some rings are typically removed to reduce to complexity of the problem. Outside the rings of air holes boundary lossy boundary conditions such as phase mathed layers, perfect electric conductor, or an air layer may be imposed.

In this work we compare these approximations with experiments and find a poor resemblance for the cladding mode fields. Using a finite element method (COMSOL) with a powerful mode solver we simulate the full cross-section of the PCF. In Fig. 1 we have shown optical micrographs of a PCF (a through b). The cladding mode is excited by a long-period grating with a laser operating at 635 nm. Below is shown the numerically calculated fields (1 through 3). Two cladding modes are shown as the resonant cladding mode is four fold degenerate. The experimental and the numerical cladding modes look slightly different since in experiment the cladding modes scatter into other cladding modes.

The study may shed light on the mechanisms behind the inscription of LPGs in PCFs using heat treatment by $CO_2$ laser or electric arc which are still unknown.

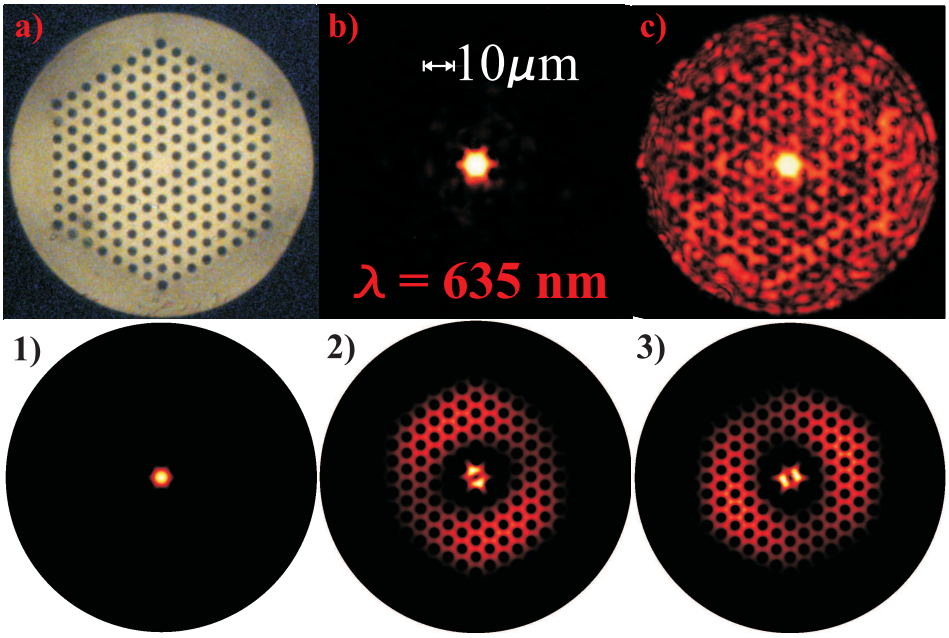


FIG. 1: Experimental optical microscope images of PCF structure (a), core mode (b) in a fiber without grating, and cladding mode at the resonant wavelength. (1-3) the numerically calculated fields for the core mode 1. In 2-3 is shown the two different degenerate mode fields. Each mode field has two polarizations

# Donor and acceptor modes in nonlinear microstructured optical fibers

M. Zacares[1], G. Renversez[2], F. Drouart[2], G. March[1], A. Nicolet[2] and A. Ferrando[1]
[1] *Interdisciplinary Group, Universidad Polytecnica de Valencia, Camino de Vera, 46022 Valencia, Spain*
[2] *Institut Fresnel (UMR CNRS 6133) and Université Paul Cézanne Aix-Marseille III*
*Faculté des Sciences et Techniques de St Jérôme, 13397 Marseille Cedex 20, France*
*e-mail: gilles.renversez@fresnel.fr*

We generalize to the case of a nonlinear matrix with a positive Kerr term the concept of donor and acceptor modes previously described by Ferrando *et al.* in the linear case. We obtain our results using several numerical methods applied to both finite size and infinite structures.

The aim of our work is to generalize to the case of a nonlinear matrix the concept of donor and acceptor modes in photonic crystal fibers described by Ferrando *et al.* in reference[1] (see also reference[2]). In the linear case, it is well known that a small variation in the refractive index, $\delta n^2$, will produce a change in the effective refractive index of the mode. A donor defect (typically an inclusion such that its diameter is smaller than the ones of the surrounding inclusions) produces an increase of the local refractive index and will give rise to a mode originating in the next-lower conduction band ($\delta n_{eff} > 0$). An acceptor defect (typically an inclusion such its diameter is bigger than the ones of the surrounding inclusions) will generate modes that will arise from the next-higher conduction band generate modes that will arise from the next-higher conduction band ($\delta n_{eff} < 0$). The nonlinear case is richer because it is possible to play with another degree of freedom: the power of the fields. Nonlinearity induces a local variation in the refractive index. It acts as a defect, even in the completely periodic case. For a Kerr-focusing nonlinearity, $\delta_n$ and therefore the effective refractive index of the nonlinear solution will increase ($\delta n_{eff} > 0$)

Playing with the nonlinearity, geometry of the defect and position of the bands it is possible to obtain nonlinear localized-delocalized transition. We observe two kinds of scenario depending on the nature of defect. For donor defects, in the linear case there are localized solutions in the first bandgap. If a focusing nonlinearity is included, a family of localized solutions can be found. All these solutions are localized and are linked to the linear modes of the first bandgap. The effect of power is to increase the effective refractive index of the nonlinear solution and to localize the field. In this case no transition is observed. For acceptor defects, the scenario is slightly different. In the linear case, there are localized modes in the second bandgap but not in the first one. In the nonlinear case, transitions associated to localization/delocalization can be found. We describe these transitions using several numerical methods applied to both finite size and infinite structures[3].

**References**

[1] A. Ferrando, E. Silvestre, J.-J. Miret, P. Andrès, and M. V. Andrès. *Optics Letters*, 25(18):1328–1330, 2000.
[2] E. Yablonovitch, T. J. Gmitter, R.D. Meade, A. M. Rappe, K. D. Brommer, and J. D. Joannopoulos. *Phys. Rev. Let.*, 67(24):3380–3383, 1991.
[3] F. Zolla, G. Renversez, A. Nicolet, B. Kuhlmey, S. Guenneau, and D. Felbacq. *Foundations of Photonic Crystal Fibres.* Imperial College Press, London, 2005.

# Q-Factor Calculations with the Finite-Difference Time-Domain Method

Aliaksandra Ivinskaya and Andrei V. Lavrinenko
*COM•DTU, Department of Communications, Optics and Materials, Technical University of Denmark, DK-2800 Kgs Lyngby, Denmark*
*aiv@com.dtu.dk*

A sphere as a resonator with analytically predicted quality factor is used to test different approaches to calculate the *Q*-factor. The fit to the exponential energy density decay shows the best result consistent with the analytics up to the third digit.

## Summary

Many approaches for calculation of the *Q*-factor with the FDTD have been proposed, but there is lack of clear comparison between them. This variety of approaches is due to large number of output data after computational cycle as compared, for example, with frequency-domain (FDFD) algorithms where the *Q*-factor appears only as a generalized characteristic of the whole system. The analysis of one field component is usually based on the exponential fit in the time domain or the lorentzian fit, the Pade approximation, the Baker algorithm, etc. in the frequency domain. Another way is to use the energy density *U* or the Pointing vector *P* (both comprising six field components) for evaluation of the quality factor from the exponential fit or via $Q=\omega U/P$ in the time domain.

We considered natural resonances on a dielectric sphere of the radius $r$=0.16 μm with the refractive index $n$=6.0 in air, with analytically calculated $Q$=43.17 [1]. We made FDTD calculations with five detectors located at different positions inside and outside the sphere. The most accurate and robust way to define the quality factor turned out to be the exponential fit of the time-averaged energy density, as shown in Fig. 1. Results for all five detectors differed only in the third digit. We conclude that there is no need to collect information through the whole domain and it is enough to use only one point detector, placed arbitrarily inside the sphere. Investigations of single electric or magnetic field components, with the lorentzian fit in the frequency domain or the exponential fit in the time domain, gave unstable *Q*-factor with relative error about 30% in some cases.

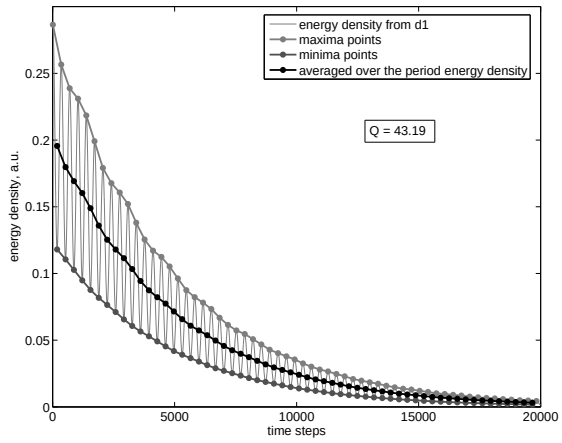


Fig.1. Example of the exponential decay of the period-averaged energy density used to define the quality factor of a sphere.

## References

[1] A. Julien and P. Guillon, IEEE Trans. Microwave Theory Tech. **34**, 723-729 (1986).

# Wave Chaotic Behaviour Generated by Linear Systems

V.A. Buts[1], A.G. Nerukh[2], N.N. Ruzhytska[2], and D.A. Nerukh[3]
[1]*National Scientific Centre «Kharkov Institute of Physics and Technology», Kharkov, 61108, UKRAINE*
[2]*Kharkov National University of RadioElectronics, 14 Lenin Ave.,Kharkov, 61166, UKRAINE*
*hm@kture.kharkov.ua*
[3]*Chemistry Department, University of Cambridge, Lensfield Road, Cambridge, CB2 1EW, UK*

It is shown that the requirement for chaotic dynamics and chaotic characteristics to be inherent exclusively to non-linear systems needs further elaboration. Non-apparent non-linearity in the system simplification or parameters analysed can be crucial and should be analysed with great care.

**Summary**

First, we pay attention to the fact that the equations of geometrical optics, which describe the chaotic dynamics of light beams, are derived by simplifying the Maxwell's equations that are linear. Therefore, it seems that roughening and simplification of the initial linear physical models leads to the necessity of investigating nonlinear equations which can have chaotic solutions. It is worth noting that these considerations can be used for the analysis of a wider range of physical processes. As an example we consider the simplest physical model where the described peculiarity in the dynamics of linear systems can be realized. In this model we consider electromagnetic wave scattering on periodically inhomogeneous medium occupying the half-space. The periodic inhomogeneity has two different periods. The incident wave scattered by the inhomogeneity of the first period generates a wave of the diffraction of the order minus one. The conditions for the excitation of the same wave diffraction by the inhomogeneity of the second period are realized with some detuning. Thus, there is the case of a three-wave dynamical diffraction. Equations describing the dynamics of the complex amplitudes of these three interactive waves are linear. Since their dynamics, in general, and all characteristics are regular. However, in the case of weak coupling between the waves a system of reduced equations for amplitudes and phases can be readily obtained. This reduced system is nonlinear and simpler than the initial one and this allows to obtain an analytic criteria for the onset of the dynamical chaos. Qualitative agreement between the analytical and numerical results is obtained, namely, stochastic instability develops as soon as conditions for the intersections of the geteroclinic trajectories are fulfilled. In this the case the spectra broaden, the correlation function decreases and the real parts of the maximal Lyapunov exponents become positive.

Second, we show that some important characteristics in the solutions of purely linear problems can have chaotic dynamics. It is caused by the fact that these characteristics themselves are nonlinear. As an example of such problem a linear parametric problem of the electromagnetic field in the homogeneous dielectric medium which permittivity is modulated in time beginning from some moment is considered. If the initial field is a plane monochromatic wave and the modulation is in the form of rectangular pulses then the problem has an exact analytical solution which describes the temporal process of the wave transformation. Since under the modulation the permittivity changes abruptly from the initial value to the new one and back then the transformation process consists of a progressive repetition of the known effect of each wave splitting onto a pair of forward and backward propagating waves at each jump of the permittivity. Exact relationships between these wave amplitudes reveal a controlling sequence which determines the whole transformation. The analysis shows that the temporal course of this sequence can have distinctly non-regular behaviour, which chaotic character is visually confirmed by the Lamerey diagram and by the calculation of the Hurst exponent and the Lyapunov exponent. It is shown that the Hurst exponent takes magnitudes corresponding to the white noise and the Lyapunov exponent becomes positive.

# A variational formulation of guided wave scattering problems

Manfred Hammer
*MESA$^+$ Institute for Nanotechnology, University of Twente, Enschede, The Netherlands*
*m.hammer@math.utwente.nl*

A functional of the six electromagnetic components is proposed as a variational basis for 3-D frequency domain problems in integrated optics. Stationarity implies that the Maxwell equations in the interior of the domain of interest and transparent influx conditions for incoming waveguides on its boundary port planes are satisfied.

## Summary

Consider the abstract 3-D guided-wave scattering problem as introduced schematically in Fig. 1. The frequency domain Maxwell equations are to be solved inside the computational domain $\Omega$.

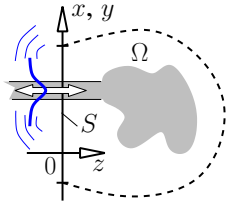


*Figure 1: An exemplary port plane $S$ constitutes part of the boundary of the domain $\Omega$. Axes $x$ and $y$ of a local coordinate system span $S$, the $z$-axis is oriented towards the interior of $\Omega$. Incoming waveguides are parallel to the $z$-axis, i.e. the exterior is $z$-homogeneous. Extension to further input/output ports is straightforward.*

Transparent influx boundary conditions (TIBCs) for the electromagnetic fields $\boldsymbol{E}$, $\boldsymbol{H}$ on $S$ can be stated as

$$\boldsymbol{E} = \sum_m 2F_m\tilde{\boldsymbol{E}}_m - \sum_m \frac{1}{N_m}\langle\tilde{\boldsymbol{E}}_m,\boldsymbol{H}\rangle\tilde{\boldsymbol{E}}_m\,,\quad \boldsymbol{H} = \sum_m 2F_m\tilde{\boldsymbol{H}}_m - \sum_m \frac{1}{N_m}\langle\boldsymbol{E},\tilde{\boldsymbol{H}}_m\rangle\tilde{\boldsymbol{H}}_m\,. \tag{1}$$

Here $(\tilde{\boldsymbol{E}}_m,\tilde{\boldsymbol{H}}_m)$ are the electric and magnetic profiles of the complete set of normal modes [1] on $S$ (partly continuous and partly discrete index $m$, the combination $(\tilde{\boldsymbol{E}}_m,\tilde{\boldsymbol{H}}_m)$ represents a wave that travels towards the interior of $\Omega$). Orthogonality properties $\langle\tilde{\boldsymbol{E}}_l,\tilde{\boldsymbol{H}}_k\rangle = \delta_{lk}N_k$ hold, with nonzero $N_k$, for the product $\langle\boldsymbol{A},\boldsymbol{B}\rangle = \iint_S(\boldsymbol{A}\times\boldsymbol{B})\cdot\boldsymbol{e}_z\,\mathrm{d}x\,\mathrm{d}y$. Modal coefficients $F_m$ specify the external influx.

A variational representation of the former problem is given by the functional

$$\begin{aligned}\mathcal{F}(\boldsymbol{E},\boldsymbol{H}) \;=\; & \iiint_\Omega \left\{\boldsymbol{E}\cdot(\boldsymbol{\nabla}\times\boldsymbol{H}) + \boldsymbol{H}\cdot(\boldsymbol{\nabla}\times\boldsymbol{E}) - \mathrm{i}\omega\epsilon_0\epsilon\boldsymbol{E}^2 + \mathrm{i}\omega\mu_0\boldsymbol{H}^2\right\}\mathrm{d}x\,\mathrm{d}y\,\mathrm{d}z \\ & - \sum_m 2F_m\left\{\langle\tilde{\boldsymbol{E}}_m,\boldsymbol{H}\rangle - \langle\boldsymbol{E},\tilde{\boldsymbol{H}}_m\rangle\right\} + \sum_m\frac{1}{2N_m}\left\{\langle\tilde{\boldsymbol{E}}_m,\boldsymbol{H}\rangle^2 - \langle\boldsymbol{E},\tilde{\boldsymbol{H}}_m\rangle^2\right\}\end{aligned} \tag{2}$$

(an expression from [1], extended by the boundary integrals; cf. the formulation for scalar 2-D second order systems with homogeneous exterior of [2]). If $\mathcal{F}$ becomes stationary, then $\boldsymbol{E}$ and $\boldsymbol{H}$ satisfy the frequency domain Maxwell equations in $\Omega$, they satisfy the TIBCs (1) on $S$, and the transverse components of both $\boldsymbol{E}$ and $\boldsymbol{H}$ vanish on all other parts $\partial\Omega\backslash S$ of the boundary.

$\mathcal{F}$ constitutes a variational basis for rigorous numerical (FEM) treatments of the scattering problems, but also for more approximate modeling: A generalized version [3] of coupled mode theory (CMT) can be derived by restricting (2) to suitable CMT field templates.

### References

[1] C. Vassallo. *Optical Waveguide Concepts*. Elsevier, Amsterdam, 1991.

[2] A. Sopaheluwakan. *Characterization and Simulation of Localized States in Optical Structures*. University of Twente, Enschede, The Netherlands, 2006. Ph.D. Thesis.

[3] M. Hammer. Hybrid analytical / numerical coupled-mode modeling of guided wave devices. *Journal of Lightwave Technology*, 2007 (submitted).

# Slow-light enhanced optical detection in liquid-infiltrated photonic crystals

M.E.V. Pedersen, L.S. Rishøj, H. Steffensen, S. Xiao, and N.A. Mortensen
*MIC- Department of Micro and Nanotechnology, NanoDTU, Technical University of Denmark, DK-2800 Kgs Lyngby, Denmark*
nam@mic.dtu.dk

**Summary**

Optical techniques are finding widespread use in chemical and bio-chemical analysis, and Beer-Lambert-Bouguer (BLB) absorption in particular has become one of the classical workhorses in analytical chemistry. During the past decade, there has been an increasing emphasize on miniaturization of chemical analysis systems and naturally this has stimulated a large effort in integrating microfluidics and optics in lab-on-a-chip microsystems, partly defining the emerging field of optofuidics. At the same time, there is an increasing attention to slow-light phenomena as well as the fundamentals and applications of light-matter interactions in electromagnetically strongly dispersive environments. We theoretically and numerically consider the classical problem of BLB absorption in a liquid-infiltrated photonic crystal.

We show how slow light in an optofluidic environment facilitates enhanced light-matter interactions, by orders of magnitude, with strong opportunities for improving existing miniaturized chemical absorbance cells. The principle of a BLB measurement is illustrated in panel (a) of Fig. 1. Since $\alpha_I$ correlates with the concentration of the absorbing chemical species, Beer's law provides optical means for detecting and quantifying the concentration of chemical solutions. Obviously, the effect relies heavily on having a sufficiently long optical path length and the longer $L$ is the lower a concentration can be monitored for a given sensitivity of the optical equipment measuring $I/I_0$. Lab-on-a-chip implementations of chemical absorbance cells are thus facing almost exhausting challenges since the miniaturization, i.e. reduction of $L$, decreases the sensitivity significantly. This problem has already been confirmed experimentally for lab-on-a-chip systems with $L$ of the order 100 to 1000 microns. In this work, we show a route to achieve enhancement factors much larger than unity, thus potentially compensating for the cost of miniaturization and reduction in optical path length.

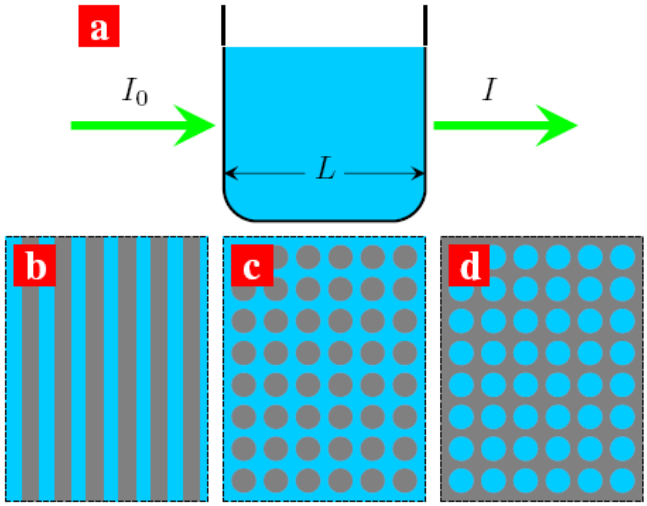


**Fig 1.** Panel (a) shows a typical BLB setup with an optical probe, with intensity $I_0$, incident on a sample with absorption parameter $\alpha_I$ due to a concentration of some chemical species. Panels (b), (c), and (d) show different examples of liquid infiltrated photonic crystals providing a strongly dispersive electromagnetic environment for the interaction light with dissolved bio molecules.

# Breakdown of Wigner-Weisskopf theory for spontaneous emission: A quantitative analysis

Philip Kristensen, Bjarne Tromborg, Peter Lodahl and Jesper Mørk
*COM•DTU, Department of Communications, Optics and Materials, Technical University of Denmark, DK-2800 Kgs Lyngby, Denmark*
ptk@com.dtu.dk

Using a Laplace transform technique we solve the equations of motion governing spontaneous emission from a two-level system in a photonic crystal structure. In this way we derive analytically an expression for the breakdown of the Wigner-Weisskopf approximation and the onset of non-Markovian decay dynamics.

## Summary

Spontaneous emission is a genuine display of the quantum mechanical nature of light-matter coupling and is described properly only in a full quantum optical model. For the two-level system the emission dynamics is governed by a complicated integro-differential equation, which includes the light-matter coupling strength, $\beta$, and the optical local density-of-states (LDOS), $\rho$ [1]. In the weak-coupling regime, the Wigner-Weisskopf approximation [2] applies, leading to an exponential decay with a rate proportional to the value of the LDOS at the emission frequency. However, if the LDOS displays strong frequency dependence, the Wigner-Weisskopf approximation may break down. In this case an emitted photon may couple back to the two-level system leading to non-Markovian decay [3]. Using a Laplace transform technique we solve the equation for an arbitrary LDOS. The figure shows examples of different model LDOS along with the corresponding decay curves.

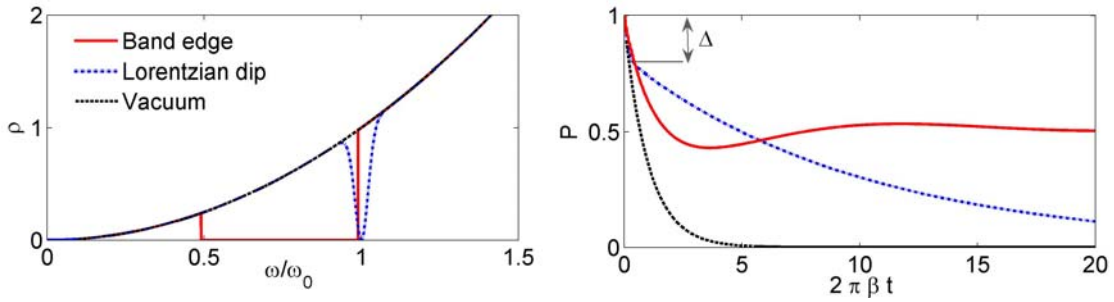


Left: Examples of different normalized LDOS; band edge (full), a Lorentzian dip (dash-dot) and vacuum (dash), which for this choice of normalization is simply $\omega^2$. In all cases, non-Markovian decay will occur only if the light-matter coupling strength is large. Right: Corresponding decay curves for the excited state occupation probability, for the case of $\beta = 10^{-3}$. In the case of the band edge the decay is fractional, corresponding to the atom-photon state decaying to a stationary entangled state.

The emission dynamics is analyzed in the frequency domain. This allows for an analytical expression for the onset of breakdown of the Wigner-Weisskopf approximation. The approach relies on the fact that if the decay is exponential, a single-pole approximation will satisfy the initial condition (leading to $\Delta = 0$ in the figure). In this way we show that $\beta d / d\omega(\rho / \omega) > 1$ is a sufficient (but not necessary) condition for breakdown of the Wigner-Weisskopf approximation. From measurements of the light-matter coupling strength in quantum dots we are in this way able to identify photonic systems in which measurements of non-Markovian decay should be possible.

## References

[1] N. Vats, S. John and K. Busch, Physical Review A. **65**, 043808 (2002).
[2] E. Wigner and V. Weisskopf, Zeitschrift für physik. **63**, 54-73 (1930).
[3] S. John and T. Quang, Physical Review A, 50, 1764-1969 (1994).

# Band Structure Calculation Methods for complex and frequency dependent Photonic Crystals

Michael Bergmair[1] and Kurt Hingerl[1]
[1] *CD-Laboratory for Surface Optics, Institut für Halbleiter- und Festkörperphysik, Universität Linz, Altenbergstraße 69, 4040 Linz, AUSTRIA*

michael.bergmair@jku.at

We use simulation techniques to derive band structure of frequency dependent photonic crystals (PC). In one dimension metallic and polaritonic PCs are investigated for all angles of incidence including surface states. Calculations can also be done for two and three dimensional systems.

## Summary

Photonic crystals are investigated in recent literature for almost twenty years. Kuzmiak et al. [1] presented two methods to derive band structure for metallic PCs. The first method is a modified plane wave expansion (PWE) where the frequency dependent dielectric function $\varepsilon(\omega)$ leads to a non-linear matrix equation which is solved by reformulating this equation to an eigenvalue problem. This method works in one, two and three dimensions but requires a large computation time.
The second method is a Kronig-Penney like description which allows to calculate the dispersion only for one dimensional PCs. In this model one uses the continuity conditions of the electric field as well as Bloch's theorem. The resulting equation allows to derive the wave number for any frequency. This yields for a frequency dependent (and via Kramers-Kronig complex) dielectric function of a PC a complex wave vector **k**. The imaginary part of the wave vector is a measure for the spatial damping.
In the following we restrict ourself to one dimensional systems where we use either a Drude model (metallic PC) or a Lorentzian dielectric function (polaritonic PC) and investigate all angles of incidence. For normal incidence there is a degeneracy between the two polarizations (TE and TM). In this case one observes an additional band gap next to the structural ones. This metallic or polaritonic band gap is located at frequencies where the dielectric function has a large imaginary part (huge absorption).
This metallic/polaritonic band gap is complete for all angles of incidence except for solutions which propagate parallel to the periodically orientated metallic/polaritonic sheets. These states exist only for the polarization where the magnetic component is parallel to the layers and are strongly connected to surface plasmons or surface polaritons. One will note that these states are coupled over adjacent layers [2]. A detailed investigation of these states, especially the propagation length, is quite difficult because a non-linear complex equation has to be solved for two variables. The results and discussion will be presented in our contribution.

## References

[1] V. Kuzmiak and A. Maradudin, Phys. Rev. B, **55** 7427, 1997
[2] M. Bergmair, M. Huber and K. Hingerl, APL, **89**, 081907, 2006

.

# Multistable Lasing in Coupled Microcavities and Nanopillar Waveguides: Mode Switching Dynamics

Sergei V. Zhukovsky[1], Dmitry N. Chigrin[1], Andrei V. Lavrinenko[2], and Johann Kroha[1]
[1] *Physikalisches Institut, Universität Bonn, Nussallee 12, D-53115 Bonn, Germany*
[2] *COM•DTU, Department of Communications, Optics and Materials, Technical University of Denmark, DK-2800 Kgs Lyngby, Denmark, ala@com.dtu.dk*

We show analytically and numerically that coupled cavity-based microresonators support multistable lasing. Each mode can be made to lase on demand by injection seeding, offering a concept for a switchable microlaser. We investigate the dynamics of mode-to-mode switching and the effects of the cavity noise.

Mode hopping and multistabilities are known to occur in lasers with a substantially broad gain profile regarding the spacing between neighboring resonator modes. Coupled microcavities, however, can be designed to support spectrally close modes with nearly identical spatial intensity distribution. In this paper, we show that this facilitates strong coupling between modes, which in turn gives rise to bi- or multistability. This is in agreement with recent experimental findings on bistable lasing in twin semiconductor microdisks [1]. We further predict analytically that in such a multistable resonator, each mode can be made to lase on demand by preparing the resonator state at the onset of laser generation, e.g., by injecting a pulse with spatial structure matching the mode symmetry (the injection seeding) [2].

These results were confirmed in FDTD numerical simulations. Switchable lasing is observed both in twin coupled defects in a photonic crystal lattice [3] and in 4-row coupled nanopillar waveguides [4]. In both cases, the mode-to-mode switching can be performed by re-seeding the resonator after having turned the pump off for a cool-down. The cool-down duration is on the order of picoseconds and is in a direct relation with the re-seeding signal amplitude (Fig. 1). This exponential relation shows an excellent agreement with the prediction of the analytical model.

Besides analyzing the mode switching dynamics, we investigate the interplay between the cavity noise, the seeding signal and the lasing onset. Time mismatch between the seeding and the onset is shown to effectively diminish the seeding, causing the noise-dominated rather than the selective lasing.

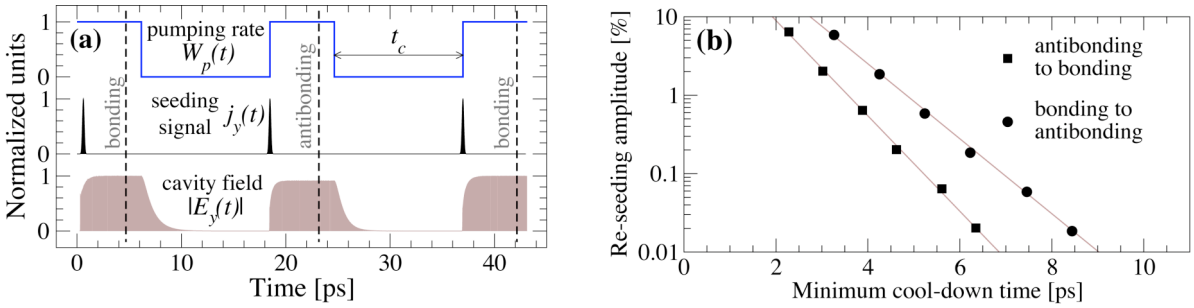


**Fig. 1. (a)** The time diagram of switching between the two modes (bonding and antibonding) in twin coupled defects; **(b)** the relation between minimum cool-down time $t_{c\,(\min)}$ and re-seeding amplitude.

## References

[1] S. Ishii and T. Baba, Appl. Phys. Lett. **87**, 181102 (2005).
[2] A.E. Siegman, *Lasers* (University Science Books, Sausalito, CA, 1986).
[3] S.V. Zhukovsky, D.N. Chigrin, A.V. Lavrinenko, and J. Kroha, arXiv:cond-mat/0701619.
[4] S.V. Zhukovsky, D.N. Chigrin, A.V. Lavrinenko, and J. Kroha, arXiv:cond-mat/0611351, to appear in Phys. Stat. Sol. (b) (2007).

# Parallelogramic metal gratings as a benchmark for the modal- and diffraction-order-based slicing techniques

M.Foresti[1, 2], A.V.Tishchenko[1]
[1] *Laboratoire Hubert Curien, 18 rue Benoît Lauras, Bâtiment F, Saint-Etienne, France, 42000*
[2] *Saint-Gobain Recherche, 39 Quai Lucien Lefranc, Aubervilliers, France, 93303 Cedex*
*maud.foresti@saint-gobain.com, tishchen@univ-st-etienne.fr*

A comparison is made between two slicing approaches for the calculation of the S-matrix of a deep 1D parallelogramic metal grating: the widely used diffraction order basis and the modal basis. The reference is given as the modal solution of the surface-relief grating as a whole.

## Summary

Diffraction on deep metal surface-relief gratings is a difficult electromagnetic problem. No reference method is known even in the 1D case except for lamellar gratings where modal methods [1, 2] are known to give an accurate solution. The technique of slicing is widely applied to calculate the diffraction S-matrix of a relief grating from the S-matrices of thin periodic sublayers considered as a shallow lamellar grating. The slicing technique is usually applied by using the basis of the diffraction orders between slices. A stable and accurate solution is always obtainable in the case of dielectric gratings, but it fails in the case of metal gratings and TM incidence.

We will show that the modal method can advantageously be used as an alternative basis in a slicing technique and that it always converges towards the exact solution. This basis is the modal space created by the modal spectra of the grating sublayers. All the S-matrices between different layers are expressed via modal amplitudes rather than those of diffracted waves. Although mentioned implicitly [2], and even explicitly [3], such potential has never been implemented to the best of our knowledge.

The contribution will focus on the numerical comparison between the two approaches for the calculation of deep relief gratings in cases where an exact reference method exists. The first type of examples is binary rectangular gratings. The second type of examples refers to parallelogramic grooves of which we have previously reported the rigorous modal solution [4] which will serve as a reference. Critical examples will be shown where the diffraction-order-based technique always fails and where the modal-based technique always converges towards the exact solution. We believe that this is a breakthrough which can now safely open to diffraction problems involving 1D metal gratings of arbitrary profile and composition. Further evidence of this will be reported during the talk.

## References

[1] L. C. Botten, M. S. Craig, R. C. McPhedran, J. L. Adams, and J. R. Andrewartha, “The dielectric lamellar diffraction grating,“ 1981, Optica Acta, **28**, 413-428.
[2] M. G. Moharam, T. K. Gaylord, “Diffraction analysis of dielectric surface-relief gratings,” J. Opt. Soc. Am., **72**, 1385-1392 (1982)
[3] J. Y. Suratteau, M. Cadilhac, and R. Petit, “Sur la détermination numérique des efficacités de certains réseaux diélectriques profonds, “ 1983, J. Opt. (Paris), **14**, 273-288.
[4] M. Foresti, A. V. Tishchenko, “Exact solution to diffraction on a grating with parallelogramic grooves by the true modal method, “Proc. SPIE, **6182**, p. 319-328 (2006).

# Competing quadratic and cubic nonlinear phenomena in metamaterials

D. de Ceglia[1,2], A. D'Orazio[1], M. De Sario[1], V. Petruzzelli[1],
F. Prudenzano[3], M. A. Vincenti[1], M. G. Cappeddu[4], M. J. Bloemer[2], M. Scalora[2]

[1] *Dipartimento di Elettrotecnica ed Elettronica,Politecnico di Bari, Via Orabona 4, 70125 Bari-Italy*
deceglia@deemail.poliba.it

[2] *Charles Bowden Research Centre, Redstone Arsenal, Bldg. 7804, Huntsville, 35803 AL-USA*
[3] *Dipartimento di Ingegneria dell'Ambiente e per lo Sviluppo Sostenibile, Politecnico di Bari, Viale del Turismo 8 74100, Taranto-Italy*
[4] *Università di Roma, Dipartimento dei Materiali, via Eudossiana 18, I-00184 Rome- Italy*

In this paper we discuss nonlinear, multi-harmonic conversion processes in metamaterials with quadratic and cubic nonlinear responses. Particular attention is devoted to metallic-based structures, for the enhancement of nonlinear effects.

## Summary

Until now studies on second and third order nonlinear effects in metamaterials have been conducted separately. In particular, it has been demonstrated that dedicated designs of these artificial materials can lead to strong quadratic, or cubic nonlinear responses [1]. Significant second harmonic generation has been predicted in negative index metamaterials even in the presence of large linear absorption [2]. Furthermore it has been shown that the large values of nonlinear coefficients of metals can be accessed by using metallo-dielectric stacks [3]. In this work we numerically investigate nonlinear pulse propagation in metallic-based metamaterials in order to ascertain how simultaneous effects due to quadratic and cubic nonlinearities alter the frequency conversion process. We observe these phenomena in different operational regimes corresponding to different values of the second and third order nonlinear coefficients. Self-phase modulation, quadratic cascaded effects and multi-harmonic generation are analyzed under these unusual conditions.

## References

[1] I. V. Shadrivov, S. K. Morrison, and Yu. S. Kivshar, Opt. Express **14**, 9344-9349 (2006); M. Lapine, M. Gorkunov, and K. H. Ringhofer, Phys. Rev. E **67**, 065601 (2003).
[2] M. Scalora, G. D'Aguanno, M. J. Bloemer, M. Centini, D. de Ceglia, N. Mattiucci, and Y. S. Kivshar, Opt. Express **14**, 4746 (2006).
[3] R.S. Bennink, Y.K. Yoon, R.W. Boyd, J.E. Sipe, Opt. Lett. **24**, 1416 (1999); N.N. Lepeshkin, A. Schweinsberg, G. Piredda, R.S. Bennink, R.W. Boyd, Phys. Rev. Lett. **93**, 123902 (2004); M.C. Larciprete, C. Sibilia, S. Paoloni, M. Bertolotti, F. Sarto, and M. Scalora, Jour. of App. Phys. **93**, 5013 (2003); M. Scalora, N. Mattiucci, G. D'Aguanno, M.C. Larciprete, and M.J. Bloemer, Phys. Rev. E **73**, 016603 (2006).

# An adaptive finite element method for the optimization of photonic crystal fibers

S. Burger, J. Pomplun, F. Schmidt

Group Computational Nano-Optics (CNO), Division Scientific Computing, Department Numerical Analysis and Modelling, Konrad-Zuse-Zentrum für Informationstechnik Berlin (ZIB) Berlin-Dahlem, Germany
*frank.schmidt@zib.de*

We discuss the optimization of the design of hollow-core photonic crystal fibers with respect to low loss and high damage threshold. Design and geometry optimization have been performed by the European Southern Observatory, whereas we developed the numerical components. The forward solver consists of a combination of automatic triangulation, a vectorial high order finite element discretization and error-controlled adaptive grid refinement, the optimization loop employs standard multidimensional minimization procedures. The optimal solution shows a 99.8% power fraction within the air core.

# Transformation of Radiating Cylindrical Waves between Skew Axes and Application to an Optical Fiber Helix

I. D. Chremmos [1] and N. K. Uzunoglu[1]
[1] *Microwave and Fiber Optics Laboratory, School of Electrical and Computer Engineering*
*National Technical University of Athens, 9 Iroon Polytechniou Str., Zografos 15780, Athens, Greece*
jochremm@central.ntua.gr

The transformation of radiating cylindrical waves between two cylindrical coordinate systems with skew axes, recently derived by the authors, is reviewed in detail. As an application, an elegant analytical solution for the evanescent field of an optical fiber helix is presented for the first time.

## Summary

The transformation of radiating cylindrical waves (Hankel function radial dependence) between two cylindrical coordinate systems with skew (non-parallel) axes was recently derived by the authors and is here reviewed [1]. This generalizes the classic Graf's addition theorem for Hankel functions , which has been extensively used, in the past 100 years, to express cylindrical waves in a displaced polar coordinate systems. The analytical proof of the new theorem is based on the fundamental complex integral representation of Hankel function. An appropriate deformation of the integration contour and change of variables is applied to obtain a Fourier transform expression of the cylindrical wave around the new system with skew axis.

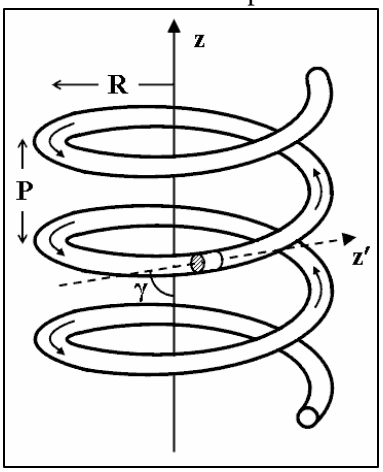


The transformation was derived in the framework of the first rigorous EM analysis of the coupling between two non-parallel optical fibers [2]. As a new application in this presentation, an elegant analytical solution for the evanescent field of an optical fiber helix (Figure) is attempted for the first time. The structure has been recently studied from a different point of view [3]. Here we are interested in the external field produced by the fiber helix. In the absence of external sources, the electric field anywhere in the structure, is given by the familiar integral inside the fiber volume, resulting from Green's theorem:

$$\mathbf{E}(\mathbf{r}) = (k_f^2 - k_0^2)\iiint \underline{\mathbf{G}}_0(\mathbf{r},\mathbf{r}')\cdot\mathbf{E}(\mathbf{r}')dV'$$

where $\underline{\mathbf{G}}_0$ is free-space dyadic Green's function. The field inside the fiber $\mathbf{E}(\mathbf{r}')$ is assumed to be that of a straight fiber, which is reasonable for weakly coupled helix turns (sufficiently large helix pitch P) and small bending loss (sufficiently large helix radius R and high glass-air relative index contrast) [3]. To compute the integral, the cylindrical waves produced by any elementary fiber slice (Figure) must be expressed in the central global coordinate system of the helix axis, so that they can be added. A helix has the property of constant angle of elevation (p/2–?), and, therefore, the utilization of the derived transformation allows an analytical expression for the total field, after integrating along the infinite fiber helix. A further complicated periodic segmentation of the fiber length must be employed for the field in the region $\rho > R$. Fully analytical final expressions for the vector field anywhere outside the fiber are derived, which are reported for the very first time to our knowledge.

## References

[1] I. Chremmos and N. Uzunoglu, J. Opt. Soc. Am. A **23**, 1884-1888 (2006).
[2] I. Chremmos *et al.*, IEEE J. Lightwave Technol. **24**, 3779-3788 (2006).
[3] M. Sumetsky, Opt. Express **12**, 2303-2316 (2004).

# Air-clad fibers: pump absorption assisted by chaotic wave dynamics

Niels Asger Mortensen
*MIC- Department of Micro and Nanotechnology, NanoDTU, Technical University of Denmark, DK-2800 Kgs Lyngby, Denmark*
nam@mic.dtu.dk

**Summary**

Air-clad fibers have a huge potential for high-power fiber lasers and amplifiers. The large index contrast between air and silica makes the cladding support pump light of very high numerical aperture, thus facilitating pumping by relatively cheap high-NA pump sources [1]. The pump light is corralled by the air-clad and while light propagates down the fiber, photons are absorbed and converted to stimulated emission by a rare-earth doped fiber core at the center of the inner cladding. Skew rays or whispering gallery modes are well-known obstacles to efficient pump absorption since they do not have a significant overlap with the core. Such modes are particular inherent to cylinder symmetric fiber geometries, such as standard MCVD-fabricated fibers. Typically, the problem is circumvented by breaking the high cylindrical symmetry and D-shaped claddings have become a standard approach to suppression of skew rays. More generally, geometries which are classically chaotic will favor strong pump absorption. In the ergodic limit, absorption scales as $A_c/A_{cl}$, where $A_c$ is the area of the absorbing rare-earth doped core and $A_{cl}$ is the area of the inner cladding. Pump absorption in air-clad fibers is typically very high and it has been speculated [1] that this is coursed by chaotic ray dynamics. Non-integrable air-clad geometries seem to be inherent to the fabrication method where the shapes of the air holes arise in an interplay and competition of e.g. the glass viscosity and glass-air surface tension. Fig. 1 illustrates one example of an air-clad fiber [2] which has a classically chaotic geometry with a convex boundary (from the point of view of the pump light) which will scatter incident waves in a highly indeterministic way. In this work we use finite-element simulations to show how the wave dynamics has fingerprints inherited from the classically chaotic geometry.

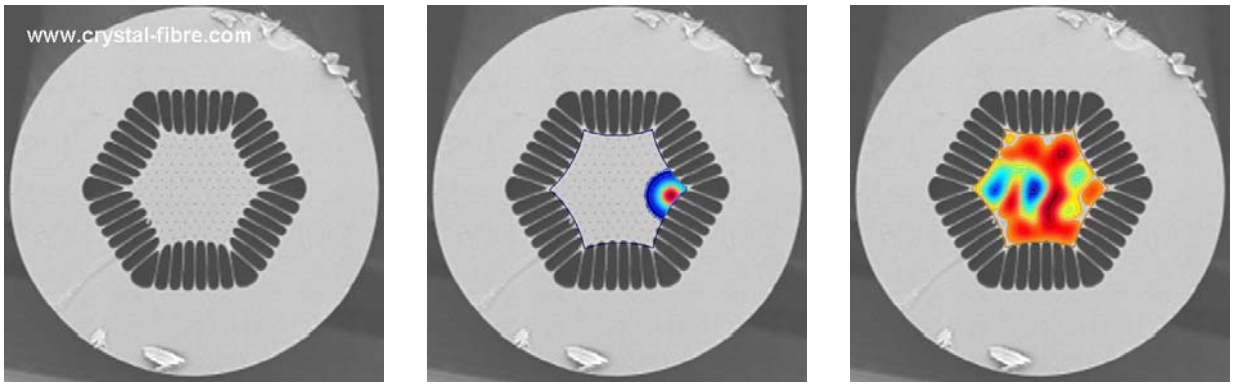


Fig. 1. Scanning-electron micrograph of the cross section of an air-clad fiber [1]. The pump light is corralled by an inner cladding with a diameter of the order 180 microns. Conversion to stimulated emission occurs by absorption in a 30 micron ytterbium-doped core in the centre of the fiber. The superimposed simulations show chaotic wave dynamics of a Gaussian pump excitation.

**References**

[1] J. Broeng *et al.*, Proc. SPIE **5335**, 192 (2004).

[3] J. Limpert *et al.*, Opt. Express **11**, 818-823 (2003).

# Spectral properties of splay-aligned mesogens in Liquid Crystal Photonic Bandgap Fibres

Giovanni Tartarini[1,3], Roberta Palermo[1], Francesca Cornazzani[1], Thomas Tanggaard Alkeskjold[2], Anders Bjarklev[2], Paolo Bassi[1,3]

[1] *DEIS, University of Bologna, Viale Risorgimento 2, 40136 Bologna, Italy,*
[2] *COM•DTU, Technical University of Denmark, DK-2800 Kgs Lyngby, Denmark*
[3] *also with MIST.E-R, Laboratory for MIcro and Submicro enabling Technologies of Emilia-Romagna*

Through a detailed electromagnetic analysis we investigate the characteristics of Liquid Crystal infiltrated Photonic Crystal Fibers guiding by the Photonic Bandgap effect (LC-PCFs). Spectral features related to the so-called splay-alignment of LC mesogens will be analyzed.

## Summary

Many applications of LC-PCFs have been demonstrated in communications, sensing and signal processing [1,2] or can be envisaged, based on the many interesting optical properties of LCs.

An important physical aspect to be analyzed using LCs of both Nematic or Smectic mesophases is the orientation of the mesogens which fill the capillary holes. Besides the axial orientation (i.e. parallel to the capillary as well as to the waveguide axis *z*), a variety of molecular alignments is possible, related for example to their chirality or non-chirality and/or to their interaction with the surface of the capillary hole. One important aspect is the possibility to induce a gradual inclination of the mesogens against the z axis, which is increasing going from the center of the holes to the surface of the capillary, and has a circular symmetry inside the hole itself; the so-called splay-alignment. For some LC's this arrangement may be the natural one, determined by minimizing the free energy of the LC, or it may also be pursued through appropriate capillary coating techniques. Splay-alignment is in some devices favorable since this gives a more controllable behavior when external fields are applied [2].

We have performed a theoretical study of the characteristics of LC-PCFs when the mesogens of the LC exhibits the above described disposition. To this purpose, we utilize a numerical simulator, based on the Finite Element Method (FEM), which, thanks to the particular solutions adopted, is particularly useful in the accurate study of guided and leaky modes in waveguiding structures which exhibit a general anisotropy [3].

We will show that the range of wavelengths where the Band Gap Effect can be observed and exploited is greatly influenced by the degree of tilting of the mesogens. A particularly interesting result is that this causes a shift towards longer wavelengths of the short wavelength bandgap edge, while the long wavelength bandgap edge is practically not influenced by the mesogens tilting. Through a detailed analysis of the modes supported by the LC-PCFs, all the presented results will be motivated from a rigorous electromagnetic point of view. The predictions coming from this work are of use in view of an actual realization and characterization of capillary coated LC-PCFs.

## References

[1] L. Scolari, T. T. Alkeskjold, D. S. Hermann, A. Anawathi, M. D. Nielsen, A. Bjarklev, J. Riishede and P. Bassi, Optics Express, vol. 13, 7483-7496, (2005)

[2] T. T. Alkeskjold, Ph.D. Thesis, Research Center COM, DTU (2005)

[3] G. Tartarini, R. Stolte, H. Renner, Optics Communications, vol. 253, 109-117 (2005)

# Modeling Photonic Crystal and Plasmonic Devices

Shanhui Fan

Ginzton Laboratory, Stanford University
Stanford, USA
*shanhui@stanford.edu*

Abstract not available

# On Meta-Meta-Materials – an approach for magnetic resonances in the visible

C. Rockstuhl[1], T. Scharf[2], T. Pertsch[1], and F. Lederer[1]

[1] *Friedrich-Schiller-Universität Jena, Max-Wien-Platz 1, 07743 Jena, Germany*
carsten.rockstuhl@uni-jena.de

[2] *University of Neuchâtel, Rue A.-L. Breguet 2, 2000 Neuchâtel, Switzerland*

We present a new approach to observe magnetic activity in the visible. We employ Mie resonances in spheres that are made of an appropriately designed Meta-Material to obtain the necessary high permittivity.

**Summary**

Meta-Materials (MMs) are artificially structured media aimed to provoking a tailored response to an external wave-field. In most cases a top-down approach is applied for their fabrication. For MMs operating in the visible usually metallic nanostructures are sculptured using time and cost intensive techniques. Alternatively, MMs were proposed that base on Mie-resonances excited in closely packed spheres made of materials with a high permittivity, e.g. polaritonic materials. However, such polaritonic materials have there resonances providing the necessary large permittivity in the far-infrared. Hence, exploiting this concept in the visible appears to be impossible. To gap this bridge we present a genuine bottom-up approach to obtain a negative permeability in the visible. We employ a medium composed of densely packed spheres. The sphere material derives its properties from a MM itself; hence the term Meta-Meta-Material (MMM) is introduced. As the MM we employ densely packed metallic nanoparticles, where the medium shows a Lorentzian resonance in the effective permittivity in the spectral vicinity of the collective plasmon resonance. The different levels of the design are shown in Fig. 1. Various computational tools are applied for the rigorous simulation of the material and compared to effective medium theories.

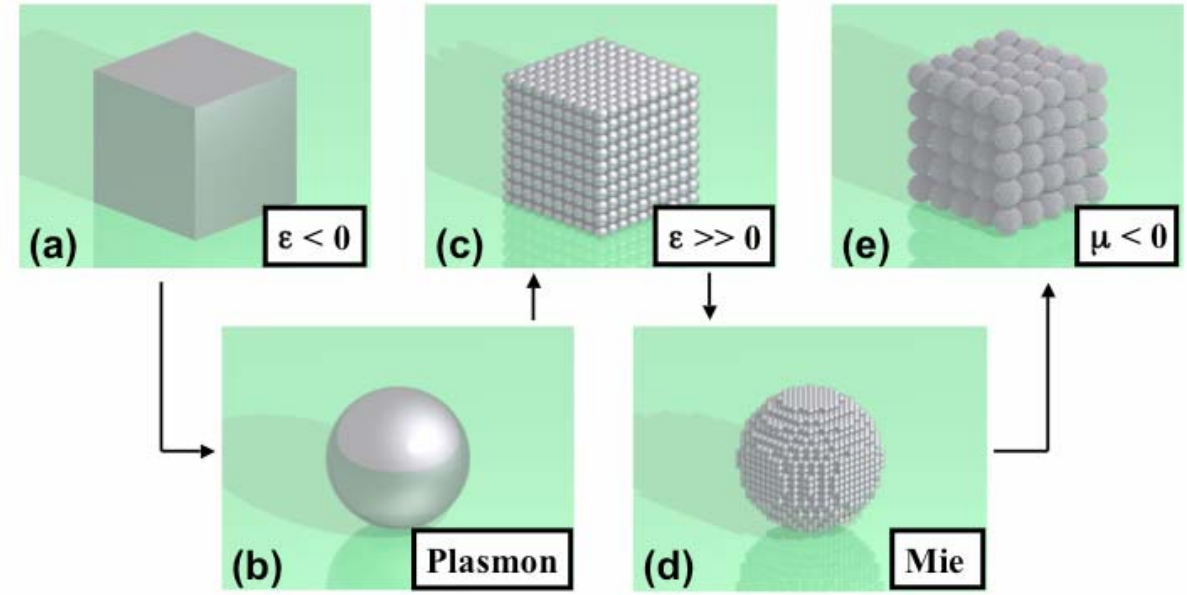


Fig. 1: Sketch of the various levels used for constructing a Meta-Meta-Material. Out of noble metals (a) nanoparticles are made, which support plasmonic resonances (b). A material made of those nanoparticles (c) shows a strong dispersion in the permittivity. Assembled spheres from this MM (d) allows for a strong excitation of a Mie-resonance in the magnetic mode of the assembly. When such spheres are densely packed (e) a medium with negative effective permeability in the spectral domain of this Mie-resonance is obtained.

# Tailoring group velocity by topology optimization

Roman. Stainko[1] and Ole Sigmund[2]

[1] *MAT•DTU, Department of Mathematics, Technical University of Denmark, DK-2800 Kgs Lyngby, Denmark*

*roman.stainko@mat.dtu.dk*

[2] *MEK•DTU, Department of Mechanical Engineering Solid Mechanics Section, Technical University of Denmark, DK-2800 Kgs Lyngby, Denmark*

In this work we show how the group velocity of a constructed guided mode can be tailored using the method of topology optimization. We will explain the numerical modelling of the optimization method and present some examples of photonic crystals with tailored dispersion properties.

## Summary

Interesting phenomena of photonic crystals (PhCs), like bandgaps and waveguiding, have lead to a tremendous increase of research interest in this area. High-end functionalities in electro-optical circuits urge to optimize these structures. So far mostly trial and error methods have been applied to improve the behaviour of the PhCs components, like e.g. to maximize the bandgap of PhCs or to reduce the losses of waveguides in PhCs. Recently also topology optimization was applied to synthesize e.g. high transmission waveguide bends and junctions.

In this work we extend the topology optimization method not only to create a bandgap around an a-priorily chosen guided mode, but also to have the possibility to tailor the group velocity of the guided mode in the slow-light regime below the light line.

To achieve that goal we do not solve the eigenvalue problem given by the Helmholtz equation but rather excite the system for a given wave vector and a given frequency. Then we maximize the confinement factor of the resulting field in the defect core with respect to the given excitement, wave vector and frequency. By choosing several pairs of frequencies and wave vectors the optimization progress yields a guided mode that is defined by these pairs. For the analysis of the excited system we apply a Galerkin finite-element procedure using standard quadratic bilinear elements. The optimization problem is solved with a mathematical programming tool, the method of moving asymptotes, in combination of the sensitivities of the objective function and some additional constraints. In order to benefit from a fast optimization method, the sensitivity analysis is done analytically using the adjoint method. To ensure that the final optimal designed PhCs with the wanted dispersion properties can be manufactured we apply filter methods that rule out the possibility of too fine scaled structures to appear.

In the presentation we will discuss the modelling of the method as well as the numerical aspects of the optimization in greater detail. We will finish with some examples and animations, showing the potential of the new method.

# Accurate Analysis of Modal and Leaky Characteristics of Silicon-on-Insulator Photonic Wires

Hung-chun Chang, Sen-ming Hsu, and Chin-ping Yu
*Department of Electrical Engineering, Graduate Institute of Electro-Optical Engineering, and Graduate Institute of Communication Engineering, National Taiwan University, Taipei, Taiwan 106-17, R.O.C.*
hcchang@cc.ee.ntu.edu.tw

Consistent analysis results for guided modes on silicon-on-insulator photonic wires are achieved by using full-vectorial finite-element and finite-difference solvers with perfectly matched layer (PML) boundaries. Two different wire structures are considered and highly accurate substrate leakage losses are presented.

## Summary

Photonic wires, or photonic wire waveguides, are high index contrast optical waveguides with core region of sub-micron cross-sectional sizes. We consider the silicon-on-insulator (SOI) structures, with the waveguide cross-section as shown in Fig. 1. Such structure is promising for achieving future high-density integrated photonic circuits [1]. We analyze the structure in detail using two different methods, the finite-element imaginary-distance beam propagation method (FE-ID-BPM) [2] and the Yee-mesh-based finite-difference frequency-domain (FDFD) method [3]. In the FE analysis, linear tangential and quadratic normal (LT/QN) basis functions are employed. In the FDFD solver, proper boundary condition matching is performed across the dielectric interfaces [3]. Thus, both methods are highly accurate. And the PML absorbing boundary conditions have been incorporated into the numerical models so that leakage properties of the modes can be determined. The thickness of the silicon core is 220 nm. We vary the core width from $w$ = 300 to 500 nm and the $SiO_2$ layer from $d$ = 0.75 to 3 μm and examine the substrate leakage losses of the fundamental mode. Although $w$ is small, we find that the horizontal half width of the computational domain should be at least 5 μm to reach correct values for the leakage loss. In our calculation, the numerical accuracy of the leakage loss can be down to $10^{-15}$ dB/cm, and the agreement between the results from the two methods confirms the correctness of the calculation. We have also developed a power flow diagram to illustrate the Poynting power flow in the transverse plane and to examine the effect of the size of the computational domain on the analysis results. We have also studied another wire structure with square silicon core embedded entirely in the $SiO_2$ cladding [4]. The propagation characteristics for both horizontal and vertical polarizations have been examined.

## References

[1] P. Dumon, W. Bogaerts, V. Wiaux, J. Wouters, S. Beckx, J. V. Campenhout, D. Taillaert, B. Luyssaert, P. Bienstman, D. V. Thourhout, and R. Baets, IEEE Photon. Technol. Lett. **16**, 1328-1330 (2004).
[2] K. Saitoh and M. Koshiba, IEEE J. Quantum Electron. **38**, 927-933 (2002).
[3] C. P. Yu and H.C. Chang, Opt. Express **12**, 6165-6177 (2004).
[4] F. Grillot, L. Vivien, S. Laval, and E. Cassan, J. Lightwave Technol. **24**, 891–896 (2006).

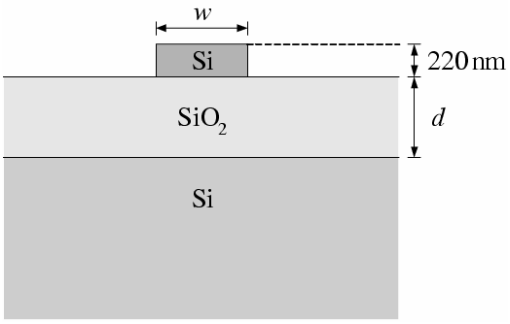


Fig. 1. Cross-section of SOI photonic wire waveguide.

# SOI grating structure for perfectly vertical fiber coupling

Günther Roelkens (1), Dries Van Thourhout (2), Roel Baets (3)
1) Photonics Research Group, Ghent University-IMEC, Sint-Pietersnieuwstraat 41, B-9000 Ghent,
gunther.roelkens@intec.ugent.be
2) Photonics Research Group, Ghent University-IMEC, Sint-Pietersnieuwstraat 41, B-9000 Ghent,
dries.vanthourhout@intec.ugent.be
3) Photonics Research Group, Ghent University-IMEC, Sint-Pietersnieuwstraat 41, B-9000 Ghent,
roel.baets@intec.ugent.be

**Abstract:** *We present the design of a grating coupler structure allowing efficient coupling to a perfectly vertically positioned single mode fiber. This design no longer implies tilting of the fiber to avoid a large second order reflection, reducing the cost of packaging. By incorporating a slight asymmetry in the grating structure design, a grating fiber coupling efficiency of 50% to single mode fiber and 65% to high numerical aperture fiber can be obtained, with a 3dB bandwidth of 55nm. Constraints in the design are related to the manufacturability using 248nm deep UV lithography. The fabrication tolerance of the device is assessed, which is compatible with the state-of-the-art Silicon processing techniques.*

## Introduction

Silicon-on-Insulator (SOI) is emerging as the platform for large scale integration of optical functions due the high omni-directional refractive index contrast between the Silicon core ($n_{Si}$=3.476) and the $SiO_2$ cladding ($n_{SiO2}$=1.447). Moreover, standard CMOS technology can be used to fabricate these photonic integrated circuits, increasing the reproducibility and yield, and lowering the cost of fabrication due to the economy of scale [1]. An inherent drawback of the high omni-directional refractive index contrast is however the large mismatch in mode size between the SOI waveguide and the single mode fiber, making efficient optical coupling to the photonic integrated circuit a non-trivial task. A promising approach is the use of a grating structure to couple the light from a single mode fiber into the photonic integrated circuit. This approach allows wafer scale testing of the integrated circuit as no polished facet is required for coupling [2]. Although one-dimensional grating structures behave very differently for TE and TM polarization, two-dimensional grating structures can be used to tackle this problem by using a polarization diversity approach [3]. Several grating designs are described in literature, both based on vertically etched slits in the Silicon waveguide layer [2] as on slanted grating structures [4]. While the latter directly enable the use of a perfectly vertically oriented optical fiber, the definition of the angled slits is not compatible with standard CMOS processing. Recently, we showed that high coupling efficiency to optical fiber can be obtained using vertically etched slits by optimizing the grating design [5]. A uniform grating structure exhibiting a fiber coupling efficiency of 66% was designed, while using a non-uniform grating structure 78% coupling efficiency could be obtained. The coupling efficiency was in this case dramatically improved by locally adding a Silicon epitaxial layer on top of the 220nm thick single mode Silicon waveguide layer prior to grating etching. However, these designs relied on slightly tilting the optical fiber with respect to the vertical axis (typically 10 degrees off vertical). This was required to avoid a large second order Bragg reflection back into the SOI waveguide in the case of perfectly vertical coupling, which dramatically reduces the fiber coupling efficiency. This can also be understood from symmetry considerations, as equal coupling efficiency in both exit waveguides of the grating structure is obtained when perfectly vertically illuminating a uniform grating structure, resulting in an absolute maximal fiber coupling efficiency of 50%. The requirement of the slight tilting of the optical fiber has important consequences for practical applications, which would require angled polishing of the fiber ferrule and mounting of the ferrule under an angle with respect to the photonic integrated circuit normal direction [6]. In order to avoid this costly complication in the packaging of the photonic integrated circuit, the possibility for perfectly vertical coupling in an efficient way is assessed here, by designing an asymmetric grating structure in order to avoid the large second order Bragg reflection. The grating structure can be made asymmetric by tailoring the width and pitch of the individual grating teeth. This is however not interesting from a fabrication point of view, as the practical realization of these type of structures is hampered by the different etch rate for slits with a different width and optical proximity effects in the lithographic definition of the non-uniform grating structure. In this paper, we will combine the previously mentioned approach of locally adding a Silicon epitaxial layer to improve the fiber coupling efficiency and incorporating an asymmetry in the grating coupler structure to avoid the large second order Bragg reflection, while maintaining a uniform grating structure in which all slits are identical in width and etch depth.

## Proposed device structure

The structure we propose to allow efficient vertical fiber coupling is schematically depicted in figure 1. A 220nm Silicon waveguide core layer on top of a 2μm buried $SiO_2$ layer is assumed. Locally, a Silicon epitaxial layer of thickness *t* is grown in order to in-

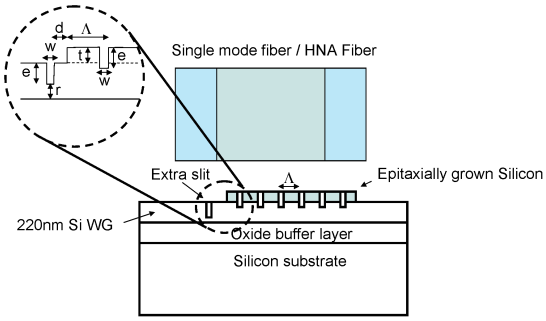


**Fig. 1:** Layout of the proposed fiber coupler structure together with a definition of the different parameters of the design

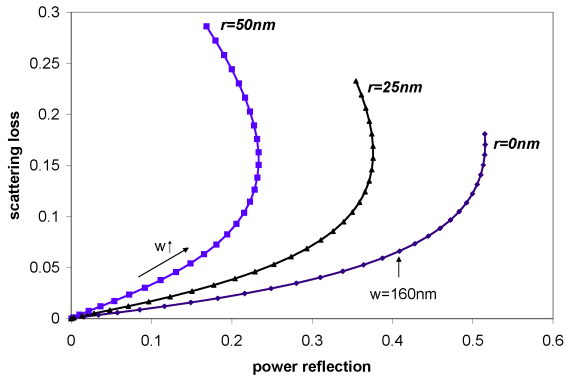


**Fig. 2:** Scattering loss of a single slit in a 220nm SOI waveguide as a function of the power reflection for various slit widths and etch depths

crease the directionality of the grating (being the ratio of the upwards diffracted optical power to the total diffracted power) as explained in [5]. The asymmetry in the grating structure is created by etching one additional slit in the 220nm thick Silicon waveguide layer instead of in the thicker epitaxial layer stack. This slit will function as a partially reflecting mirror to achieve destructive interference of the second order Bragg reflection from the uniform grating structure.

## Optimization of the device structure

The grating structure was optimized using CAMFR [7], a two-dimensional fully vectorial eigenmode expansion tool. A wavelength of 1.55µm and TE polarization is assumed. As mentioned before, these grating structures are very polarization dependent, a problem that can be circumvented using a two-dimensional grating for polarization diversity operation [3]. Therefore, we will only discuss the results for TE polarization here. An analogous approach can be followed for two-dimensional grating structures. The behaviour of the etched slit in the 220nm thick Silicon waveguide layer as a partially reflecting mirror was assessed by calculating power reflection and scattered optical power as a function of the slit etch depth, using the slit width $w$ as a parameter. Results are shown in figure 2 for three different etch depths, corresponding to $r$=0 (etched through the Silicon waveguide layer), $r$=25nm and $r$=50nm. From this simulation it is clear that the completely etched

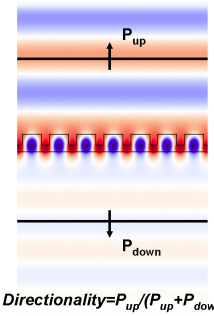


**Fig. 3:** Electric field of the vertically leaky Bloch mode with optimized directionality

through slit offers the largest reflection for a given acceptable scattering loss. Therefore, in the subsequent analysis, the slit is assumed to be etched completely through the 220nm Silicon waveguide layer. This assumption also fixes the slit etch depth in the uniform grating structure to 220nm, for ease of fabrication as explained above. In order to keep the scattering losses low while maintaining a sufficient reflection, the minimum definable slit width using 248nm deep UV lithography of 160nm was chosen for the design. This then also fixes the slit width $w$ of the diffractive grating structure in the thick Silicon layer stack to 160nm. In a second step of the optimization, the thickness of the epitaxially grown Silicon $t$ and the period of the grating structure Λ were optimized to achieve diffraction in the vertical direction at 1.55µm while maximizing the directionality (the ratio of upwards diffracted optical power to the total diffracted power) of the grating at this wavelength. This can be done by evaluating the Bloch modes at the Γ-point supported by the periodic grating structure and assessing the directionality of these leaky modes. Optimal directionality and vertical coupling at 1.55µm was obtained for a Silicon epitaxial layer thickness $t$ of 150nm and a grating period Λ of 560nm. The electric field of this TE Bloch mode is plotted in figure 3. The directionality of the optimized grating structure is higher than 80%. In order to appreciate the influence of the additional slit on the fiber coupling efficiency, the symmetric grating structure without the additional slit was simulated first. The fundamental TE mode at 1.55µm was launched in the SOI waveguide and the scattering by the grating structure was evaluated. In order to obtain the coupling efficiency to a single mode optical fiber, the electric field $\mathbf{E}_{scat}$ at a certain distance above the grating structure was evaluated and the overlap integral of $\mathbf{E}_{scat}$ and a Gaussian beam, with its mode field diameter ($1/e^2$ intensity width) as a parameter, was evaluated. This was done for various center positions of the Gaussian beam profile, thereby obtaining the optimal position of the optical fiber, the optimal mode field diameter and the maximum achievable fiber coupling efficiency. For the uniform grating structure without the additional slit and the parameters mentioned above, a fiber coupling efficiency of 33% and 26% is obtained for a mode field diameter

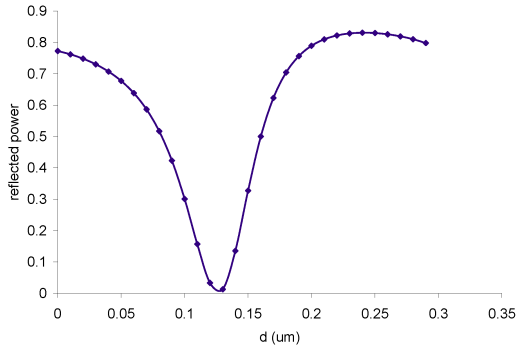


**Fig. 4:** Influence of the extra slit distance *d* on the power reflection in the SOI waveguide

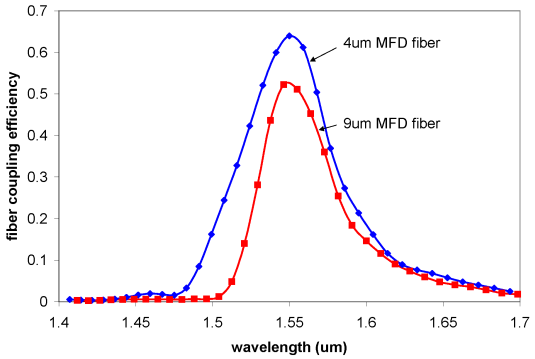


**Fig. 5:** Optimized fiber coupling efficiency as a function of wavelength for a 4µm and 9µm mode field diameter fiber

of 4µm and 9µm respectively. Reduced mode field-diameters can be obtained by splicing a high numerical aperture fiber to a single mode fiber with low optical loss at the splice [8]. This low coupling efficiency is, as mentioned above, due to the large second order Bragg reflection (55% in this case). In order to achieve destructive interference of this reflection in the proposed design, the distance *d* between the slit and the edge of the thickened layer stack needs to be optimized. The power reflection as a function of the distance *d*, for the parameters mentioned above, is plotted in figure 4. This simulation shows that nearly perfect destructive interference can be obtained by choosing an optimal distance *d* of 0.13µm. Using this optimal set of parameters, the coupling efficiency can be reassessed. The wavelength dependence of the fiber coupling efficiency is plotted in figure 5 for the case of a 4µm and 9µm mode field diameter fiber, showing that a fiber coupling efficiency of 65% and 50% can be obtained respectively, with a 3dB bandwidth of approximately 55nm, while the 1dB bandwidth is about 35nm. This implies a 3dB improvement in coupling efficiency over the symmetric grating structure. A field plot of the optimized structure, when illuminated by the 4µm diameter high numerical aperture fiber is shown in figure 6.

**Fabrication tolerance analysis**

In order to assess the manufacturability of the device using standard 248nm deep UV lithography, the

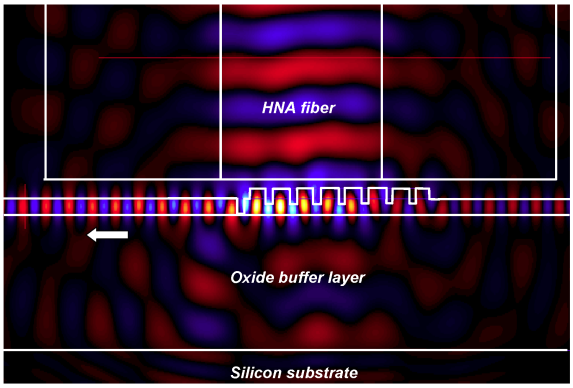


**Fig. 6:** Electric field plot of the optimized structure for a 4µm mode field diameter fiber

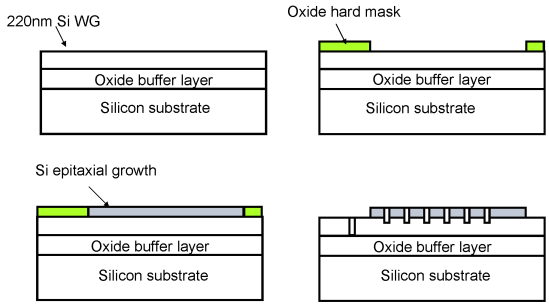


**Fig. 7:** Proposed processing sequence for the device

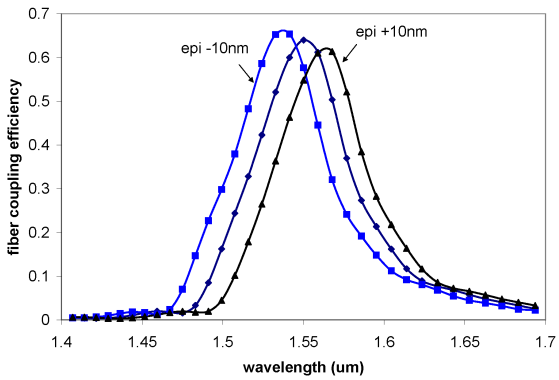


**Fig. 8:** Influence of a +/-10nm error of the epitaxial layer thickness on the fiber coupling efficiency spectrum (4µm mode field diameter fiber)

influence of deviations from the optimized design on the fiber coupling efficiency spectrum was evaluated. To see where deviations can originate from, an overview of the proposed processing scheme for the device is shown in figure 7. After deposition of an $SiO_2$ hard mask, Silicon is epitaxially grown in an opened window. After epitaxial growth, the grating structure is lithographically patterned in a photoresist layer and etched into the Silicon. By optimizing the exposure dose and applying a proximity correction to the grating structure on the mask, the dimensions of the fabricated slits can approach the optimal values. The epitaxial growth and the etching process are time based processes and a typical deviation of +/- 10nm from the targeted values can be expected. Moreover, the alignment of the grating with respect to the

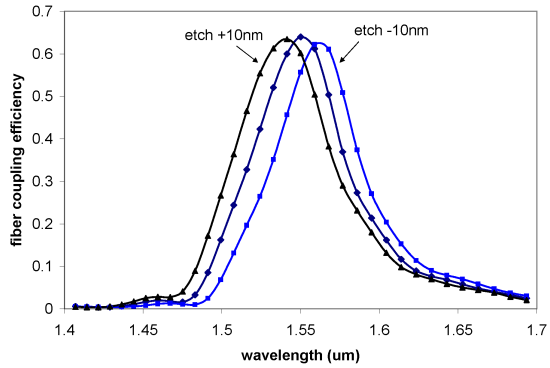


**Fig. 9:** Influence of a +/-10nm error of the slit etch depth on the fiber coupling efficiency spectrum (4µm mode field diameter fiber)

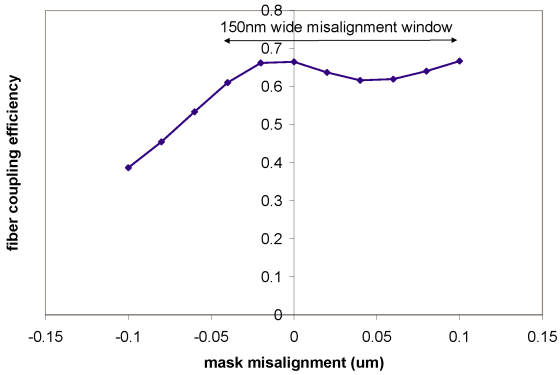


**Fig. 10:** Influence of the mask misalignment on the obtainable fiber coupling efficiency for a 4µm mode field diameter fiber

window of epitaxially grown Silicon can vary. Typically, an alignment accurary of +/-50nm can be obtained. Finally, a non-optimal position of the optical fiber results in a decrease in fiber coupling efficiency. The influence of a +/- 10nm variation on the epitaxial Silicon thickness *t* and the grating etch depth *e* is plotted in figure 8 and 9 respectively. As the additional slit is etched completely through the Silicon waveguide layer, reaching the $SiO_2$ etch stop layer, this additional slit cannot be overetched. From these simulations we can conclude that these deviations mainly result in a shift in the wavelength spectrum. In figure 10, the influence of misalignment of the epitaxial Silicon window and the grating structure on the fiber coupling efficiency at 1.55µm is plotted. From this simulation it is clear that there is a sufficiently large window for high efficiency coupling. The influence of the position of the optical fiber on the fiber coupling efficiency is plotted in figure 11. Although a higher coupling efficiency can be obtained for the reduced mode field diameter fiber, alignment tolerances are stricter in this case.

## Conclusions

In this paper we developed a Silicon-on-Insulator grating structure for efficient coupling to a vertically positioned optical fiber. A 3dB improvement over a symmetric structure is obtained. While this improvement can decrease the cost of packaging of a

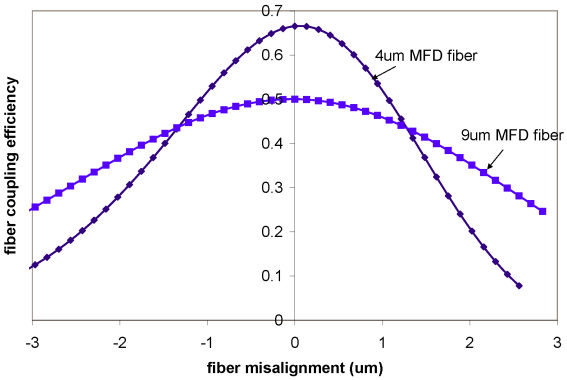


**Fig. 11:** Influence of a fiber misalignment on the obtainable fiber coupling efficiency for a 4µm and 9µm mode field diameter fiber

photonic integrated SOI circuit, it can also be used for other purposes, for example to efficiently couple light from a flip-chipped VCSEL into an SOI waveguide circuit, using the same grating. While this paper deals with the optimization of a one-dimensional grating structure, the same principle can be used in two-dimensional grating structures for polarization diversity.

## References

1 W. Bogaerts et al, J. Lightwave. Techol., no. 23, p. 401, 2005.
2 D. Taillaert et al, J. Quant. Electron., no. 38, p. 949, 2002.
3 D. Taillaert et al, Photon. Techn. Lett., no. 15, p. 1249, 2003.
4 B. Wang et al, Photon. Technol. Lett., no. 17, p. 1884, 2005.
5 G. Roelkens et al, Optics Express, no. 24, p. 11622, 2006.
6 P. Dumon et al. Optics Express, no. 14, p. 664, 2006.
7 P. Bienstman et al., IEE Proc.-Optoelectron., no. 149, p. 161, 2002.
8 J. Harper et al., Electron. Lett., no. 24, p.245, 1988.

# Spatial and Spectral Distributed Multi Population Rate Equations Model for Quantum Dot Superluminescent Diodes

Mariangela Gioannini, Ivo Montrosset
Dipartimento di Elettronica, Politecnico di Torino, mariangela.gioannini@polito.it

**Abstract:** *We present a spectral model of the emission characteristics of quantum dot superluminescent diodes including the influence of residual facet reflectivity. We analyze the transition from the amplified spontaneous emission to lasing regime and the characteristics of multi-section devices with improved performance.*

**Introduction**

Superluminescent light emitting diodes (SLD) offer the prospect of high power and wide bandwidth sources for various sensing and spectroscopy applications and in particular for optical coherent tomography, where it is required broad band and very bright light sources with a short temporal coherence. In the last years the Quantum Dot (QD) semiconductor materials have been promising used for the realization of QD-SLD [1,2], thanks to the possibility of tailoring the optical gain bandwidth with a proper engineering of the QD size and composition. Very recently multi-section QD-SLDs [3] have been proposed as a viable solution for the realization of devices with very high power and simultaneously broad band emission. A detailed numerical model for the analysis and the design of bulk SLD has been recently presented in [4], but to our knowledge only simple models have been reported for the case of QD semiconductor material [1].

The model we present in this work takes into account all the peculiar characteristics of the QD material and allows simulating the non-idealities of the device. From the material point of view we include the non-homogeneous distribution of the dot size (inhomogeneous gain broadening) and the presence of other states (wetting layer and SCH states) besides the states confined in the QDs (ground state, GS, and excited state, ES) to calculate the spectral characteristics of the emitted photons. From the device point of view we take into account the longitudinal spatial hole burning effect that is particularly strong in SLD and the effect of non zero reflectivity at the facets. We can therefore predict the amount of ripple in the output spectrum and the condition at which the transition from the SLD to the laser behavior occurs. A proper SLD model has therefore to be able to simulate the effect of the unwanted facet reflectivity and to calculate the output spectrum and the power versus current characteristics including the longitudinal spatial hole burning and the spectral hole burning effects caused by finite carrier capture/escape times in/from the various QDs of different size.

The paper is organized as follow: we will briefly describe the numerical model used and then we will validate it in a test case, comparing the characteristics of an ideal SLD (zero-facet reflectivity) with those of a laser (as cleaved facet reflectivity). We will then show how the model can be used to analyze some SLD realistic structure. In particular we will analyze the effect of residual facet reflectivity due to non-ideal anti-reflection coating and we will give two examples of analysis of multi-section SLDs.

**Numerical model**

The numerical model is based on a traveling power approach: the device is divided in several sections whose photon densities are obtained from the propagation of the forward and backward photons of the two nearest sections. Given the importance of the SLD emission spectra in practical applications, the model is also based on a spectral slicing approach [5]. In each longitudinal section of the device the model calculate the local true spontaneous emission (TSE) and the gain spectra solving a Multi Population Rate Equation system [6]. With this modeling the non-uniform QD ensemble is represented by several sub-groups of QDs, coupled through the wetting layer via the carrier capture and escape process. Each *n*-th QD group has different GS and ES energies ($E_n$) and its carrier density is depleted by the stimulated emission of the photons of that section (spatial hole burning). The various QD sub-groups are also coupled together via the homogeneous broadening of the emitted photons (spectral hole burning) that appear in the stimulated emission term. The TSE obtained by the carrier occupation of the various states is then sliced in several energy intervals with sampling step $\Delta E$. In equation (1) we report the expression of the TSE emission rate at the central energy $E_k$ of the *k*-th energy interval evaluated in the *z* section of the device:

$$R_{sp}(z,E_k)=\sum_{GS,ES}\mu_{GS,ES}N_D n_L C_{spon}\sum_n f^2_{n_{GS,ES}}(z)\cdot\rho_{opt}(E_n)\cdot G_n\cdot L(E_n-E_k) \quad (1)$$

where $\mu_{GS,ES}$ is the state degeneracy, $N_D$ is the QD density per layer, $n_L$ the number of QD layers, $C_{spon}$ is a coefficient [6], $\rho_{opt}(E_n)$ is the density of the optical modes, $f^2_{n,ES,GS}$ is the occupation probability of the GS/ES of n-th QD population in the *z* section and is obtained solving the MPRE system [6]. In expression (1) $G_n$ is the existence probability of the n-th QD population that accounts for the inhomogeneous QD distribution and $L(E_n-E_k)$ is the homogeneous

broadening function.
The photon density in the forward ($S_f$) and reverse ($S_r$) direction are then given by:

$$S_{f,r}(z,E_k) = S_{f,r}(z,E_k)\cdot\exp(g(z,E_k)\cdot\Delta z) + 0.5\cdot\beta_{sp}\cdot\frac{\Delta z^2}{v_g}\cdot R_{sp}(z,E_k)\cdot\Delta E_k$$

Where $g(E_K)$ is the gain spectrum calculated in [6], $\Delta z$ is the sampling step in the longitudinal direction, $v_g$ is the group velocity and $\beta_{sp}$ is the amount of TSE coupled with the guided mode. In the first and last section of the device we add to the term reported above also the contribution of the reverse/forward fields reflected back in the cavity.
Solving the MPRE model in each $z$ section we therefore account for the spatial hole burning effect in the longitudinal direction of the SLD and we can calculate how much the carrier population in the GS and ES are depleted by the propagating photons in the various sections.

**Numerical results**

The numerical model presented above has been validated analyzing first two test structures with the purpose of showing how the model can simulated a device with any value of end facet reflectivity and therefore account of both amplified spontaneous emission and lasing regimes. At this purpose we have considered a device with as cleaved facet reflectivity (laser, LD, behavior) and a device with zero facet reflectivity (ideal SLD behavior).

***Comparison between laser and SLD behavior***

We consider for the comparison two InAs/GaAs 4.5 mm long QD devices. We compare in the inset of Fig.1a the calculated output power versus current characteristics while in Fig.s 1a and 1b are reported the output emission spectra for the two cases at various level of current injection. The spectrum at the highest current in Fig.1, just above LD GS threshold, clearly shows a sharp peak around the GS emission while the SLD spectrum shows a dominant GS emission. The cavity gain in Fig. 2 ( a- for the LD and b- for the SLD) helps in this interpretation because the modal gain around the GS emission is clamped in the LD case whereas, in the SLD case, it presents a maximum. Increasing the current (Fig.s 1b and 2a) the LD spectrum broadens and then also the ES start lasing. On the contrary, for the SLD the ES emission becomes first equal to GS emission and than dominates since the GS starts saturating. This behavior has been measured in actual SLD and LD. Fig. 3 reports the calculated normalized longitudinal photon density distribution at the wavelengths corresponding to the GS (dashed line) and ES (solid line) output power spectral peak wavelengths. The strong longitudinal field variation in the SLD case justify the need to use a longitudinally discretized model to correctly represent the high injection regime, whereas, as it is well known, this is not strictly necessary in a laser except when the ratio of the two reflectivity is high.

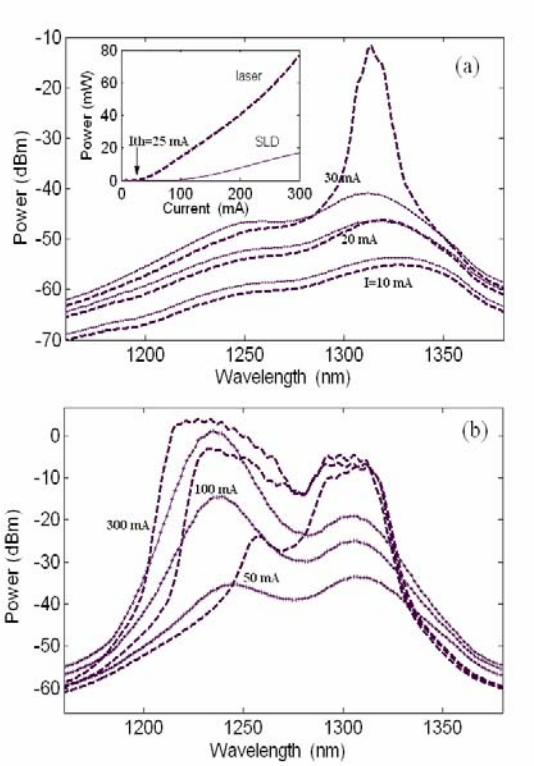


**Fig. 1:** P-I (a) and the spectral (a and b) characteristic of a SLD with zero (continuous lines) and with cleaved (dashed lines) facets reflectivity.

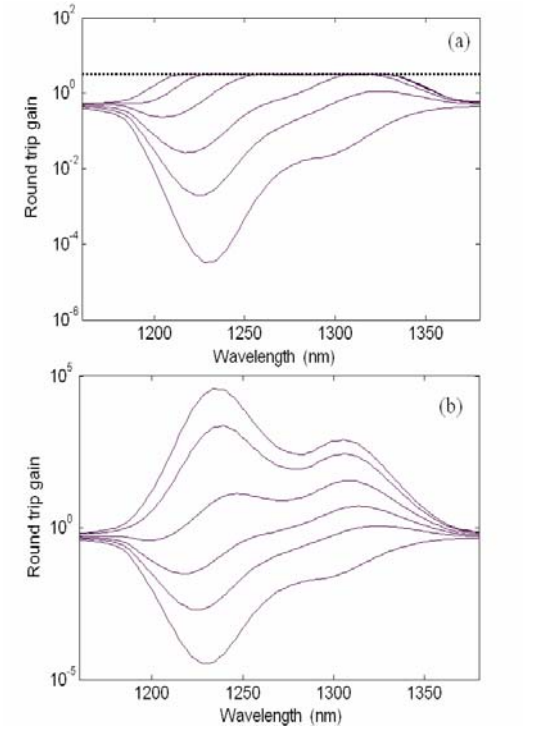


**Fig. 2:** Device round trip gain for the two cases of Fig.1. (a) cleaved FP cavity and (b) ideal SLD. The current levels of each curve are the same of Fig.1.

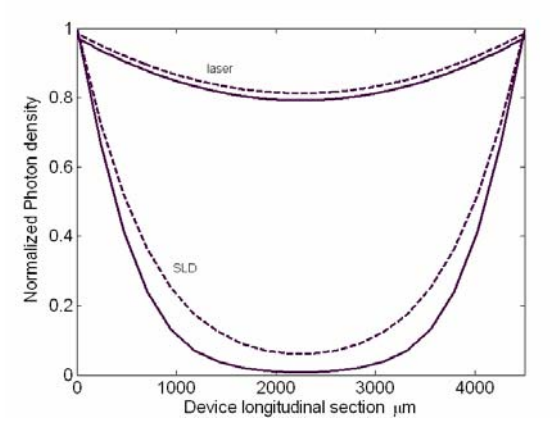


**Fig. 3:** Normalized longitudinal photon distribution at the peak emission wavelengths ( GS – dashed and ES- continuous lines) for the ideal SLD and for the FP LD.

***SLD with non-zero facet reflectivity***

In this section we report an example of simulation results of a SLD with non-zero facet reflectivity. We assume that the two facets have a residual reflectivity of $3 \cdot 10^{-4}$ due to the non-ideal anti-reflection coating. In Fig. 4 we report the calculated power versus current curve and the maximum ripple of the output spectrum evaluated at the peak of the GS and ES emission. The figure shows that the ripple remains low for the GS because the GS gain saturates at quite low values (see Fig. 2b), but it significantly increases for the ES emission. The strong ES ripple at I=150 mA evidence that the ES is getting close to the threshold condition. This result shows that if low ripple values are required (e.g. < 3dB), the SLD output power is significantly reduced.

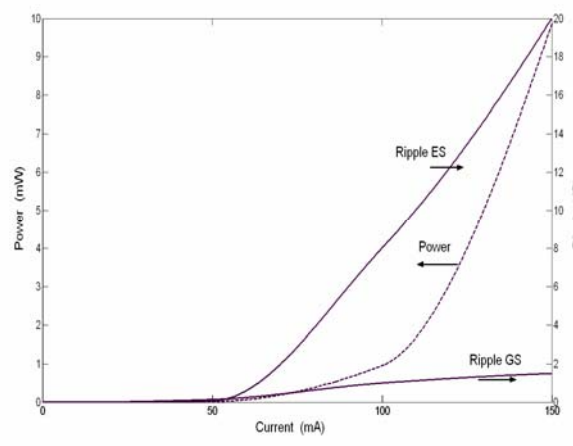


**Fig. 4:** Power versus current characteristic and maximum ripple in the output spectrum at the GS and ES peak emission wavelength. The residual reflectivity of the SLD is set to $3 \cdot 10^{-4}$

***Analysis of multi-section SLD***

The present model has therefore been used to analyze from a theoretical point of view various solutions presented in the literature to suppress the residual reflectivity [3,7] and/or increase the output power and emission bandwidth [3]. In all the cases the SLD is divided in two or more sections injected with different current levels.

In this section we analyze two examples of two sections SLD: in the first example we study a SLD with an active plus an absorber section, in the second example we analyze a SLD with two active sections pumped with different current.

The addition of the saturable absorber section was proposed several years ago [7] to suppress the lasing in bulk SLD and applied to the QD case in [3]. The purpose of this example is to show that, in the QD case, when the power in the active section increases, the absorber, being optically pumped by the generated photons, has first a reduction of the absorption and then a transition to a gain condition. In this example we consider a 3 mm long active section followed by 1.5 mm absorber with zero injected current. The facets are as cleaved. We ran several simulations keeping null the current injected in the absorber section and varying the current injected in the active section. We have observed that the many photons emitted by the ES in the active section pump first the carriers in the ES of the absorber; then these carriers relax in the GS giving an increasing of the GS carrier density. The consequence of this behavior is shown in Fig. 5, where we report the average gain of the absorber at the various current injected in the active section. The figure demonstrates that both GS and ES absorption gets smaller and smaller. However, differently from quantum well and bulk saturable absorbers, the GS absorption is not clamped to transparency, but, being refilled from the ES, it can reach a positive gain condition. As a consequence the suppression of the facet reflectivity is reduced more and more and eventually the device starts lasing first from the GS and then also from the ES.

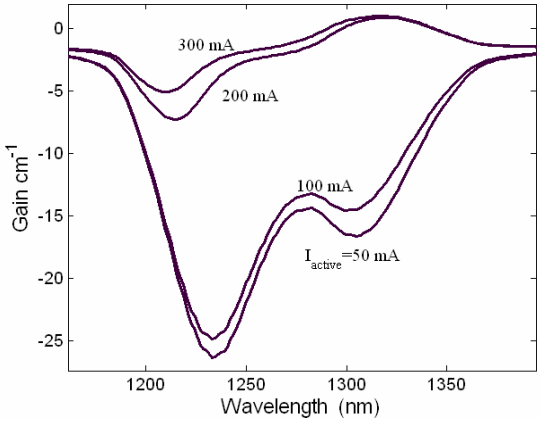


**Fig. 5:** Average gain in the absorber section as function of the current injected in the active section.

In the second example we analyze the output characteristics of a SLD divided in two active sections in-

jected with different currents and with ideally zero facet reflectivity. In this case the first section (1.5 mm with 20 mA current injection) provides the GS power; the second section (3 mm with 450 mA injection) amplifies the GS emission provided by the first section and also generates the ES power. In Fig. 6 we compare the output spectrum of the two section SLD with the one of a 3 mm uniform SLD obtained injecting the same current density. In the two sections case the GS power is suppressed of only 3.7 dB, whereas in the one section design the GS output power is suppressed of more than 9 dB. This example shows that the multi-section SLD design is a viable solution for optimizing the emission bandwidth and output power of these devices.

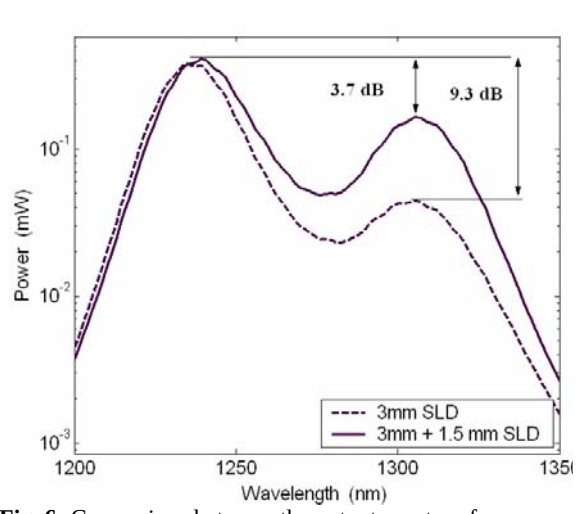


**Fig. 6:** Comparison between the output spectra of one section SLD (dashed line) and two section SLD (solid line).

## Conclusion

We have presented a numerical model for the analysis of QD-SLD. The model includes the inhomogeneous gain broadening due to the QD material, the spectral and spatial hole burning effect and the influence of non null end facet reflectivity. We have demonstrated that the model can account for the transition from the amplified spontaneous emission regime to the lasing regime and it can be used to predict the amount of ripple in the SLD output spectrum. We have also given two examples of analysis of multi-section SLD showing that the present model could be used to test the viability of new design solution of SLD with improved spectral performance.

## Acknowledgments

The author acknowledge the support of the EC IST-NMP-3 STREP project NANO UB-SOURCES.

## References

1 M. Rossetti, A. Markus, A. Fiore, L. Occhi, C. Velez, "*Quantum dot superluminescent diodes emitting at 1.3 μm*", IEEE Photon. Tech. Lett., no. 3, pp. 540-542, 2005.

2 S.K. Ray, K.M.Groom, H.Y. Liu, M. Hopkison, R.A. Hogg, "*High poer 1.3 μm quantum dot superluminescent diodes*", Photonics West, January 2006.

2 S.K. Ray, K.M.Groom, H.Y. Liu, M. Hopkison, R.A. Hogg, "*High power 1.3 μm quantum dot superluminescent diodes*", Photonics West, January 2006.

3 Y.C. Xin, A. Martinez, T. Saiz, T.A. Nilsen, A-Moscho, Y. Li, A.L. Gray, A. Vahktin, L.F. Lester, *"Novel quantum dot 3-section superluminescent diode",* International Conference on Solid State Devices and Materials, Paper B-6-3, Yokohama (Japan), 2006

4 J. Park, X. Li, *"Theoretical and numerical analysis of superluminescent diodes",* IEEE J. Light. Tech., no. 6, pp. 2473-2479, 2006.

5 J. Park, X. Li, W.P. Huang, *"Comparative study of mixed frequency-time domain models of semiconductor optical amplifiers",* IEE Proc. Optoelectron., no. 3, pp. 151-159, 2006.

6 M. Gioannini, A. Sevega, I. Montrosset, *"Simulation of differential and linewidth enhancement factor of quantum dot semiconductor lasers"*, Springer Optical and Quantum Electronics, no. 4-6, pp. 381-394, 2006.

7 N.S.K. Kwong, K.Y. Lau, N. Bar-Chaim, *"High power high efficiency GaAlAs superluminescent diodes with an internal absorber for lasing suppression"*, IEEE J. Quantum Electron. , no. 4, pp. 696-704, 1989.

# Full-vectorial time-domain modelling of photonic crystal semiconductor lasers

Wolfram H.P. Pernice (1), Dominic F.G. Gallagher (2) and Frank P. Payne (1)
1) Oxford University, Department of Engineering Science, Parks Road,Oxford, OX1 3PJ, UK,
wolfram.pernice@eng.ox.ac.uk
2) Photon Design, 34 Leopold Street, Oxford, OX4 1TW, UK

**Abstract:** *We present a novel numerical scheme for the simulation of photonic crystal lasers with nonlinear response. The gain of the lasing material is closely modelled over a large wavelength range. High computational efficiency is achieved by using refined meshes and implementing the method for distributed computing.*

**Introduction**

Photonic crystals show promise for shaping the optical properties of semiconductor lasers. They are for example used to optimise beam quality of VCSEL lasers [1] and to achieve low-threshold [2] or ultrafast lasers [3]. However, the design of such structures provides serious challenges to numerical methods available to date. For one, the material properties of the lasing material have to be described accordingly in the algorithm. In addition, the structural size of the device under consideration often overextends the computational hardware available in standard research facilities.

We present an efficient numerical solution to these challenges. We use the finite-difference time-domain (FDTD) method [4] due to its flexibility to handle complex geometric and material systems. Material gain is included into the standard FDTD algorithm by linking the gain to a frequency dependent conductivity. Because data for material gain in a quantum well structure is readily available [5], we choose to incorporate active material behaviour using the conductivity, which can be expressed in terms of the material gain and therefore allows us to describe complex vertical layer structures. Using a semi-deterministic fitting algorithm, the gain function can be cast into a suitable mathematical form that can be used in the FDTD method, while preserving causality in the time domain. Our fitting routine yields accurate results for a large wavelength range. Similarly, we achieve high accuracy for modelling the dielectric function of the metal grating used in the validation of the algorithm.

The hardware limitations are overcome by using a non-uniform meshing algorithm, yielding higher mesh densities for areas with small geometrical features. A new interpolation method is used in order to reduce spurious reflections from mesh boundaries. The algorithm is also developed for use on parallel computers making it possible to fit large structures into distributed memory.

We validate our algorithm by simulating different photonic crystal laser structures. We consider a PC membrane laser, a high-Q cavity laser and a polymer laser based on a metallic nano-particle grating.

**Extended Maxwell's equations and FDTD formulation**

For an adequate representation of the material gain we need to consider both the frequency dependent behaviour of the lasing material and fluctuations of the carrier density due to spatial hole burning and carrier depletion. As shown by [6], the material gain can be linked to a frequency dependent conductivity $J_t$, which we include in the standard set of Maxwell's equations as

$$\varepsilon \frac{\partial E}{\partial t} = \nabla \times H - J_t \qquad \mu \frac{\partial H}{\partial t} = -\nabla \times E \tag{1}$$

$J_t$ can be a single Lorentzian or as in this paper a sum of $N$ individual Lorentzian poles. By using a multipole formulation the fit to the material gain yields much more accurate results than alternative formulations [7]. Each single Lorentzian pole yields a second order differential equation in the time domain as

$$T_k^2 \frac{\partial^2 J_k}{\partial t^2} + 2T_k \frac{\partial J_k}{\partial t} + (1+\omega_k^2 T_k^2) J_k = \frac{\sigma_k}{1+I/I_S}\left(E + T_k \frac{\partial E}{\partial t}\right) \tag{2}$$

where $I$ denotes the optical intensity and $I_S$ the saturation intensity. The coefficients $T_k$, $\omega_k$ and $\sigma_k$ for each pole are dependent on the carrier density and denote the relaxation time, the resonant frequency and the peak gain, respectively. The non-linear dependence of the gain saturation on the optical intensity, which is determined by the spectral hole-burning and/or hot carrier effects, is included in our gain model by the factor $(1+I/I_S)^{-1}$. As given by [8] the carrier density is linked to the electric field and the current density as

$$\frac{\partial N}{\partial t} = \frac{2}{\hbar\omega_0} E \sum_{k=1}^{N} J_k - \frac{N}{\tau} + W_P \tag{3}$$

where $\tau$ is the carrier lifetime, $\omega_0$ is the frequency of the gain peak and $W_P$ the electrical pump rate. The above equations provide the complete updating scheme that is discretized using centred finite differences in both space and time as shown by [4]. It is, however, important to make sure that fields on the left- and right-hand side of the equations are centred on equivalent time-steps, as failing to do so leads to numerical instability [7]. We therefore apply a semi-implicit discretization scheme, which is solved to yield explicit updating equations for all fields.

**Semideterministic fitting routine**

In order to include the material gain in our algorithm, we need to obtain the Lorentzian parameters in equation 2 as a function of carrier density. The fitting routine therefore needs to obtain a set of parameters for each of the material gain sets. We use the commercial product Harold [5] to obtain material gain data for our quantum-well gain structure. The fitting routine is performed before the actual FDTD algorithm is started. It is important to control the fitting routine such that the fitted parameters vary smoothly with increasing carrier density. Therefore we apply a semi-deterministic fitting routine as shown schematically in figure 1, using an adaptive non-linear least-squares algorithm as described in detail in [9]. We fit each individual gain curve with a set of four Lorentzians. Each pole corresponds to a determined

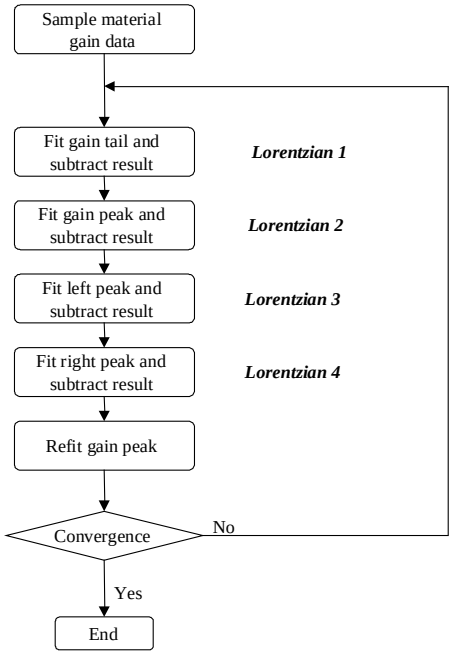


**Fig. 1:** Flow chart for the fitting routine for gain materials.

spectral position in order to fit the gain peak, curvature and absorption in the vicinity of the peak with high accuracy. We fit one pole at a time and then subsequently subtract the fitted result from the original data. This way dominant resonance peaks in the gain spectrum are individually removed. We first fit the absorption tail of the gain curve, followed by the gain peak. Subsequently spurious resonances to the left and right of the peak are removed with one additional pole each. Because the sum of these four Lorentzians might not represent the peak gain well, we refit the gain peak. This cycle of fitting can be applied repeatedly. We find that the algorithm converges very quickly to the local optimum in only one or two iterations. Representative results from our algorithm are shown in figure 2. As required, the fitting algorithm yields a close match to the gain

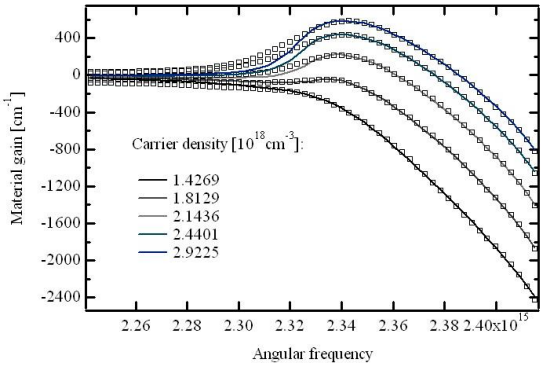


**Fig. 2:** Fitted gain curves for varying carrier density. Each fit is composed of four Lorentzian resonances that preserve gain peak and curvature as well as long-wavelength absorption.

peak, curvature and long-wavelength absorption tail. We note that a better fit to the left side of the peak could be obtained by selecting a greater number of poles. However, this increases the computational burden of the FDTD algorithm and also worsens the trajectory of the Lorentzian parameters. In figure 3 we show the trajectories for the peak Lorentzian as a function of carrier density. In order to facilitate evaluation in the FDTD updating scheme, we approximate the trajectory with a polynomial, fitted

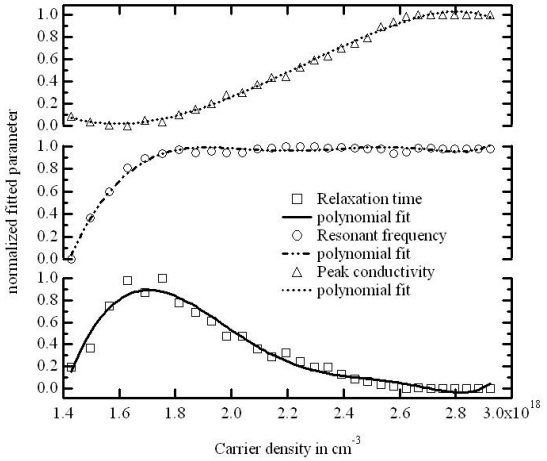


**Fig. 3:** The trajectory of the parameters of the peak Lorentzian with varying carrier density. Shown is also a polynomial fit of fifth order.

also in a least-squares sense. Because the parameters vary without major jumps, a polynomial of fifth order is sufficient to represent the trajectory. Polynomials can be evaluated at minimal costs and are therefore ideally suited for a fast FDTD algorithm.

**Mesh refinement and distributed computing**

As suggested by [4], the FDTD algorithm requires a spatial resolution of roughly 20 grid points per wavelength in order to yield a numerical accuracy of 1 %. Because this criterion is dependent on the refractive index of individual geometrical features, small shapes with high refractive index impose an unnecessary stringent grid resolution for the computational domain. We therefore implement a mesh refinement scheme, which provides higher resolution

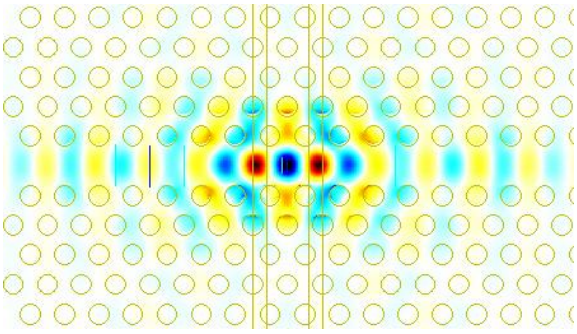

**Fig. 4:** Lasing mode at steady state for the high Q laser.

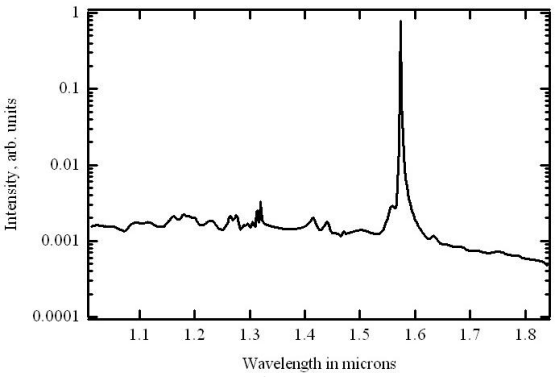


**Fig. 5:** Spectral response of the nano-cavity laser. The lasing peak is positioned at the resonance frequency of the cavity at 1.574 microns.

in areas with high refractive index, such as metallic particles. We choose a refinement factor of two. This refinement scheme can however by recursively applied to yield smaller grid steps. A factor of two is chosen because higher refinement steps yield higher reflections from refinement boundaries. A further reduction in reflection can be obtained by using a parabolic interpolation scheme in order to obtain boundary points for the refined region.

Though the use of non-uniform meshes reduces memory requirements significantly, three-dimensional problems still challenge computational hardware. Because many research facilities do not have access to supercomputing equipment, it is convenient to use in-house cluster systems formed by linking personal computers to a distributed environment. We split the computational domain into regions that fit into the memory of each machine. An mpi-based message passing system is employed to make sure that neighbouring domains have access to required information. The distributed version of the software not only allows us to reduce calculation time, but more importantly increases the size of problems that can be treated by the FDTD.

**Numerical experiments**

In order to evaluate the proposed algorithm we numerically investigate several photonic crystal laser geometries.

***Ultra-high Q cavity laser***

In a first example we compute the lasing spectrum for a nano-cavity membrane laser. The nano-cavity is designed as described by [10]. Nano-cavity lasers have attracted interest in recent years due to low threshold and fast tuning speeds. The ultra-high Q cavity provides a nice way to realize a laser, because the optical pumping can be provided through the waveguide channel in the photonic crystal lattice. The cavity is composed of a hetero photonic crystal lattice with lattice constants I=410 nm and lattice constant II=420 nm. The membrane thickness was set to 287 nm. This cavity design shows a resonance peak at 1.574 microns. The high quality factor of the cavity results from the dual lattice nature of the structure. Wavelengths are allowed in the region with larger lattice constant that cannot propagate in the regions with smaller lattice constant. When the waveguide in photonic crystal II is short enough, the frequencies that photons are allowed in this region become quantized - similar to the situation for electrons in a semiconductor quantum structure. We apply our algorithm to this particular structure. We choose a grid spacing of 25 nm and propagate the fields for 5 ps to ensure that the laser has reached steady state. The lasing output is recorded in the air space above the membrane. In figure 4 we show the

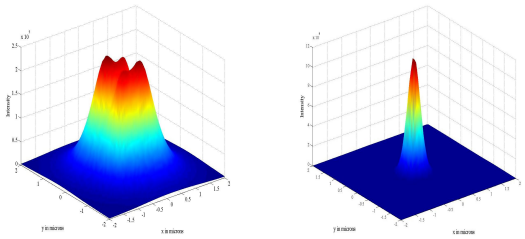

**a)** **b)**

**Fig. 6 a)** Far field obtained for a single defect cavity. **b)** Far field for 7 coupled nanocavities.

lasing mode once the laser has reached steady state. The cavity mode is clearly visible for the resonant frequency of 190.5 THz. The spectral response of the laser reveals a central peak at 1.574 microns as shown in figure 5.

***Nano-cavity array membrane laser***

In a second example we consider the beam characteristics of coupled nano-cavity lasers. Such membrane laser arrays have can provide ultra-fast modulation speeds [3]. Here we consider a thin membrane of 280 nm thickness. A hexagonal photonic lattice with lattice constant 365 nm is inscribed into the membrane, where the hole diameter is set to 175 nm. InP is chosen as a material system with 4 quantum wells included in the membrane to yield a peak gain around 1.25 microns. Cavities are generated in the membrane by removing a single hole from the lattice. Choosing only one defect atom allows us to preserve the symmetry of the lattice and therefore obtain better mode shaping properties. In this experiment we study the far field behaviour of single and coupled cavities. As shown

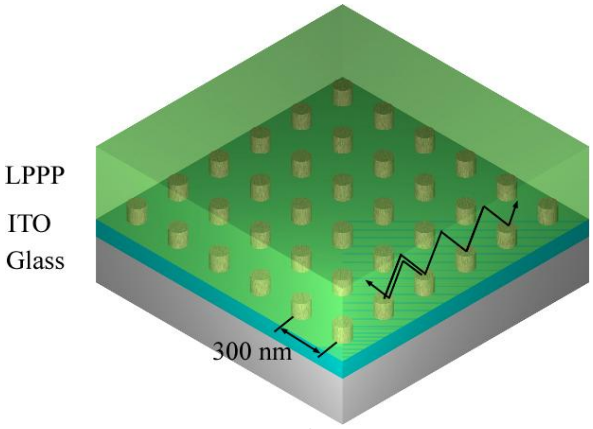


**Fig. 7:** Geometrical structure of the polymer PC laser. Optical feedback is provided through second-order Bragg scattering as indicated by the black arrows.

in figure 6a), a single cavity does not result in a directional output beam. However, by coupling 7 cavities a supermode exists in the photonic crystal lattice that does yield a directional output, as demonstrated in figure 6b). Furthermore, the output intensity is increased by a factor of approximately 4.8. The simulation confirms therefore the possibility to improve the output characteristics of coupled cavity lasers with numerical techniques.

***Polymer laser with a metallic nano-particle grating***

In the last numerical example we investigate lasing behaviour in a polymer laser. Since the demonstration of stimulated emission in organic semiconductors this field of research has attracted increasing interest. In this study we employ the optical feedback mechanism described by Stehr et al. [2] consisting of a grating of gold nano-discs. The simulated structure is shown in figure 7. A 110 nm thin layer of indium tin oxide (ITO) on a glass substrate is used as the substrate for the metal grating. The gold discs of diameter 110 nm and 30 nm height form a two-dimensional photonic crystal lattice with a lattice constant of 300 nm. The grating provides feedback through second order Bragg scattering. A thin methyl-substituted ladder-type poly(para phylene) (LPPP) layer of 460 nm thickness is chosen as a gain medium with an emission peak at 490 nm. We consider six rows of photonic crystals in this investigation. The global grid resolution is set to 20 nm. In order to achieve high accuracy for the metal disks, we enclose them in a subgridding region of refinement factor 4, meaning that we use a mesh density that is four times higher than in the global grid. The computational domain is terminated with uniaxial perfectly matched layers in order to absorb reflections from the grating structure. The total simulation time is set to 5 pico-seconds and the lasing output is recorded above the LPPP layer in air. In figure 8 we show the spectral response of the polymer laser. A clear peak is visible at 476 nm in the blue visible range. This peak corresponds to the Bragg wavelength of the grating in second order mode. The lasing output is coupled out of the LPPP layer through the first order mode as shown in [2].

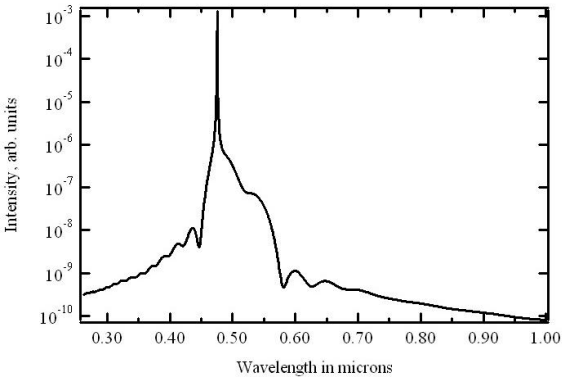


**Fig. 8:** Spectral response of the polymer PC laser.

**Conclusions**

We have presented a novel flexible FDTD algorithm that is capable of simulating lasing in complex material systems in three dimensions. We fit the gain material to a multi-pole Lorentzian model using a semi-deterministic fitting algorithm providing accuracy over a wide spectrum. Saturation effects and spatial hole burning are included through rate equations and a non-linear saturation model. The algorithm uses mesh refinement techniques and is developed for use in a distributed cluster system thus allowing for numerical investigation of large devices. The validity of the approach was demonstrated by simulating a variety of photonic crystal laser structures. We investigated lasing in nano-cavity membrane lasers and polymer based lasers with a gold nano-particle grating.

**Acknowledgements**

Wolfram H.P. Pernice would like to thank Photon Design for funding a DPhil. Research studentship.

**References**

1 N. Yokouchi et al., IEEE Sel.Top. Quantum Electr., vol. 9, no. 5, pp. 1439-1445, 2003.
2 J. Stehr et al., Advanced Materials, vol. 15, p. 1726, 2003.
3 H. Altuc et al., Nature Physics, vol. 2, pp. 484-489, 2006.
4 A. Taflove and S. C. Hagness, "Computational Electrodynamics: The Finite-Difference Time-Domain Method", Boston: Artech House, 2005.
5 Harold, Photon Design, 34 Leopold Street, OX4 1TW Oxford, U.K.
6 S. C. Hagness et al., Radio Sci., vol. 31, no. 4, pp. 931-941, 1996.
7 M. Bahl et al., IEEE Journal of Quantum Electronics, vol. 41, no. 10, pp. 1244-1252, 2005.
8 A. E. Siegman, Lasers. Mills Valley, CA: Univ. Sci. Books, 1986.
9 J. E. Dennis et al., ACM Trans. Math. Softw, vol. 7, no. 3, pp. 348-368, Sept. 1981.
10 B-S. Song et al., Nature Materials, vol. 4, pp. 2007-2010, 2005.

# Efficient modeling of nonlinear wave propagation and radiation dynamics in nano-photonic systems

Kurt Busch

Institut fuer Theoretische Festkoerperphysik, Universitaet Karlsruhe, Karlsruhe, Germany
*kurt@tfp.uni-karlsruhe.de*

Abstract not available

# Modelling light extraction in 3D organic LEDs containing photonic crystals

Peter Bienstman[1], Peter Vandersteegen[1] and Roel Baets[1]

[1] *Photonics Group, Department of Information Technology, Ghent University*

*Sint-Pietersnieuwstraat 41, 9000 Gent, Belgium*

*Peter.Bienstman@UGent.be*

We discuss the modelling of light extraction in organic LEDs containing photonic crystals. These periodic structures can be placed both at the substrate/air interface and at the substrate/organic interface, but they require a different numerical treatment.

## Summary

Organic light-emitting diodes form an attractive future light source, in view of their potentially low cost, high energy efficiency and their diffuse, large-area emitting surface. However, just like any LED these devices suffer from limited light extraction because of the high-index materials involved. More specifically, light can be trapped in the organic layers or in the glass substrate. In order to improve light outcoupling, a 2D periodic structure can be placed either at the interface between the organic layer and the glass, or, several millimeter away from the emitter, at the interface between the glass and the air.

We present a comprehensive model to study light extraction from such devices. The model first uses the standard method of expanding the field of the spontaneously emitting dipole into propagating and evanescent plane waves [1]. The resulting field profile coming from the multiple reflections at the top and bottom mirror of the microcavity is then calculated. These mirrors can contain a periodic structure. The scattering properties of these gratings are calculated using the well-known rigorous coupled wave approach (RCWA) [2].

Finally, the influence of multiple reflections inside the thick substrate beneath the microcavity is taken into account by constructing a similar model, but this time using power densities rather than amplitudes in order to reflect the incoherence effects. Again, this second, larger cavity can contain a periodic structure, e.g. a grating at the substrate/air interface, i.e. on the other side of the substrate as compared to the emitting layers.

We will present the numerical details of this model, discuss the results of various device optimizations, and also show comparisons with experimental results.

## Acknowledgements

Parts of this work were performed in the context of the European IP-OLLA project under contract IST-004607.

## References

[1] D. Delbeke, P. Bienstman, R. Bockstaele, R. Baets, JOSA A **19**, 871-880 (2002).

[2] Li, JOSA A **14**, 2758-2767 (1997).

# Emission in periodic waveguides : computational concepts and applications.

Guillaume Lecamp[1], Jean-Paul Hugonin[1] and Philippe Lalanne[1]

[1] *Laboratoire Charles Fabry de l'Institut d'Optique, CNRS, Univ Paris-Sud, Campus Polytechnique, RD 128, 91127 Palaiseau Cedex, France.*
philippe.lalanne@institutoptique.fr

It has been recognized for some time that a new generation of optoelectronic devices like low-threshold lasers or single photon sources can be drastically improved in terms of noise and speed modulation if their radiation pattern is highly directed toward a single mode namely if the fraction of spontaneous emission (SE) coupled into this mode is made close to unity. For low excitation, this fraction is defined as the SE coupling factor β. But in conventional waveguide, even those relying on high index contrast, not all the radiation funnels into a single mode and a portion γ of the SE is coupled to the radiation modes. This limitation has motivated the concept of 3D photonic-bandgap materials [1] which theoretically offers vanishing γ's. Nevertheless, in planar systems only 2D photonic crystal are achievable and in these 2D periodic structures γ is expected to be small but not zero. Currently little is known on mechanisms for decreasing γ because such mechanisms rely on the control of the dipole-field coupling over the continuum of radiation modes, a difficult electromagnetism problem.

In order to gain a better physical insight of the dipole-field coupling into the bound modes and above all into the radiation modes, we have developed a general, modal formalism for the calculation of light emission and propagation in z-periodic waveguides and in aggregates of them. Conceptually, the formalism can be seen as a generalization of the classical formalism developed for z-invariant waveguides. It allows for a semi-analytical treatment of light propagation in aggregates of periodic waveguides.

In a second part, we numerically study various photonic structures that allow the dipole to be mostly coupled into one single guided mode, namely to suppress the coupling of the dipole into radiation modes. We discuss the performances of conventional z-invariant waveguides [2] and show that photonic crystal waveguide with one-missing-row largely runs over z-invariant waveguides in terms of β factor and bandwidth (see Fig 1).

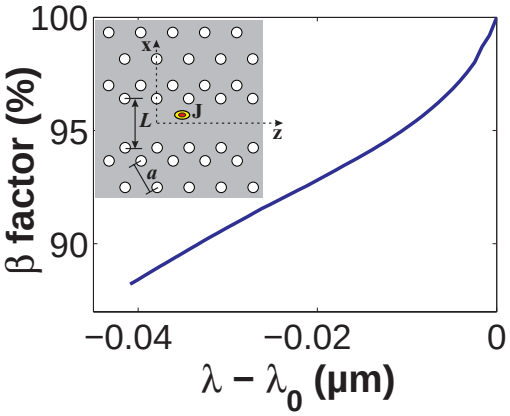


**Fig. 1** : β-factors for engineered z-periodic waveguide that provides β-factors larger than 90% over a 40nm bandwidth around $\lambda_0 = 0.95\mu m$ for the two in-plane dipole orientations.

## References

[1] E. Yablonovitch, "Inhibited spontaneous emission in solid-state physics and electronics," *Phys. Rev. Lett.*, vol. 58, pp. 2059-2062, 1987.

[2] D. Y. Chu and S. T. Ho, "Spontaneous emission from excitons in cylindrical dielectric wave-guides and the spontaneous-emission factor of microcavity ring lasers," *J. Opt. Soc. Am. B*, vol. 10, pp. 381-390, 1993.

# Plasmonic waveguides and components

Olivier J.F. Martin

Nanophotonics and Metrology Laboratory, Swiss Federal Institute of Technology Lausanne (EPFL), Lausanne, Switzerland
*olivier.martin@epfl.ch*

Abstract not available

# Numerical Modelling on New Nano-Photonic SOI Waveguide Structures for Multi-Reflector Filtering Devices

Andrei Tsarev

*Laboratory of Optical Materials and Structures*
*Institute of Semiconductor Physics, Siberian Branch of Russian Academy of Science*
*Prospect Lavrenteva, 13, Novosibirsk, 630090, Russia*
*tsarev@isp.nsc.ru*

*A novel nano-waveguide SOI structures that utilizes $p^+$-doping, nano-grooves, and 2D-grating couplers to provide better manufacturability of multi-reflector reconfigurable optical add/drop multiplexers (ROADMs) is presented. Multiple simulations by FDTD and BMP methods demonstrate the validity of new SOI design.*

## Summary

This paper present the first description and simulation by FDTD and BMP methods of novel nano-photonic SOI waveguide structures that provides better performance and manufacturability of multi-reflector reconfigurable optical add/drop multiplexers (ROADMs) that utilises multi-reflector beam expanders [1]. New structure design includes $p^+$ doping on both sides of SOI ridge waveguide with 220 nm×20 μm silicon cross section surrounded by the silica cladding. It provides small optical losses for fundamental quasi-TE mode and large losses for high-order modes (see Fig.1a) due to different free charge absorption depending on the modes field distribution. Nono-grooves etched at Brewster angle with respect to SOI ridge waveguide with $p^+$ regions provide small reflection coefficients of quasi-TE mode that has a principal role for simplifying manufacturing of novel multi-reflector ROADMs. Incorporation of these novel structures with 2D nono-grating couplers [2] provides new opportunity for polarisation diversity of ROADM. These new SOI design will be also interesting for implementation in other multiple nano-photonic optical element.

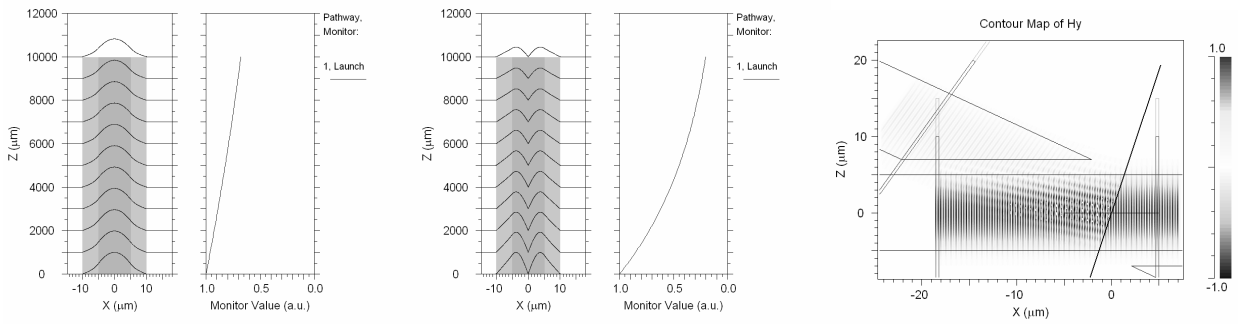


(a) (b)

Fig. 1. Simulation on new non-photonic SOI structures with $p^+$ doping on the waveguide sides.
(a) Power distribution and optical losses for quasi-$TE_0$ and quasi-$TE_1$ modes (2D BPM simulation);
(b) Power reflection of quasi-$TE_0$ mode by nono-groove (width 70 nm) etched at Brewster angle (2D FDTD simulation). Si width is 10 μm, $p^+$ doping width is 5 μm, $Dn_h$=0.002, $Da_h$= 0.16×$|Dn_h|^{5/4}$.

**Acknowledgments.** We would like to thank Company RSoft Design Group, Inc. that provides the FDTD and BMP software (see www.rsoftdesign.com) and technical support. This work has been partially supported by Grant No 05-02-08118-ofi-a from Russian Foundation for Basic Research.

## References

[1] Andrei V. Tsarev, Vittorio M. N. Passaro, and Francesca Magno, in Silicon Photonics, Editor: Vittorio M N Passaro (Research Signpost, Trivandrum, Kerala, India), chapter 3, 47-77 (2006).
[2] D. Taillaert et al, IEEE Photon. Technol. Lett., **15**, 1249-1251 (2003).

# 2D Numerical Model of Bent Waveguide Using RCWA and PML Developed to Simulate a Spectrograph in Integrated Optics

Bruno Martin[1], Alain Morand[1], Pierre Benech[1], Gregory Leblond[2], Sylvain Blaize[2], Gilles Lerondel[2], Pascal Royer[2], Etienne Lecoarer[3]

[1] *IMEP, Institut de Microélectronique, Electromagnetisme et Photonique,* UMR CNRS 5130, INPG-UJF-CNRS, *3, parvis Louis Neel, 38016, Grenoble, France*

martin@minatec.inpg.fr

[2]*LNIO, Laboratoire de Nanotechnologie et d'Instrumentation Optique,* FRE CNRS 2671, UTT, *12, rue Marie Curie BP 2060, 10010, Troyes, France*

[3]*LAOG, Observatoire de Grenoble, BP 53, 38041 Grenoble CEDEX 9, FRANCE*

This paper deals with a 2D numerical model developed in order to simulate a spectrograph in integrated optic. This numerical model is based on the RCWA using PML and is applied on a SOI or glass integrated bent waveguide transposed in an exponential conformal mapping.

## Summary

The interference pattern of a single optical wave can be obtained by splitting the wave and injecting it at the both sides of a straight waveguide. The resulting stationary wave is directly connected to the Fourier transform of the spectrum of the light source. To measure it, the waveguide is curved, thus the interference pattern is projected outside the waveguide. Indeed, curving the waveguide involves light to leak outside the bent waveguide. Moreover, controlling the leaking of the light implies controlling the number of fringes obtained in the interference pattern.

Considering this idea, a spectrograph in integrated optics on glass or on SOI is being developed. This spectrograph is a loop structure coupled with a plane waveguide that leads the radiated light in the propagation plane. To modelize this kind of structure, a 2D numerical model based on the Rigorous Coupled Wave Analysis (RCWA) combined with Perfectly Matched Layer (PML) [1] has been developed. The RCWA consists in periodically reproducing the index function of a region which enables to solve the Helmholtz in this new space. The result of this equation is a Fourier decomposition. To limit effect due to periodisation, PML are added on each side of the region of interest. This method is applied on the bent waveguide transposed in an exponential conformal map [2] where the waveguide is a straight one with a different index function. The results are then transposed in the original map. The figure illustrates the propagation of the electro-magnetic field in a region bordering a bent waveguide. The region of interest being limited increases the efficiency of the method. The radiated far-field is then obtained by the Huygens-Fresnel method.

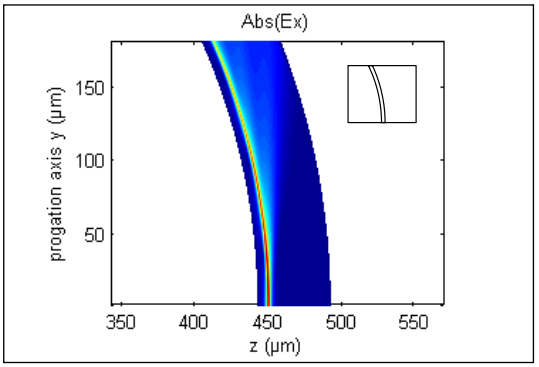


Despite some numerical issues that slightly limit accuracy of the results, this method is interesting to quickly analyse effects of the different parameters of the bent waveguide (radius, width and index contrast) and of the plane waveguide (gap between the bent waveguide and the plane waveguide) on the electro-magnetic field.

## References

[1] Qing Cao, Philippe Lalanne, and Jean-Paul Hugonin, J. Opt. Soc. Am. **19**, 335-338 (Feb. 2002).
[2] M. Heiblum and J. H. Harris 75-83, IEEE J. of Quantum Electronics, **11**, (Feb. 1975)

# Backreflection modelling in rough waveguides

Raffaella Costa[1], Francesco Morichetti[1] and Andrea Melloni[2]
[1] *Corecom, via G.Colombo 81, 20133 Milano, Italy*
[2] *DEI,Politecnico di Milano,via Ponzio 53/4, 20133 Milano, Italy*
costa@corecom.it, melloni@elet.polimi.it

A smooth waveguide with a partial lumped reflector with a random phase response is proposed to model the backreflection from a rough waveguide.

## Summary

The sidewall roughness is one of the main limiting factors for the propagation of the optical field in high index contrast waveguides, being the origin of undesired scattering losses and backreflections. The backscattering effects of the roughness have been investigated in [1-2] with a simple and approximated method based on the coupled mode theory. Although quite accurate, these approaches are often ineffective for practical applications, due to the required high computational effort.

Aim of this work is to propose an effective circuital model of the rough waveguide, useful for a fast and accurate analysis of complex circuits and for supporting the interpretation of experimental results. To this end, we have investigated also the phase of the reflected field and we propose a model consisting in the corresponding ideal smooth waveguide, with the addition of a lumped partial reflector with complex reflectivity $R\exp(j\varphi)$ placed in the middle. The modulus $R$ of the reflectivity corresponds to the average reflected spectral power while the phase takes into account the random nature of the problem. Instead of considering the phase, however, it is favourable to consider the group delay $\tau_g$ of the reflected field being directly related to a physical interpretation. The Fourier transform of the group delay of backscattered signals calculated with the matrix approach proposed by Marcuse [1] was studied for a range of different waveguides, and a typical behaviour is shown in Fig. 1a. The exponential space (time) constant has been found equal to twice the optical length Lo of the waveguide for all the considered cases. As a consequence, the $\tau_g$ owns a probability density function that is known *a priori* and the model of the rough waveguide is thus defined once the backreflected power and the length of the waveguide are known. The model proposed is thus an ideal waveguide with a lumped mirror of reflectivity R and phase $\varphi=\int\tau_g d\omega$. As an example of application we compared the fourier transform of the spectral response of a SOI rough waveguide terminated with reflecting facets calculated by the proposed model and with the coupled modes approach [1] as well as with experimental data. The latter comparison is shown in Fig.1b: the proposed model is in excellent agreement with the experimental data.

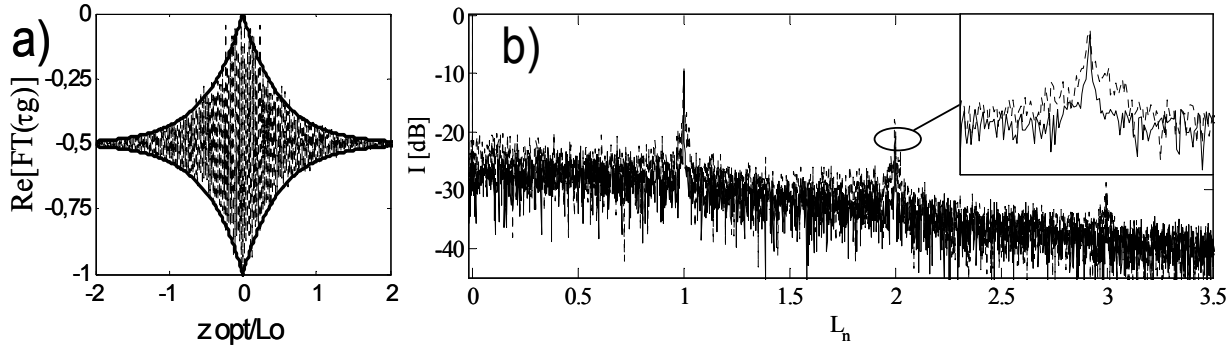


**Fig.1:** a)Real part of the FT of the group delay of the backscattered field; b) FFT of the power spectrum transmitted through a rough waveguide: experimental results (dots) and proposed model ( solid line).

**References:** [1] Marcuse D., *Theory of dielectric optical waveguide*, Ac. Press. 1991, pp.241-250.
[2] Poulton C.G *et al.*, JSTQE.2006,Vol.12, p.1306-21.

# Inverse method for the reconstruction of refractive index profile and power management in gradient index optical waveguides

Nikolai Nikolaev*, Victor V. Shevchenko°
*Peoples' Friendship University of Russia, 6 Miklukho-Maklaya St., Moscow, 117198 Russia
ne_nikolaev@mail.ru

°Institute of Radio Engineering and Electronics, Russian Academy of Sciences,Build.7, 11 Mokhovaya St., Moscow, 101999 Russia

Accurate semi-analytical technique is developed for reconstructing refractive index profiles of optical waveguide by near-field pattern. Optimising profiles of planar waveguides for managing power distribution of propagating waves is demonstrated.

## Summary

In order to optimize fabrication processes of high-quality integrated optics devices it is crucial to determine optical properties of waveguides which are directly related to their refractive index profiles. Gradient index profile waveguides, like, plastic (e.g. poly methyl methacrylate-based [1]) polymer ones, or Ti:Mg:$LiNbO_3$ [2] has many advantages offering the highest bit rate communication, easier accurate connections, higher broadband and other propagation managements. All experimental techniques developed for these purposes, like interferometric methods, measuring effective indices, near-field intensity profiles, or compositional measurements all require implementing some theoretical model for reconstructing the profile from the measurements results. Reconstructing the profile still requires great effort and long computational time as most methods used for this are based on repeating calculations of direct propagation models, with the use of, for example, Finite Difference [1] or WKB [3] methods, and then using some optimization techniques. Multiple calculations with different sets of initial parameters representing the profile not only are highly time-consuming but also their convergence is often a problem to be proved, and initial guess playing a significant role in their convergence.

Different approach is based on solving the inverse problem. We propose a semi-analytical technique developed to reconstruct the complex gradient profiles of refractive index of planar optical waveguides. Initial data for the reconstruction is Near-Field intensity pattern or propagational characteristics of transmitted waves.

Similar technique is applied to optimizing the profile to manage power transmission distribution in the waveguide core and claddings. It is shown that directing main power of the wave either along core or along some cladding layer can be achieved by choosing the right refractive index profile of the core.

The proposed technique is based on Shift Formulae Method (SFM) whose basics are described in [4]. The essence of Shift Formulae Method is special integral relationships derived from wave equations. They are named Shift Formulae and describe changes of dispersion characteristics of waves at changes of waveguide parameters or their structure. Preliminary results of the method application were shown in [5]. Analytical solution is followed by an effective computer program, with numerical results discussion.

**References**

[1] F.Caccavale, F.Segato, I Mansour, and M.Gianesin, J. Lightwave Technology, Vo. 16, No. 7, 1348-1353,1998.
[2] T.Ishigure,S.Tonaka, E. Kobayashi, and Y. Koike, J. Lightwave Technology, Vo. 20, No. 8, 1449-1456,2002.
[3] K.S.Chiang,C.L.Wong,S.Y.Cheng, and H.P.Chan, J. Lightwave Technology, Vo. 18, No. 10, 1412-1417,2000.
[4] V.V. Shevchenko, N. Espinosa-Ortiz, J. of Commun. Technology and Electronics, 38, N16, 121, 1993.
[5] N.E .Nikolaev, V.V. Shevchenko, Proc. Xth International Workshop on Optical Waveguide Theory and Numerical Modelling. April 5–6, 2002. Nottingham, UK.

# Recent Advances on Finite Element Algorithms and their Applications to Photonics

H. E. Hernandez Figueroa

School of Electrical and Computer Engineering, University of Campinas
Campinas, Brazil
***hugo@dmo.fee.unicamp.br***

Abstract not available

# A New Split Step Non-Paraxial Finite Difference Method for 3-D Wave Propagation

Debjani Bhattacharya and Anurag Sharma
*Physics Department, Indian Institute of Technology Delhi, New Delhi-110016, India*
*asharma@physics.iitd.ac.in*

A new finite difference method for 3-D propagation based on the split-step non-paraxial procedure is presented. It does not require any numerical matrix diagonalization. Numerical example on tilted rectangular waveguide shows that very good accuracy even with moderate discretization can be obtained.

## Summary

We report a finite difference split-step non-paraxial method for beam propagation in three dimensions (3-D). The computation of the propagation matrix is analytical, thereby increasing speed and accuracy. The basic principle is the same as that for 2-D propagation that we have earlier reported [1,2]; however, certain implementation issues for 3-D propagation have been solved in unique analytical ways, making it very efficient.

In the split-step finite-difference method, each propagation step can be written as [1,2]

$$\mathbf{\Phi}(z+\Delta z) = \mathbf{P}\,\mathbf{Q}(z)\,\mathbf{P}\,\mathbf{\Phi}(z) + O\left((\Delta z)^3\right) \qquad (1)$$

where $\mathbf{\Phi}(z)$ is a column vector containing the field and its derivative, $\mathbf{P}$ is a constant matrix representing propagation in a medium of constant refractive index $n_r$ and $\mathbf{Q}(z)$ is a sparse matrix defining the index distribution as a function of $z$. The splitting of the propagation operator increases the stability of the method (with respect to propagation step size), also less computational effort is required as $\mathbf{P}$ has to be computed only once. For 3-D propagation, one cannot use Eq. (1) directly due to two transverse coordinates. We overcome this difficulty by representing the transverse 2-D field as a column vector. In this case, the new F-D operator $\mathbf{A}$ for $\partial^2/\partial x^2$ becomes a block diagonal matrix whose block elements are simply a constant tridiagonal matrix used in 2-D propagation [1]. The F-D operator $\mathbf{B}$ for $\partial^2/\partial y^2$ is simply a permutation of matrix $\mathbf{A}$. To evaluate $\mathbf{P}$, matrices $\mathbf{A}$ and $\mathbf{B}$ have to be diagonalized. In our method this is done analytically. Thus, though $\mathbf{A}$ and $\mathbf{B}$ are $\left(N^2 \times N^2\right)$ matrices, the computational effort required is small due to analytical diagonalization (here $N$ is the number of samples along $x$ and $y$).

As an example we consider the tilted rectangular core waveguide considered by Shibayama *et al.* [3]. The core of refractive index 1.45 is a square of 5 μm X 5 μm and is surrounded by a medium of index 1.446. The fundamental mode is propagated. Figure 1 shows the incident, expected and the numerically propagated field after a distance of about 30 μm for a tilt of 30°. The error in the overlap integral is less that 0.01. The computations have been done on a PC using MATLAB and hence the sizes of matrices are restricted to $N$ = 64. With larger matrices, even better accuracy is expected. These and more results will be presented at the Workshop.

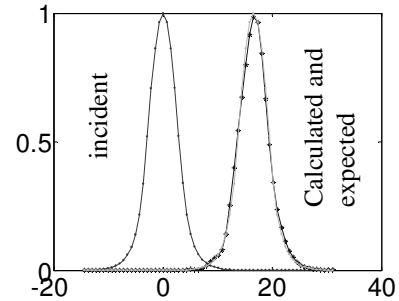


Fig. 1 Incident, expected and propagated fields in a rectangular waveguide tilted at 30°.

## References

[1] A. Sharma and A. Agrawal, *IEEE Photon. Technol. Lett.* **18**, 944 (2006).
[2] A. Sharma and A. Agrawal, OWTNM 2005, Grenoble, France (2005)
[3] J. Shibayama *et al., IEEE Photon. Technol. Lett.* **18**, 661 (2006).

# General Covariance in Computational Electrodynamics

Dzmitry M. Shyroki, Jesper Lægsgaard, Ole Bang, and Andrei V. Lavrinenko
*COM•DTU, Department of Communications, Optics and Materials,*
*Technical University of Denmark, DK-2800 Kgs. Lyngby, Denmark*
ds@com.dtu.dk

We advocate the generally covariant formulation of Maxwell equations as underpinning some recent advances in computational electrodynamics—in the dimensionality reduction for separable structures; in mesh truncation for finite-difference computations; and in adaptive coordinate mapping as opposed to subgridding.

## Summary

The Maxwell equations, in their "natural" representation, are known to be generally covariant [1]. An immense utility of such formulation pertaining to computational electrodynamics lies in clear delineation between the coordinate system chosen, which can follow the interfaces and symmetries of the given material object, and the dynamic field equations being discretized and solved, which are related to the chosen coordinates through the constitutive quantities ε and μ exclusively. This delineation enables the use of Cartesian-like, "logically rectangular" methods and solvers with any type of coordinate system actually employed.

In this contribution, we consider three areas in computational electrodynamics which would benefit substantially from the use of covariant formulations and techniques. These are:

**A. Dimensionality reduction for separable structures**. Examples include rigorous full-vector analysis of waveguide bends and twists with use of conventional simulators for straight waveguides, without the restrictions of the known approximate equivalent-index formulas; simulations, with use of existing two-dimensional, Cartesian grid based codes, of axially symmetric resonators and scatterers of arbitrary cross-section and anisotropy in the cross-section.

**B. Mesh truncation in the finite-difference computations on open domain**. Examples include formulation of the squeeze-transform layers (STLs) – the buffer regions near the domain boundaries representing the whole outer space [2,3] – which are non-dispersive, non-absorbing, outperform PMLs in guided-wave and short impulse time-domain simulations, and are the boundaries of choice whenever Hermitian formulation is required by the mode solver used.

**C. Adaptive coordinate transformation as an alternative to subgridding techniques**, to enable the uniform-grid finite-difference modelling of, e.g., quantum dots in photonic crystals and fine-structured features of nanoplasmonic devices. Our simple examples, largely following [4] in motivation and ideology, include "stretching" the ultra-thin cladding layers of the Bragg fibre, and "stretching" of the Bragg mirrors of the vertical cavity surface-emitting laser (VCSEL) with transverse nanoscale structuration.

## References

[1] E.J. Post, *Formal Structure of Electromagnetics* (North-Holland, Amsterdam, 1962).
[2] Z. Raida, Microwave Opt. Technol. Lett. **18**, 180-184 (1998).
[3] D.M. Shyroki, IEEE Microwave Wireless Comp. Lett. **16**, 576-578 (2006).
[4] A.J. Ward and J.B. Pendry, J. Mod. Opt. **43**, 773-793 (1996).

# Computing Photonic Crystal Point Defect Modes by Dirichlet-to-Neumann Maps

Shaojie Li and Ya Yan Lu
*Department of Mathematics, City University of Hong Kong*
*Kowloon, Hong Kong*

We develop an efficient numerical method for computing point defect modes of two dimensional photonic crystals. Using Dirichlet-to-Neumann maps of the defect and normal unit cells, the defect mode frequency is solved from the condition that a $K \times K$ matrix is singular, where $K$ is the number of sampling points on the boundary of the defect cell.

**Summary**

For an infinite photonic crystal with a point defect, defect modes may exist for some frequencies in bandgaps. In the standard formulation, this is an eigenvalue problem on the infinite domain where $\omega^2$ ($\omega$ is the angular frequency) is the eigenvalue. Since the eigenfunction decays to zero away from the point defect, the computation domain is usually truncated to a supercell. This eigenvalue problem is nonlinear when the medium is dispersive. Even for the linear eigenvalue problem of a non-dispersive medium, a discretization of the supercell gives rise to a large matrix. The "discretization" can be achieved by a truncated Fourier series as in the plane-wave expansion method or a discretization of the physical domain as in the finite element method. The defect modes actually correspond to interior eigenvalues that are difficult to calculate by existing iterative methods.

Recently, the Dirichlet-to-Neumann (DtN) map of a unit cell has been used to develop some efficient numerical methods for computing band structures and analyzing scattering of finite photonic crystals. The DtN map is an operator that maps the wave field on the edges of the unit cell to its normal derivative. If we have $K$ special solutions in the unit cell and choose $K$ sampling points on the boundary of the unit cell, we can approximate the DtN map by a $K \times K$ matrix. For two-dimensional photonic crystals composed of parallel circular cylinders (air-holes or dielectric rods) in a lattice, the DtN map of a unit cell can be easily constructed using the cylindrical waves as the special solutions. A boundary integral equation method has also been developed to compute the DtN map for unit cells containing cylinders of arbitrary cross section.

In this paper, we develop an efficient numerical method for computing defect modes using the DtN maps of the unit cells. The DtN maps of the defect and normal unit cells are both approximated by $K \times K$ matrices. We obtain a nonlinear eigenvalue problem which states that a $K \times K$ matrix $A$ is singular for a frequency corresponding to a defect mode. The matrix $A$ depends on $\omega$ and it is constructed from the DtN maps of the normal and defect cells. Since $K$ is typically very small, the condition that $A$ is singular can be used to find the defect mode accurately. Notice that the matrix in the standard formulation corresponds to a discretization of the supercell. Here, the matrix $A$ corresponds to a discretization of the edges of the defect cell. A supercell is actually also used in our formulation, but only the edges of the cells are involved in the manipulation, since the DtN maps contain complete information about the wave field in the interior of the unit cell if the field on the edges are known. The matrix $A$ is obtained when the wave field on all edges in the supercell, except the edges of the defect cell, are eliminated. We demonstrate our method by a number of numerical examples.

## References

[1] J. Yuan and Y. Y. Lu, Journal of the Optical Society of America A, **23**, 3217-3222 (2006).
[2] Y. Huang and Y. Y. Lu, Journal of Lightwave Technology, **24**, 3448-3453 (2006).

# Finite Element Time Domain Modelling of $90^0$ Sharp Bends

Arti Agrawal[1], B.M.A. Rahman[1], K.T.V. Grattan[1] and S.S.A. Obayya[2]
[1] *School of Engineering and Mathematical Sciences, City University, London EC1V 0HB*

b.m.a.rahman@city.ac.uk

[2] *University of Wales, Swansea*

We present the application of a newly developed finite-element time-domain method to optimisation of bend geometry for $90^0$ sharp bends in Photonics. We show important results for modal properties of Photonic Crystals and also for both Silicon on Insulator (SOI) and Photonic Crystal based bend circuits.

## Summary

At present there is a lot of interest in design of high-density Planar Lightwave Circuits (PLC) and high-index contrast structures such as SOI that can confine light tightly are being studied[1,2]. It is possible to design low loss and compact, high performance sharp right-angle bends, waveguide crossings, T-junctions and resonant cavities in SOI waveguides in a relatively small area. The compatibility of PLCs with the existing Complementary Metal Oxide Semiconductor (CMOS) technology and possibility of combining PLCs with microelectronics on a single chip makes these structures very important. Such circuits have also been demonstrated with two-dimensional Photonic Crystals (PhC)[3,4] and Photonic Crystal slabs. Active elements like Light Emitting Diodes (LED) and Vertical Cavity Surface Emitting Lasers (VCSEL) can also be made with PhCs. PhCs guide light by the mechanism of photonic band-gap guidance rather than index-guidance or total internal reflection and offer low loss light propagation. PhC slabs can be easily fabricated with current semiconductor technologies and hence are an area of intense research and development.

The design of low loss sharp bends is hampered by certain issues, namely that the bend radius has to be larger than the order of the wavelength being guided by the circuit. To achieve low loss guidance through bends, high-index contrast structures have been explored. Resonant structures that couple light from the input arm of the bend to the output arm have also been designed. In PhC bends the restriction on bend radius is lifted and smaller, tighter bends can be designed. The PhC structure provides additional degrees of freedom in design optimization that are not available with the simple index-guidance mechanism of PLCs. It is possible to remove/add dielectric posts/holes in the PhC lattice to reduce the back-reflection from the bend or to optimize the PhC lattice geometry as well as the shape of the holes/posts in the lattice. Since the PhC is scaleable it is possible to design bends for the frequency region of interest. We shall present the optimization of bend geometry in PhC and SOI structures using the efficient and accurate Finite Element based Time Domain Beam Propagation Method developed in our laboratory.

## References

[1] T. Tsuchizawa, K. Yamada, H. Fukuda, T. Watanbe, J. Takahashi, M. Takahashi, T. Shoji, E. Tamechika, S. Itabashi and H. Morita, IEEE Journal of Selected Topics in Quant. Electron., **11**, 232-240 (2005).
[2] C. Manolatou, S. G. Johnson, S. Fan, P. R. Villeneuve, H. A. Haus and J. D. Joannopoulos, Journal of Lightwav. Technol., **17**, 1682-1692 (1999).
[3] A. Mekis, J.C. Chen, I. Kurland, S. Fan, P. R. Villeneueve and J.D. Jaonnopoulos, Phys. Rev. Lett., **18**, 3787-3790 (1996).
[4] D.W. Prather, S. Shi, J. Murakowski, G.J. Schneider, A. Sharkawy, C. Chen and B. Miao, IEEE Journal of Selected Topics in Quant. Electron., **12**, 1416-1437 (2006).

# Revisiting the Rayleigh hypothesis: impacts on future electromagnetic theory and numerical modelling

A.V.Tishchenko
*Laboratoire Hubert Curien, 18 rue Benoît Lauras, Bâtiment F, Saint-Etienne, France, 42000*
*tishchen@univ-st-etienne.fr*

The Rayleigh hypothesis is shown to be true well beyond the generally accepted validity domain. It is closely verified in examples where it is usually thought that it would fail. Considering it as it fundamentally is, leads to analytical solutions to general diffraction problems and opens to new R&D developments.

**Summary**

The Rayleigh hypothesis has long been considered as a brilliant intuition with restricted validity domain and limited practical impact. Considering reflection from a periodically corrugated interface, Rayleigh looked for a solution, assuming that the field over and under the grating interface only consists of outgoing plane waves with constant amplitudes [1]. Such assumption proves to be true in regions outside the grating. Whether it is true in the grating region is still a debatable issue.

The first type of objections formulated against this hypothesis state from a physical standpoint that the fields of the diffracted orders in a homogeneous half-space can not account for the reflections and shadowing effects which would take place in a deep grating or in grooves showing re-entrant features. The second type of objections are based on numerical experiments whereby the results obtained on the basis of the Rayleigh hypothesis deviate from exact numerical results as soon as the grating depth increases beyond some limit.

We will show here that the first type of objection does not hold if the Rayleigh hypothesis is properly understood, and that the second type of objection is actually a failure of the method chosen for implementing the Rayleigh hypothesis, not of the hypothesis itself.

We will also show that, on the contrary, the Rayleigh hypothesis opens new perspectives to electromagnetic theory which have so far been overlooked.

Some authors [2-5] haven't discarded the potential of the Rayleigh hypothesis, but they haven't proceeded far enough to end up with an implementation method although Chandezon [4] has opened the way which we are exploring and paving further here.

The presentation of the potential of the Rayleigh hypothesis will be organized in three steps.

In the first step we will show that the "C" method which is reputed to exactly solve grating problems by means of a coordinate transform is actually identical to the Rayleigh hypothesis provided the basis of the fields is that of the true modes of the transformed structure instead of the diffraction orders calculated by means of a Fourier decomposition of the transformed structure.

In a second step we will show that the coordinate transform approach implemented on the basis of the modes of the transformed structure leads to an analytical solution for a wide range of grating problems, and that such analytical solution is valid for problems which have been reputed to be impossible to solve by means of the "C" method. Moreover, such analytical solutions are identical to those obtained directly on the basis of the Rayleigh hypothesis. To our knowledge, this is a first time when the solution to a general diffraction problem is found in a closed analytical form.

In a third step we will show that the results obtained on the basis of the Rayleigh hypothesis in two critical examples of structures where the Rayleigh hypothesis was generally thought to completely fail, are close to exact.

The presentation will end by describing the new perspectives in electromagnetic theory and in microoptical modelling which this new implementation of a genius hypothesis opens.

**References**

[1] Lord Rayleigh (J. W. Strutt), “On the dynamical theory of gratings,” Proc. R. Soc. London Ser. A 79, 399 (1907).

[2] K. Yasuura, H. Ikuno, “On the modified Rayleigh hypothesis and the mode-matching method,” in Summaries Int. Symp. Antennas and Propagation, Sendai, Japan, 173 (1971).

[3] P. C. Waterman, “Scattering by periodic surfaces,” J. Acoust. Soc. Am. 57, 791 (1975).

[4] J. Chandezon, D. Maystre, G. Raoult, “A new theoretical method for diffraction gratings and its numerical application,” J. Opt. Paris 11, 235 (1980)

[5] K. J. Bunch, W. N. Cain, R. W. Grow, “Use of extrapolation on wave expansions to force the satisfaction of the Rayleigh hypothesis,” J. Opt. Soc. Am. A 9, 755 (1992)

# Simulation of resonance modes in pillar-type cavities using finite element methods

*B. Kettner, F. Schmidt, L. Zschiedrich*
*Konrad-Zuse-Zentrum Berlin, Takustraße 7, D-14195 Berlin, Germany*
*Telephone: +49-30-84185-413, Fax: -107, E-mail: kettner@zib.de*

We will discuss ways of finding resonances of pillar-type nano-resonators by simulation with the finite element method. This will require solving scattering problems with point sources on unbounded domains as well as solving eigenvalue problems on unbounded domains.

**Summary**
Pillar-type cavities that may allow for optical coupling of the states of quantum dots via the cavity modes of resonators have recently been examined by M. Hetterich et. al. at CFN Karlsruhe. Such devices mainly consist of bragg-mirrors enclosing a cavity containing quantum dots that will emmit light at a given wavelength. Even though fabrication and design of these structures is quite elaborate, good numerical simulation for such cavities is a challenging task still requiring further improvement.
For a good numerical simulation of such devices, two problem classes have to be taken into account. To simulate the emission of the quantum dots in the cavity, we have to solve the scattered field resulting from a point source enclosed in the cavity. This means solving a scattering problem in an unbounded domain for a given frequency $\omega$. For a closer investigation of the resonance modes, a time-harmonic ansatz for the vectorial magnetic field $\mathbf{H}$ leads to the eigenvalue problem

$$\begin{aligned} \nabla \times \frac{1}{\epsilon(\vec{x})} \nabla \times \mathbf{H}(\vec{x}) &= \omega^2 \mu(\vec{x}) \mathbf{H}(\vec{x}), \\ \nabla \cdot \mu(\vec{x}) \mathbf{H}(\vec{x}) &= 0, \vec{x} \in \Omega \\ +\text{boundary condition} & \end{aligned}$$

where $\Omega$ is the computational domain and $\omega$ is an eigenvalue corresponding to a frequency. The boundary condition for this formulation of the problem has to be further specified. Transparent boundary conditions are required for realsitic modeling.
First simulations were done as scans of scattering problems with varying wavelengths on a cross-section through a pillar-type cavity and exhibited sharp resonant peaks which were confirmed by measurements done at CFN Karlsruhe. In a next step solving the eigenvalue problem on the unbounded domain confirmed these calculations and revealed resonance modes at the previously determined wavelengths.
First full 3D-simulations of a pillar-type cavity were then conducted, solving the eigenvalue-problem for the axisymmetric geometry taking into account the transparent boundaries and pitch of the pillar-walls. Even these complex calculations confirmed the resonance modes found in the 2D simulations of the cross-section and deliver a good representation of the cavity modes that results in deeper understanding of the processes in such devices.

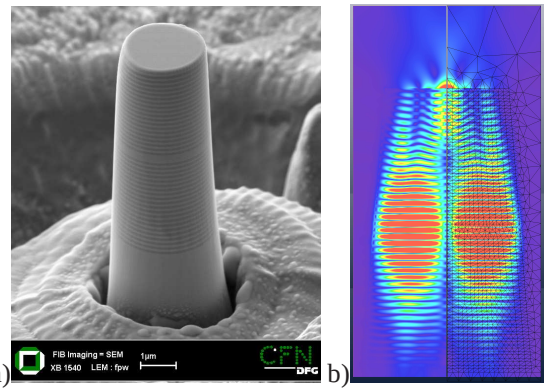


Fig. 1. a) b)

(a) Pillar-type cavity with a diameter of $2.7\mu m$ produced by CFN Karlsruhe (b) Simulation grid for axisymetric solution of the eigenvalue problem together with the magnitude of the computed eigenmode.

# Influence of geometry on the quality factor of a micro pillar

Niels Gregersen,[1] Torben R. Nielsen[1] and Jesper Mørk[1]
[1] *COM•DTU, Department of Communications, Optics and Materials, Technical University of Denmark, DK-2800 Kongens Lyngby, Denmark*
ngr@com.dtu.dk

In a micro-cavity pillar, a high quality (Q) factor is achieved by optimizing the geometry parameters. The Q factor generally decreases when the geometry deviates from the design optimum, but we identify a higher order mode interaction countering this decrease.

## Summary

A semiconductor micro pillar (MP) is an attractive candidate for a material system capable of emitting single photons [1]. The cavity is surrounded by two distributed Bragg reflectors (DBRs) along the vertical direction (Fig. 1), and total internal reflection provides confinement in the lateral plane. The highly reflecting DBRs result in a high Q factor and a small mode volume can be achieved by choosing a small pillar diameter. This choice results in strong diffraction effects, so we have computed the Q factor using the eigenmode expansion technique [2] which allows for a full 3D vectorial simulation of the optical field.

Along the vertical axis, maximum reflectivity of the Bragg stacks is achieved with layer thicknesses equal to $\lambda / (4\, n_{eff})$, where $n_{eff}$ is the effective index of the fundamental mode, and equal layer radii ensure a high mode overlap. We have perturbed this mode overlap by introducing an inclination angle of the side wall of the pillar, simulating realistic fabrication-induced underetch, and we have studied the effect on the Q value (Fig. 2).

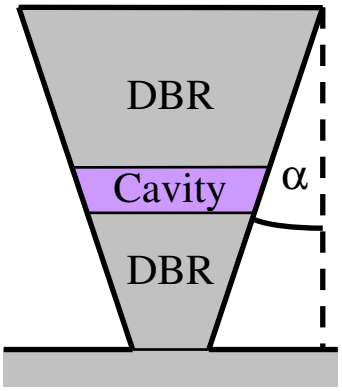


Fig. 1. Illustration of micro pillar.

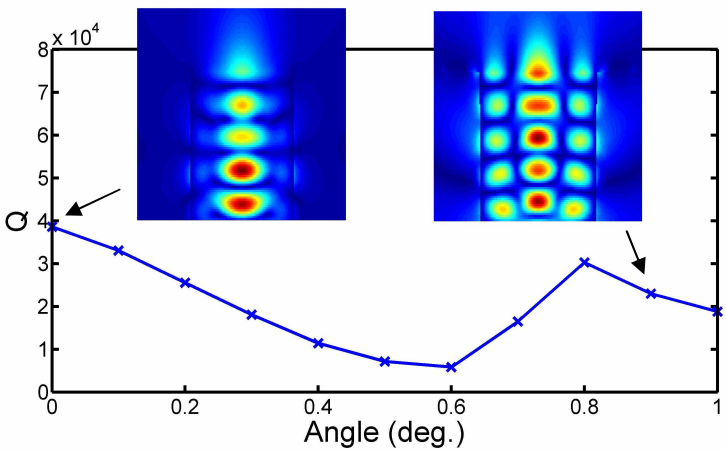


Fig. 2. Q factor as function of inclination angle α. Inserts: Radial electric field profile in top DBR mirror.

From a 1D consideration, one would expect the Q value to decrease uniformly as the mode overlap is reduced, however, we observe an increase for angles above 0.6°. The radial electric fields in the top of the micro pillar are shown for two angles, and we observe that the increase in Q is caused by interaction with higher order modes that assist in maintaining high Bragg mirror reflectivity.

## References

[1] K. J. Vahala, Nature **424**, 839 (2003).
[2] P. Bienstman, H. Derudder, R. Baets, F. Olyslager and D. D. Zutter, IEEE Trans. Microw. Theory Tech. **49**, 349-354 (2001).

# Control of Near-Field Pattern in 2D Circular Resonator by Adjusting in Time of Media Parameters

Nataliya Sakhnenko, Alexander Nerukh
*Kharkov National University of Radio Electronics, 14 Lenin Ave., Kharkov, 61166, Ukraine*
n_sakhnenko@yahoo.com

The purpose of this paper is to present an analytical investigation of source field transformation in 2D cylindrical resonator due to time changing of refractive index. The basic interest is to gain insight into details of the electromagnetic field evolution during the transient period.

## Summary

Time changing of the dielectric permittivity in unbounded space leads to change of a wave frequency [1] and conservation of a wave number. In the presence of boundaries this process is more complex and it depends qualitatively on configuration of the initial field. For the case of initial field without external source (e. g. mode of the resonator) changing of refractive index leads to the changing of frequency and wave number, but near field pattern conservation [2]. If the initial field has external source (e.g. point source) then the temporal change of dielectric permittivity inside the resonator leads to complicated transient process caused by excitation of all modes of the resonator in its new state and transformation of the near-field pattern. In this paper we consider point source that is located at distance $1.5\mu m$ from the circular resonator boundary (on the right from resonator in Fig.1) and radiates electromagnetic wave with $\lambda = 1.95\mu m$. Radius of the resonator is $1\mu m$. Refractive index is $3.385$. For these parameters we observe near field pattern similar to $E_{5,2}$ mode (initial field in Fig.1). Then we suppose that at zero moment of time refractive index changes into value 3.42. Fig.1 demonstrates transformation of the initial near-field pattern with time (T) and forming of field pattern corresponding to $E_{8,1}$ mode.

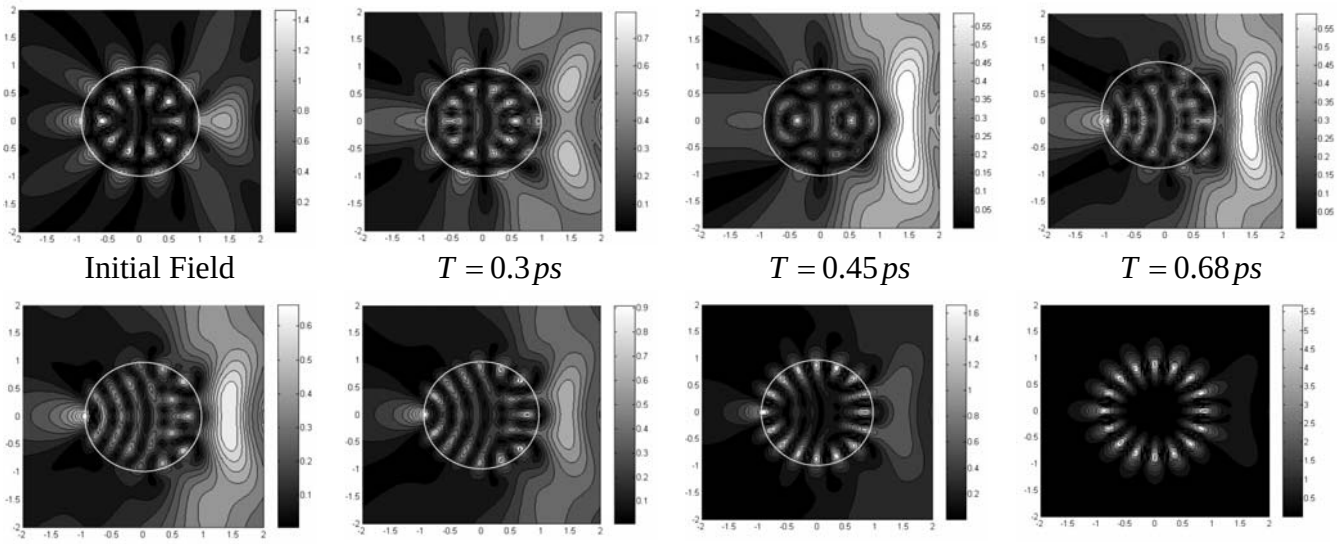

Initial Field $T = 0.3\,ps$ $T = 0.45\,ps$ $T = 0.68\,ps$

$T = 2.28\,ps$ $T = 4.56\,ps$ $T = 11.4\,ps$ $T = 45\,ps$

Fig.1 Electromagnetic field evolution during transient period

## References

[1] F.R. Morgenthaler, IRE Trans Microwave Theory and Techn, MTT-6, 167-172 (1958).
[2] N. K. Sakhnenko, T.M. Benson, P. Sewell and A. Nerukh, Optical and Quantum Electron. **38**,71-81 (2006).

# Beam Propagation Method for simulation of Quantum Dot flared laser and SLD

Paolo Bardella, Ivo Montrosset, José María Blanco Triana
*DELEN, Dipartimento di Elettronica, Politecnico di Torino, Corso Duca degli Abruzzi 24, Torino, Italy*
ivo.montrosset@polito.it

We present a 2D model for the analysis of Quantum Dot devices using a BPM. This model takes into account both the ground state (GS) and the excited state (ES) and computing the evolution of the fields in the cavity it is able to analyze P-I characteristics of lasers and SLDs.

## Summary

Semiconductor devices made with QDot materials are increasingly drawing the attention for the realization of optical sources. The study of such devices requires a correct description of the carrier density in the wetting layer (WL) and the occupation of the excited state (ES) and ground state (GS). A 2 dimensional BPM simulator with these characteristics has been implemented using the formulation proposed in [1]

$$D\nabla^2 n_{WL} + \frac{J}{q} - \frac{n_{WL}}{\tau_{r,WL}} - \frac{4\rho_{ES}}{\tau_{e,ES,WL}} - \frac{(1-\rho_{ES})n_{WL}}{\tau_{c,WL,ES}} = 0$$

$$\frac{n_{WL}(1-\rho_{ES})}{4\tau_{c,WL,ES}} + \frac{\rho_{GS}(1-\rho_{ES})}{2\tau_{e,GS,ES}} - \frac{\rho_{ES}(1-\rho_{GS})}{\tau_{c,ES,GS}} - \frac{\rho_{ES}}{\tau_{e,ES,WL}} - \left(A_{ES}\rho_{ES} + B_{ES}\rho_{ES}^{\ 2} + C_{ES}\rho_{ES}^{\ 3}\right) - v_g\sigma_{ES}(2\rho_{ES}-1)S_{ES} = 0$$

$$\frac{2\rho_{ES}(1-\rho_{GS})}{\tau_{c,ES,GS}} - \frac{\rho_{GS}(1-\rho_{ES})}{\tau_{e,GS,ES}} - \left(A_{GS}\rho_{GS} + B_{GS}\rho_{GS}^{\ 2} + C_{GS}\rho_{GS}^{\ 3}\right) - v_g\sigma_{GS}(2\rho_{GS}-1)S_{GS} = 0$$

where $n_{WL}$ is the number of carriers per dot in the WL; $\tau_e$ and $\tau_c$ are the escape and capture times; $\sigma_{ES}$ and $\sigma_{GS}$ the dot capture sections; *A*, *B*, and *C* the recombination coefficients. Lateral and longitudinal diffusion of non-confined carriers $n_{WL}$ is also taken into account. For a given current, stationary solutions are found iteratively searching for field profiles for the GS and ES emissions that remain unchanged after a round trip in the cavity. The results have been validated with a simple mean field model, but the advantages of this BPM model are the easy study of tapered lasers and SLDs, the possibility to get complete information about the transversal electric fields associated to GS and ES, and the calculation of $M^2$ factor to investigate coupling efficiency with the fiber. As an example, Fig.1 shows a result of QDot laser P-I simulation: the simulator predicts the saturation of the GS power in agreement with experimental results.

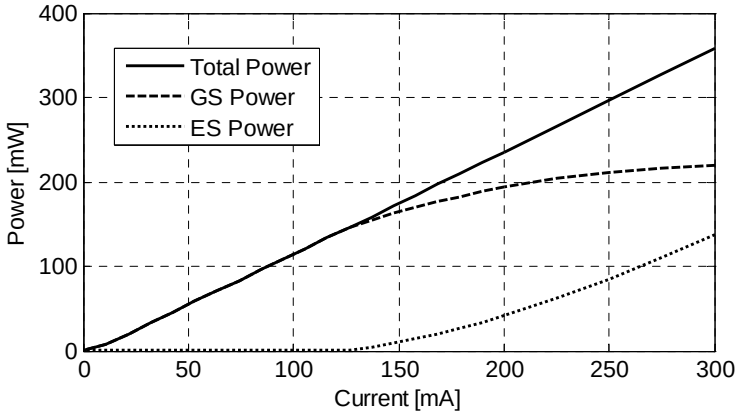


**Fig.1** P-I curves showing optical power associated with GS and ES

## References

[1] K. Veselinov et al., Opt. and Quantum Electron. **38**, 369-379 (2006).

# Models of Non-Stationary Light Beam Propagation for Non-Linear Waveguide Excitation Problems

Elena Romanova[1], Vijay Janyani[2], Ana Vukovic[3], Phillip Sewell[3] and Trevor Benson[3]
[1] *Saratov State University, Astrakhanskaya 83, Saratov 410012, Russia, romanova@optics.sgu.ru*
[2]*Malaviya National Institute of Technology, Jaipur 302017, India, vijayjanyani@gmail.com*
[3]*George Green Institute for Electromagnetics Research, University of Nottingham, Nottingham, UK*

The propagation of non-stationary light beams through sharp discontinuities in non-linear planar waveguides is considered. The objective is to understand fundamental processes, as an aid to the future design of guiding structures with pulse shaping and signal processing functionality.

## Summary

Recent achievements in the development of highly non-linear materials for photonics, coupled with the rapid development of nano-fabrication technologies, have stimulated interest in the modelling of high intensity light propagation in non-linear waveguide structures. Our previous work considered the CW problem of non-linear waveguide excitation using the theory of solitons [1]. The 2D Non-Linear Schrodinger Equation (NLSE) was also used to model quasi-static propagation of non-stationary light beams and higher orders of non-linearity and dispersion were taken into account in a generalized 2D+T NLSE [1]. In a medium with instantaneous Kerr non-linearity, pulse shaping is governed by self-steepening and dispersion effects leading to a constant leakage of field from the waveguide core [1]. An alternative to this approach is a Transmission Line Modelling (TLM) method in which material non-linearity is described via a Duffing model [2]. TLM is a time-domain numerical method and so makes no inherent assumptions and provides vital spatiotemporal information about pulse dynamics.
Here, the two models are used to study the propagation of light pulses through waveguide junctions having different linear and (or) non-linear properties. Despite its demonstrated usefulness in fs optics, the model based on the NLSE doesn't take into account reflections and backward propagation. TLM studies of a non-linear slab waveguide excited by its linear mode with a fs temporal envelope reveal power dependent instantaneous and continuous reflections and the modified shapes of both transmitted and reflected pulses. As an example, Figure 1 shows reflected and transmitted pulses, calculated using TLM for a TE polarized beam having an initial Gaussian pulse envelope, from a junction of linear and non-linear slab waveguides. In the paper, the influence of reflections on pulse shaping and the subsequent validity of the NLSE will be discussed in detail.

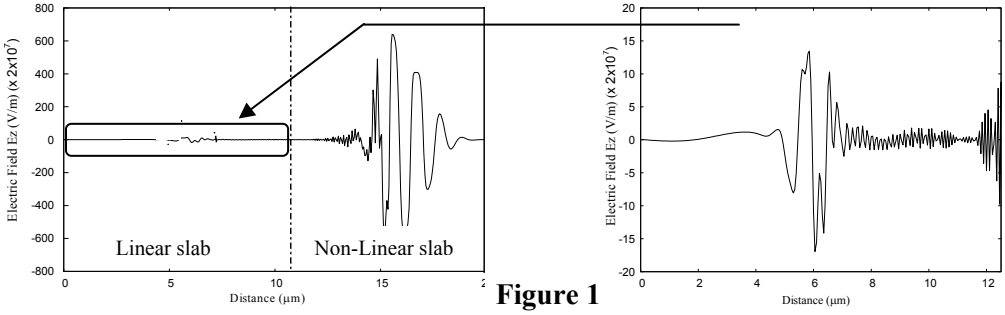


**Figure 1**

Variation of electric field along waveguide axis after pulse reflection from a linear/non-linear junction.

## References

[1] E.A.Romanova, L.A.Melnikov, S.B.Bodrov, A.M.Sergeev, in: *Frontiers in Planar Lightwave Circuit Technology* (Springer, 2006, 147-187).
[2] V. Janyani, A. Vukovic, J. D. Paul, T. M. Benson, and P. Sewell, Optical and Quantum Electron., **37**, 3-24 (2005).

# Model of the Refractive Index Change Induced by a Single Femtosecond Pulse

Jovana S. Petrovic, Vladimir Mezentsev and Ian Bennion

*Research Group, Aston University, Aston Street,B4 7ET, Birmingham, United Kingdom*
*petrovij@aston.ac.uk*

A model of permanent refractive index change induced by a single femtosecond laser pulse is presented. Model of the laser – material interaction is thermally coupled to the model of the stress induced index change. Different inscription regimes with respect to the critical power of self focusing have been studied.

## Summary

Tightly focused femtosecond pulses are capable of producing permanent spatially well localised and temperature stable refractive index change in a variety of materials, which has been used for fabrication of optoelectronic components such as waveguides, couplers, multiplexers, optical memory, fibre gratings, sensors, see e.g. [1]. Although there is still a plenty of space for research on the device side, the essential improvement can be made only after the processes involved in femtosecond laser inscription have been fully understood. Here we propose a comprehensive model that thermally couples the plasma induced by the fs pulse to the stress induced refractive index change.

When the femtosecond pulse is focused inside the material, its intensity in and near the focal point is high enough to cause the nonlinear absorption of the pulse, forming high temperature plasma in just several femtoseconds. The transfer of energy from the plasma to the lattice involves thermal diffusion of electrons and structural changes in material that last much longer than the plasma generation and longer than the presence of the pulse in the focal region. The structural modifications such as densification and cracks lead to a permanent index change. Based on these observations the model of femtosecond inscription comprises two parts that describe: (i) pulse propagation and plasma generation, (ii) thermo-mechanical changes in material and the corresponding refractive index change. They are treated separatelly whereby the kinetic properties of the generated plasma obtained from (i) are used to generate initial conditions for (ii).

Pulse propagation is modelled by the NLSE coupled with the plasma balance rate equation featuring avalanche and multi-photon ionisation [2]. The system is solved by the implicit finite difference scheme with the resolution in the propagation direction adjusted at each step. Due to the high temperature gradient the rapid cooling of the glass results in a quenching effect. It is modelled by the heath diffusion equation coupled to the stress field equilibrium equation via the dependence of the glass viscosity on temperature, and solved by a commercial finite element solver. For the inscription conditions that do not cause optical breakdown and cracks in material, the densification of the glass due to strain was used in the empirical analog of the Clausius-Mossitti relation to calculate the refractive index change. In other cases, microexplosions that lead to the voids in material are likely to happen and the model would have to be corrected to treat the shock wave formation. Finally, the numerical results for different input powers are compared to the index changes obtained in corresponding experimental conditions.

## References

[1] Photonics Spectra, October 2006
[2] M. D. Feit and J. A. Fleck, Appl. Phys. Lett. **24(4)**, 169-172 (1974)
[3] T. Bennet and L. Li, J. Appl. Phys. **89(2)**, 942-950 (2001).


DTU

JCMwave

RSOFT
Design Group

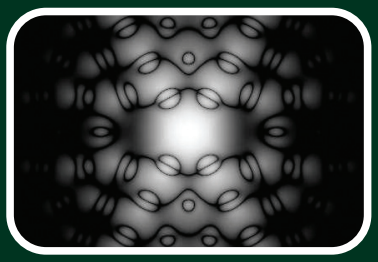

COM•DTU